Patent Application of

Andrew M. Sifferman

for

TITLE: CORRECTION FOR NON-PARALLEL ULTRASONIC BEAMS IN A CORRELATION SPEED SENSOR

CROSS-REFERENCE TO RELATED APPLICATIONS

This application claims the benefit of US Provisional Patent Application No. 61/406,112, filed Oct. 23, 2010 by the present inventor, which is incorporated by reference.

FEDERALLY SPONSORED RESEARCH

Not Applicable

SEQUENCE LISTING OR PROGRAM

Not Applicable

BACKGROUND OF THE INVENTION

[0001] 1. Field of the Invention

[0002] This invention relates to speed sensors typically used in boats, and more particularly to speed sensors employing the correlation of acoustic signals received by ultrasonic transducers.

[0003] 2. Description of the Related Art

[0004] A correlation speed sensor, also known in the art as a correlation log or an ultrasonic speed sensor, is an electronic device used to measure the speed of a vessel through water, although such a device may be used in other applications, or in other mediums. At the time of this writing, such prior art devices are manufactured and sold on the open market by Airmar Technology Corporation, of New Hampshire, and Consilium Marine AB, of Sweden.

[0005] FIG. 1 illustrates a correlation speed sensor of the prior art. The sensor is typically contained within a housing 110 made of plastic, bronze, or stainless steel, and is installed in the hull 112 of a vessel. The sensor typically contains a pair of identical piezoelectric ultrasonic transducers 101 and 102 mounted in tandem along an axis of motion 114. The ultrasonic beams 103 and 104 of the transducers are aligned approximately parallel to each other, and they transmit into the water below the vessel in a direction normal to the surface of the hull. Usually, the first transducer 101 is located in the forward position on the vessel, and the second transducer 102 in the afterward position, allowing the sensor to measure speed through the water along the vessel's axis of forward motion. Generally, the transducers are encapsulated in a non-hygroscopic polymer, which is omitted from FIG. 1 for illustrative clarity.

[0006] FIG. 2 illustrates a block diagram of the circuitry within a typical correlation speed sensor of the prior art. In addition to the two transducers 201, 202 (FIG. 2), a correlation speed

sensor typically contains a transmitter circuit 203 to drive the transducers, a pair of amplifier/filter circuits 204 to condition received echoes, a pair of envelope detectors 205, a pair of analog-to-digital converters 206, and a microcontroller 200. These circuits might be located within the sensor housing (110, FIG. 1), or alternatively located within an external module (not shown). The transmitter circuit 203 produces electrical signals (i.e. pings) to be converted by the transducers 201, 202 into acoustic energy that is projected into the water. Echoes are received by each transducer 201, 202 and amplified by the corresponding amplifier/filter circuit 204. The amplifier/filter circuits 204 feed the amplified echo signals to the envelope detectors 205. The envelope detectors 205 each remove the ultrasonic carrier from the received and amplified signal, leaving only the envelope of the signal, which is a signal proportional to the intensity of the received echo. The envelope detectors 205 then feed the detected signal envelopes into the inputs of analog-to-digital converters 206. The analog-to-digital converters 206 are sampled under control of the microcontroller 200. The microcontroller 200 performs the signal processing and calculations necessary to determine the speed of the flow of the water past the sensor, and provides the results to a display or recording device via a digital communication interface 207.

[0007] In accordance with the prior art, the operation of a typical correlation speed sensor is as follows. Referring again to FIG. 1, the two transducers 101 and 102 simultaneously ping into the water. Each transducer produces a beam of acoustic energy 103, 104 traveling through the water at a constant speed in a direction perpendicular to the transducer's projecting surface. The transmitted energy reflects off of randomly occurring particulate matter 116 suspended in the water, producing a series of echoes back to the transducer elements. The time at which an echo is detected relative to its originating ping is determined by the distance of the reflecting object from the surface of the transducer, and the speed of sound propagating through the water, according to the relation

$$\text{time} = \frac{(\text{distance} \times 2)}{\text{soundspeed}}$$

where the speed of sound through water is well known to be approximately 1484 meters per second. The factor of 2 in the above equation is to account for the round-trip travel of the sound energy from the transducer to the reflecting object, and then back to the transducer again.

[0008] During the period of time that the series of echoes from the ping is returning to the transducers, the circuitry within the sensor samples, from both transducers in unison, the signal strength of echoes received from particles occurring within a specific layer of water 105 at a fixed depth, or vertical distance, from the transducers. The specific layer of water 105 is sometimes referred to in the art as a range bin, or a sampling window. Correlation speed sensors of the prior art may also employ more than one sampling window, as exemplified in FIG. 1 by the second sampling window 106 at a further vertical distance from the transducers 101, 102 than the first sampling window 105.

[0009] The flow of water closest to the surface of a vessel's hull is distorted by a phenomenon well known in the art as the boundary layer effect. Because of this distortion, the magnitude and direction of the flow of water within the boundary layer is not representative of the flow of water beyond the boundary layer. In order to achieve an accurate measurement of vessel speed, it is therefore necessary for the correlation speed sensor to restrict its sampling window(s) to depths beyond the boundary layer. For example, in FIG. 1 the sampling windows 105, 106 might be located 3 to 5 inches away from the faces of the transducers.

[0010] As the vessel moves through the water, a plurality of pings and subsequent echoes will normally occur during the course of the traversal of each reflecting object 116 through the ultrasonic beams 103, 104 of the transducer elements 101, 102.

[0011] If the vessel is moving forward, then the flow of water past the sensor will cause a given set of reflecting objects 116 to be first encountered and detected by the first transducer 101 in the forward position. At a subsequent time later that is determined by the speed of the vessel and the horizontal distance d_0 (FIG. 1) between the centers of the ultrasonic beams 103, 104, the substantially same set of reflecting objects 116 will be detected by the second transducer 102 in the afterward position. Thus, as shown in FIG. 3 (prior art), the received discrete signal waveform 302 from the afterward transducer is similar to the received discrete signal waveform 301 from the forward transducer, but shifted in time.

[0012] The time shift is typically determined by calculating a difference function from the autocorrelations and the cross-correlation of the signals from the two transducers. Discrete autocorrelation functions may be written as

$$AC_1(t) = \sum_{i=0}^{N-1} S_1[i] \times S_1[i+t]$$

for the first transducer, and

$$AC_2(t) = \sum_{i=0}^{N-1} S_2[i] \times S_2[i+t]$$

for the second transducer, where N is a total number of samples, $S_1[i]$ is the i^{th} sample from the first transducer, $S_2[i]$ is the i^{th} sample from the second transducer, and t is a number of contiguous samples representing a time shift. A cross-correlation between the signals from the two transducers may likewise be written as

$$CC(t) = \sum_{i=0}^{N-1} S_1[i] \times S_2[i+t]$$

[0013] FIGS. 4A and 4B (prior art) illustrate an autocorrelation function $AC_1(t)$ (401) based on a signal from a first transducer, and an autocorrelation function $AC_2(t)$ (402) based on a signal from a second transducer. Because the two transducers are assumed to be identical, the two autocorrelation curves 401, 402 are theoretically identical. The duration of each autocorrelation curve 401, 402 is established by the width of the corresponding transducer's ultrasonic beam along the axis of motion and the speed of the vessel. Both autocorrelation curves peak at t=0 because by definition an autocorrelation is the correlation of a signal with itself, and there is no time shift associated with an isolated signal.

[0014] FIG. 4C (prior art) illustrates a cross-correlation function CC(t) (403) based on signals from both transducers. The peak 404 of the cross-correlation occurs at a time shift τ determined by the spacing between the two ultrasonic beams and the speed of the vessel.

[0015] FIG. 5A (prior art) shows a curve 501 representing the average of the autocorrelation functions $AC_1(t)$ and $AC_2(t)$, and a cross-correlation curve CC(t) (503) based on parallel ultrasonic beams, superimposed onto the same graph. The peak 504 of the cross-correlation corresponds with time shift τ. The intersection 507 between the auto-correlation and cross-correlation curves occurs at $\tau/2$, as shown in FIG. 5A.

[0016] The time shift τ between the two signals may be determined by calculating a difference function between the autocorrelations and the cross-correlation of the signals from the two transducers. FIG. 5B (prior art) illustrates one such difference function (505)

$$F(t) = \frac{AC_1(t) + AC_2(t)}{2} - CC(t)$$

[0017] The zero crossing 506 occurs at $\tau/2$, and may be determined by finding the value for t when F(t)=0, according to well-known principles of the art. Other methods of determining the time shift are also possible.

[0018] According to the prior art, once the time shift τ between the received signals has been determined, the relative speed of the water with respect to the sensor may then be calculated using the well-known relation of speed being equal to distance traveled per unit of time, or

$$\text{speed} = \frac{d_0}{\tau}$$

where d_0 is the predetermined fixed horizontal distance between the centers of the transducer elements, as shown in FIG. 1 (prior art).

[0019] A significant disadvantage with this prior approach is that the horizontal distance d_0 (FIG. 1) between the transducer elements is used in the calculation for speed, when in fact the dimension that would properly be used, if it were known, is the actual distance that the reflecting objects traverse through the water between the centers of the ultrasonic beams.

[0020] FIG. 6 illustrates a side elevation view of a transducer assembly showing two transducers 101, 102 mounted on a baseplate 100, and having parallel ultrasonic beams 103, 104. The horizontal distance between the two transducer elements is shown in FIG. 6 as dimension d_0. The distance traveled by the reflecting objects is represented as dimension d_1 for the first sampling window 105, and dimension d_2 for the second sampling window 106.

[0021] In the prior art, the two ultrasonic beams are assumed to be exactly parallel to one another; therefore the horizontal distance between the centers of the beams is assumed to be

constant over the range of depths traversed by the beams, and will naturally be equal to the distance d_0 between the centers of the transducer elements themselves. This may be understood pictorially by referring to FIG. 6, in which the horizontal distance d_1 between the centerlines 601, 602 of the parallel ultrasonic beams 103, 104 at the depth of sampling window 105 is clearly the same as the distance d_0 between the centers of the transducers 101, 102. Likewise, the distance d_2 at the depth of the additional sampling window 106 is clearly the same as the distance d_0. That is,

$$d_0 = d_1 = d_2$$

only because it has been assumed that the ultrasonic beams are parallel.

[0022] This prior assumption that the two ultrasonic beams are in fact parallel can be, however, flawed in practice. Manufacturing process variations can and do contribute to dimensional errors that often result in the ultrasonic beams being non-parallel.

[0023] In a typical correlation speed sensor, each of the two transducer elements is composed of a piezoelectric material that has been polarized and manufactured to specific dimensions. During the assembly process, it is intended that the transmitting faces of the two transducers be mounted so as to be coplanar with respect to one another – if achieved, this would result in their ultrasonic beams being parallel, since the beam of acoustic energy produced by each transducer element travels through the medium in a direction normal to its transmitting surface. Achieving this coplanarity consistently in practice, however, can be difficult. For example, one method of mounting the transducer elements is to position and affix them to a common baseplate 100 (FIGS. 1 and 6) using a suitable adhesive (not shown). But deviations in the flatness of the baseplate, the thickness and/or uniformity of the adhesive, and/or the dimensions of the transducer elements; and/or the presence of contaminant particles trapped between the baseplate and each transducer,

can all contribute to errors that result in the transmitting surfaces of the two transducers being in fact mutually non-coplanar.

[0024] FIG. 7 is a perspective view of a correlation speed sensor application that illustrates the disposition of two transducers 101, 102 with respective non-parallel ultrasonic beams 103, 104 monitoring two sampling windows 105, 106. The transducers are shown mounted on a baseplate 100, and enclosed in a housing 110. The sensor is installed in the hull 112 of a vessel moving along axis of motion 114. The transducers 101, 102 are each shown as being tilted relative to baseplate 100, and as a result, their respective ultrasonic beams 103, 104 are also independently tilted. The tilting of the beams may be due, for example, to an uneven thickness of the adhesive (not shown) bonding the transducers to the baseplate, and/or to contaminant particles (not shown) lodged between the baseplate and the transducers. As a result of the ultrasonic beams being non-parallel, it is easy to see in FIG. 7 that the horizontal distance d_1 between the centerlines 601, 602 of the ultrasonic beams at the depth of sampling window 105 is not the same as the distance d_0 between the transducers 101, 102. Likewise, the horizontal distance d_2 between the centers of the ultrasonic beams at the depth of the additional sampling window 106 differs from both d_0 and d_1. In summary, as a result of the ultrasonic beams being non-parallel,

$$d_1 \neq d_0$$

$$d_2 \neq d_0$$

$$d_1 \neq d_2$$

and in general, for any sampling window j at vertical distance y_j from the face of the transducers, $d_j \neq d_0$. Therefore, the signals measured in sampling windows 105, 106 are associated with a flow of particles through different horizontal distances d_1, d_2 than the distance d_0 between the transducers.

[0025] If the dihedral angle between the planes of the transducer transmitting surfaces is nonzero, then the distance between the centerlines 601, 602 (FIG. 7) of the resultant non-parallel ultrasonic beams 103, 104 will vary linearly according to the depth of the sampling window. If the ratio between the depth of the samples (relative to the transducers) and the distance between the centers of the transducer surfaces is high (which is likely to be the case due to the need to sample echoes originating from outside the boundary layer), then a small deviation in the angle between the planes of the transducer surfaces can translate to a large deviation in the distance between the beam centers at the sampling depth. This large deviation, if left uncorrected, can result in a correspondingly large error in the speed value reported by the sensor.

[0026] For example, consider a typical correlation speed sensor of the art having a transducer width of 0.4 inches along the axis of motion, a transducer center-to-center spacing of 0.44 inches, and a sample depth of 4 inches. If a contaminant particle having a diameter of only 0.001 inch lodges under the outside edge of one of the two transducers, causing its ultrasonic beam to tilt toward the other transducer's ultrasonic beam, this would result in a +2.3% error in the reported speed.

[0027] In a second, more extreme, example, if contaminant particles .005 inch in diameter lodge under the inside edge of both transducers, causing their ultrasonic beams to tilt away from each other, an error of −18.5% would result. The same .005 inch particles lodged under the outside edges of the transducers would cause the beams to tilt toward each other, resulting in an error of +29.4%.

[0028] Because these deviations are caused by an inherent difficulty in controlling manufacturing processes, clearly the resultant error can vary widely from one manufactured unit to the next.

[0029] It is furthermore well established in the prior art that to improve precision and accuracy, additional sampling windows at different vertical distances from the transducers may be employed to increase the amount of statistical data available for determining the time shift between the two signals. When employing this technique, the disadvantage cited above propagates to all sampling windows, since each unique preferred horizontal distance d_j between the ultrasonic beams at sampling window j is substituted within the calculation for speed by the inferior distance d_0 between the transducer elements.

SUMMARY OF THE INVENTION

[0030] In accordance with one embodiment of the present invention, a correlation speed sensor contains two identical ultrasonic transducers. The transmitting surfaces of the two transducers are very nearly coplanar, but slight variations in manufacturing processes introduce a small dihedral angle between the two transmitting surfaces. This dihedral angle results in the transmitted ultrasonic beams being nearly, but not exactly, parallel. As a result, the horizontal distance between the centers of the ultrasonic beams varies linearly according to the vertical distance from the transducers, and for a given vertical distance is not readily determined without the benefit of the present invention. Because the accuracy of a correlation speed sensor depends on accurately knowing the horizontal distance between the ultrasonic beams within each sampling window, a need exists for a way to determine this distance.

[0031] As such, a primary advantage of the embodiment is that it more accurately determines the distance between the centers of the two ultrasonic beams, along a specific axis of motion, at any vertical distance from the transmitting surfaces of the transducers within the near field range of the transducers.

[0032] A further primary advantage of the embodiment is that it improves the accuracy of the speed reading reported by a correlation speed sensor.

[0033] A further advantage of the embodiment is that it promotes consistency in the reported speed readings between any two manufactured correlation speed sensors operating under similar test conditions.

[0034] A still further advantage of the embodiment is that it achieves these benefits without the need for an additional manufacturing process associated with a calibration correction for non-parallel ultrasonic beams.

[0035] A yet further advantage of the embodiment is that it achieves these benefits without change to the physical configuration of the transducers, baseplate, and/or other mechanical aspects of the speed sensor as employed in the prior art.

[0036] Further aspects and advantages of this and other embodiments will become clear as the invention is described and shown in further detail.

BRIEF DESCRIPTION OF THE DRAWINGS

[0037] The present invention will be more clearly understood from the description of the preferred embodiments as set forth below with reference to the accompanying drawings, wherein:

[0038] FIG. 1 is a perspective view illustrating a correlation speed sensor of the prior art installed in the hull of a vessel, the sensor having two transducers with parallel ultrasonic beams monitoring randomly located reflective particles suspended in a fluid medium;

[0039] FIG. 2 is a block diagram of electronics and related components in a correlation speed sensor according to the prior art;

[0040] FIG. 3 is a prior art plot of echo signal amplitude versus time of two discrete sample waveforms based on similar but time-shifted reflection signals;

[0041] FIG. 4A is a prior art graph of an autocorrelation function based on a signal received from a first transducer;

[0042] FIG. 4B is a prior art graph of an autocorrelation function based on a signal received from a second transducer;

[0043] FIG. 4C is a prior art graph of a cross-correlation function based on signals received from first and second transducers having parallel ultrasonic beams;

[0044] FIG. 5A is a prior art graph of an autocorrelation function and a cross-correlation function based on parallel ultrasonic beams, both functions superimposed onto the same graph;

[0045] FIG. 5B is a prior art graph of a difference function based on parallel ultrasonic beams;

[0046] FIG. 6 is a side elevation view of a transducer assembly that illustrates the disposition of two transducers having parallel ultrasonic beams, monitoring two sampling windows;

[0047] FIG. 7 is a perspective view illustrating a correlation speed sensor installed in the hull of a vessel, the sensor having two transducers whose ultrasonic beams are tilted apart from each other;

[0048] FIGS. 8A and 8B are a perspective view and a side elevation view, respectively, of a transducer assembly having two transducers whose ultrasonic beams are tilted apart from one another and skewed; to aid in visualizing the angle between the ultrasonic beams as it relates to the embodiments described herein;

[0049] FIG. 8C is a side elevation view of a transducer assembly having two transducers whose ultrasonic beams are tilted toward one another and skewed; to aid in visualizing the angle between the ultrasonic beams as it relates to the embodiments described herein;

[0050] FIG. 9A is a graph of an autocorrelation function and a cross-correlation function based on ultrasonic beams that are tilted apart from one other, both functions superimposed onto the same graph;

[0051] FIG. 9B is a graph of a difference function based on ultrasonic beams that are tilted apart from each other;

[0052] FIG. 10A is a graph of an autocorrelation function and a cross-correlation function based on ultrasonic beams that are tilted toward each other, both functions superimposed onto the same graph;

[0053] FIG. 10B is a graph of a difference function based on ultrasonic beams that are tilted toward each other;

[0054] FIG. 11 is a side elevation view of a transducer assembly having two transducers whose ultrasonic beams are tilted apart from one another, and particularly illustrating geometric features used in determining the angle between the ultrasonic beams according to certain embodiments herein;

[0055] FIG. 12 is a side elevation view of a transducer assembly having two transducers whose ultrasonic beams are tilted toward one another, and particularly illustrating geometric features used in determining the angle between the ultrasonic beams according to certain embodiments herein;

[0056] FIGS. 13A-13B are a flow chart that describes a process for determining the angle between the ultrasonic beams according to principles of a first embodiment of the present invention;

[0057] FIG. 14 is a flow chart that describes a subroutine for collecting samples in two sampling windows according to principles of the first embodiment;

[0058] FIG. 15 is a side elevation view of a transducer assembly having two transducers whose ultrasonic beams are tilted apart from one another, monitoring a single sampling window;

[0059] FIG. 16 is a flow chart that describes a process for determining speed using a single sampling window, according to principles of the first embodiment;

[0060] FIGS. 17A-17B are a flow chart that describes a process for determining the angle between the ultrasonic beams according to principles of a second embodiment of the present invention;

[0061] FIG. 18 is a flow chart that describes a subroutine to collect samples in a single sampling window, according to principles of the second embodiment;

[0062] FIGS. 19A-19C are a flow chart that describes a process for determining the angle between the ultrasonic beams, and the distance between the transducers, according to principles of a third embodiment;

[0063] FIG. 20 is a side elevation view of a transducer assembly having two transducers whose ultrasonic beams are tilted apart from one another, monitoring three sampling windows; and which also illustrates a hypothetical scenario involving three reflective particles;

[0064] FIGS. 21A-21B are a flow chart that describes a process for determining speed using one or more sampling windows, according to principles of a fourth embodiment;

[0065] FIG. 22A is a graph of autocorrelation and cross-correlation functions based on samples from three sampling windows in ultrasonic beams that are tilted apart from one another, all functions superimposed onto the same graph;

[0066] FIG. 22B is a graph of difference functions based on samples from three sampling windows in ultrasonic beams that are tilted apart from each other;

[0067] FIG. 23 is a flow chart that describes a process for determining speed using one or more sampling windows, according to principles of a fifth embodiment;

[0068] FIG. 24 is a block diagram illustrating the functionality of a subroutine performing the processes of Sample Collection, Sample Rate Conversion, and Combine Samples, according to principles of the fifth embodiment;

[0069] FIGS. 25A-25B are a flow chart that describes a process of sample collection, according to principles of the fifth embodiment;

[0070] FIGS. 26A-26B are a flow chart that describes a process of sample rate conversion, according to principles of the fifth embodiment;

[0071] FIG. 27 is a flow chart that describes a process of combining samples, according to principles of the fifth embodiment;

[0072] FIG. 28A is a plot of raw samples collected over time from two transducers in three sampling windows, corresponding to the hypothetical scenario of FIG. 20 in which three reflective particles simultaneously pass through the three sampling windows, according to principles of the fifth embodiment;

[0073] FIG. 28B is a plot of rate-converted samples versus time, illustrating the outputs of three concurrently-running Sample Rate Conversion processes receiving as inputs the raw samples of FIG. 28A, according to principles of the fifth embodiment;

[0074] FIG. 28C is a plot showing the rate-converted samples of FIG. 28B after having been compressed in time, according to principles of the fifth embodiment;

[0075] FIG. 28D is a plot illustrating the output of a Combine Samples process having received as input the samples of FIG. 28C, according to principles of the fifth embodiment;

[0076] FIG. 29A is a graph of autocorrelation and cross-correlation functions based on rate-converted and time-shifted samples from three sampling windows in ultrasonic beams that are tilted apart from one other, all functions superimposed onto the same graph; and

[0077] FIG. 29B is a graph of a difference function based on the combined samples from three sampling windows in ultrasonic beams that are tilted apart from each other.

[0078] It is noted that throughout the various figures, like reference numbers refer to like components wherever possible. Furthermore, in general, reference numbers follow a convention wherein the first one or two digits of the reference number represent the figure number in which

a component is first introduced. For example, centerline 601 is introduced in FIG. 6, and appears also with the same reference number in FIGS. 7, 8A, 8B, 8C, 11, 12, 15, and 20.

DETAILED DESCRIPTION OF THE INVENTION

[0079] While the invention is susceptible to embodiments in many different forms, there are shown in the drawings and will be described herein, in detail, the preferred embodiments of the present invention. It should be understood, however, that the present disclosure is to be considered an exemplification of the principles of the invention and is not intended to limit the spirit or scope of the invention by the embodiments illustrated.

Terminology and Definitions

[0080] The terms "fluid," "fluid medium," and "water" are used interchangeably throughout this disclosure. Correlation speed sensors are most commonly employed in boats and ships, where the fluid medium is naturally water. The principles of the present invention apply equally to the application of correlation speed sensors in fluid mediums other than water.

[0081] As used herein, the term "vertical," when used in reference to a transducer or its ultrasonic beam, refers to a direction normal to the face of the transducer and along the axis of its ultrasonic beam. The term "horizontal," when used in reference to features of a correlation speed sensor, refers to a direction along the axis of motion of the sensor. It is noted that because the transducers in this disclosure are assumed to be tilted slightly relative to their ideal orientations, the choice of this terminology might unfortunately result in a "horizontal" feature being not strictly orthogonal with a "vertical" feature. Because of the slightness of the tilt angles assumed herein, this peculiarity in the terminology should be regarded as inconsequential.

[0082] As used herein, the term "depth" refers to the distance along the axis of an ultrasonic beam between a specified feature in the water and the transmitting face of the corresponding transducer.

[0083] As used herein, the term "sampling window" refers to a layer of water at a specific vertical distance from the transducers, that is monitored for echoes from reflective targets.

Description of Geometric Model

[0084] Before commencing to describe the principles of the embodiments, it will be instructive to describe in detail a geometric model of a correlation speed sensor with non-parallel ultrasonic beams as it relates to the embodiments described herein.

[0085] As previously stated, it is noted that like reference numbers refer to like components wherever possible throughout the various figures.

[0086] FIGS. 8A and 8B are a perspective view and a side elevation view, respectively, of a transducer assembly that illustrates the disposition of two transducers 101, 102 mounted to a baseplate 100, and arranged in tandem along an axis of motion 114. The transducers 101, 102 have respective ultrasonic beams 103, 104 with respective centerlines 601, 602. Indicator 801 defines the orientations of three mutually orthogonal axes X, Y, and Z relative to the transducers and baseplate. The X axis is parallel to the axis of motion 114. The surface of baseplate 100 to which the transducers 101, 102 are mounted is in an XY plane, and normal to the Z axis. The two transducers 101, 102 are shown in FIGS. 8A and 8B as being tilted away from each other in such a way that the centerlines 601, 602 of their respective ultrasonic beams 103, 104 do not intersect; i.e. the centerlines are skew lines.

[0087] It is not a requirement of the embodiments that the centerlines 601, 602 of the ultrasonic beams be skewed; in a given instance of a correlation speed sensor the centerlines might intersect in a common plane, or might in fact be parallel, and the principles of the embodiments will still apply. The scenario of FIGS. 8A and 8B in which the centerlines are skewed serves as a general case that lends itself to illustrating the principles of the embodiments.

[0088] FIG. 8C is a side elevation view of a transducer assembly that is identical in configuration to FIGS. 8A and 8B, except that the two transducers 101, 102 in FIG. 8C are tilted toward one another instead of away from each other as in FIGS. 8A and 8B.

[0089] In an ideal manifestation of a correlation speed sensor, the two ultrasonic beams 103, 104 would be parallel, as shown in FIG. 1 (prior art) and FIG. 6. Variations in manufacturing processes, however, sometimes cause the transducers 101, 102 to be tilted a slight amount, which causes an angular displacement of their respective ultrasonic beams 103, 104, as shown in FIGS. 7, 8A, 8B, and 8C. The cause of the tilt is not germane to the present invention, although possible causes can be envisioned, such as an unevenly distributed adhesive (not shown) between the baseplate 100 and the transducers 101, 102, and/or one or more contaminant particles lodged between the transducers and the baseplate, and/or baseplate 100 having an uneven surface.

[0090] In FIGS. 8A, 8B, and 8C, the reader will note that there appears to be a gap separating each transducer 101, 102 from baseplate 100; the gap is shown for the purpose of illustrative clarity with regard to the orientation of the transducers 101, 102 relative to an ideal baseplate 100. In an actual correlation speed sensor application, this gap would be filled most likely with an adhesive.

[0091] In the following descriptions of the embodiments, reference is made often to "the angle between the ultrasonic beams," also referred to as θ. To facilitate visualizing more precisely what is meant by the term "the angle between the ultrasonic beams," FIGS. 8A, 8B, and 8C

depict an imaginary plane 805 that extends in the X and Z directions. Line 806 is an orthographic projection of the centerline 601 of ultrasonic beam 103 onto XZ plane 805. Line 807 is an orthographic projection of the centerline 602 of ultrasonic beam 104 onto XZ plane 805. For the purposes of the embodiments described herein, θ is defined to be the angle between orthographic projections 806, 807 onto XZ plane 805 of the centerlines 601, 602 of the ultrasonic beams 103, 104. If the ultrasonic beams 103, 104 are tilted away from each other, as shown in FIG. 8B, angle θ is defined to have a positive sign. If the ultrasonic beams 103, 104 are tilted toward each other, as shown in FIG. 8C, angle θ is defined to have a negative sign. This definition of "the angle between the ultrasonic beams" is not to be construed as being limiting in any way, and it is to be understood that other definitions for "the angle between the ultrasonic beams" may be applied without departing from the spirit or scope of the present invention.

[0092] Referring still to FIGS. 8A, 8B, and 8C, it is noted that in practice, a tilt of either or both of transducers 101, 102 might be associated with a slight positional displacement of the centers 802, 803 of the transmitting faces of transducers 101, 102, relative to their ideal, non-tilted positions (i.e. the positions they would have held if the transducers' transmitting faces were coplanar). Line 804 is drawn through the centers 802, 803 of the transmitting faces of transducers 101, 102 for the purpose of illustrating this point. If the transducers were mounted ideally, having parallel ultrasonic beams 103, 104, then line 804 would be parallel to the X axis and the axis of motion 114. A tilt of the transducers, however, might cause the centers 802, 803 of the transmitting faces of transducers 101, 102 to shift slightly in position along one or more of the axes X, Y, or Z, which would cause the direction of line 804 (still passing through the centers 802, 803 of the transducers) to shift slightly in either elevation or azimuth. It is a simplifying assumption of the embodiments described herein that the amount of this positional displacement of the transducer centers 802, 803, as a result of the tilting of the transducers, is negligible and may be ignored. This assumption is justified so long as the vertical distance between the transducers 101, 102 and the sampling window 105 is large in comparison to the horizontal distance d_0 between the transducers. Because of the need to restrict the sampling windows to

depths beyond the boundary layer, this condition is easily met. For example, in a typical correlation speed sensor application, the vertical distance between the transducers and the sampling windows is about 3 to 5 inches, while the horizontal distance d_0 between the transducers is about 0.44 inches. Having made this simplifying assumption, the distance d_0 between the centers of the transducers 101, 102, in accordance with the embodiments described herein, is therefore assumed to be fixed, regardless of the presence or magnitude of a tilt of either or both transducers. These assumptions relative to the embodiments described herein do not necessarily extend to other possible embodiments of the invention; it would certainly be possible to employ a correction for tilted transducers that takes into account the positional displacement of the centers of the transducer faces, without exceeding the scope or spirit of the present invention.

[0093] FIGS. 9A and 9B illustrate the effect on the autocorrelation and cross-correlation functions, and the resulting difference function, caused by the ultrasonic beams being tilted away from each other as shown in FIG. 8B. It will be instructive to compare FIGS. 9A and 9B with FIGS. 5A and 5B (prior art), which illustrate the ideal case where the ultrasonic beams are parallel. Curve 901 (FIG. 9A) represents the average of the autocorrelation functions $AC_1(t)$ and $AC_2(t)$, which when compared to curve 501 (FIG. 5A) is seen to be unaffected by the angle between the transducers. Curve 903 (FIG. 9A) represents a cross-correlation function CC(t) based on signals from two transducers whose ultrasonic beams are tilted away from each other as shown in FIG. 8B. The peak 904 of the cross-correlation occurs at a time shift τ established by the horizontal distance d_1 (FIG. 8B) between the centerlines 601, 602 of the two ultrasonic beams 103, 104 (FIG. 8B) at the depth of the sampling window 105 (FIG. 8B), and the speed of the vessel. Since the mutual tilting of the ultrasonic beams in the present case causes the horizontal distance d_1 between the beams to widen, the cross-correlation curve 903 (FIG. 9A) is shifted to the right when compared to the case where the beams are parallel (curve 503 in FIG. 5A). The amount of shift 908 (FIG. 9A) corresponds directly to the additional spacing $(d_1 - d_0)$ between the ultrasonic beams 103, 104 (FIG. 8B) at the depth of the sampling window 105. The

intersection 907 between the autocorrelation and cross-correlation curves is still seen in FIG. 9A to occur at $\tau/2$ (cf. intersection 507 in FIG. 5A).

[0094] FIG. 9B illustrates a difference function 905

$$F(t) = \frac{AC_1(t) + AC_2(t)}{2} - CC(t)$$

generated using the autocorrelation 901 and cross-correlation 903 curves of FIG. 9A. When compared to the difference function curve 505 of FIG. 5B, it is readily seen that the shifting of cross-correlation curve 903 (FIG. 9A) to the right (caused by tilting the ultrasonic beams away from each other as in FIG. 8B), causes a distortion evident in difference function curve 905 (FIG. 9B). Although the curve is distorted, the zero-crossing 906 still occurs at $\tau/2$, which allows the time shift τ to be determined using the same procedure as used for the case with parallel ultrasonic beams; that is, by finding t when F(t)=0, according to well-known principles of the art.

[0095] FIGS. 10A and 10B illustrate the effect on the autocorrelation and cross-correlation functions, and the resulting difference function, caused by the ultrasonic beams being tilted toward each other, as shown in FIG. 8C. Curve 1001 (FIG. 10A) represents the average of the autocorrelation functions $AC_1(t)$ and $AC_2(t)$, which when compared to curves 501 (FIG. 5A, prior art) and 901 (FIG. 9A) is again seen to be unaffected by the angle between the transducers. Curve 1003 (FIG. 10A) represents a cross-correlation function CC(t) based on signals from two transducers whose ultrasonic beams are tilted toward each other as shown in FIG. 8C. As was the case in FIGS. 5A (prior art) and 9A, the peak 1004 (FIG. 10A) of the cross-correlation occurs at a time shift τ established by the horizontal distance d_1 (FIG. 8C) between the centerlines 601, 602 of the two ultrasonic beams 103, 104 (FIG. 8C) at the depth of the sampling window 105 (FIG. 8C), and the speed of the vessel. Since the mutual tilting of the ultrasonic beams in the present case causes the horizontal distance d_1 (FIG. 8C) between the beams to become shorter,

the cross-correlation curve 1003 (FIG. 10A) is shifted to the left when compared to the case where the beams are parallel (curve 503 in FIG. 5A). The amount of shift 1008 (FIG. 10A) corresponds directly to the reduced spacing ($d_0 - d_1$) between the ultrasonic beams 103, 104 (FIG. 8C) at the depth of the sampling window 105. The intersection 1007 between the autocorrelation and cross-correlation curves is still seen in FIG. 10A to occur at $\tau/2$ (compare with intersection 507 in FIG. 5A, and intersection 907 in FIG. 9A).

[0096] FIG. 10B illustrates a difference function 1005 generated using the autocorrelation 1001 and cross-correlation 1003 curves of FIG. 10A. When compared to the difference function curve 505 of FIG. 5B, it is readily seen that the shifting of cross-correlation curve 1003 (FIG. 10A) to the left (caused by tilting the ultrasonic beams toward each other as in FIG. 8C), causes a distortion evident in difference function curve 1005 (FIG. 10B). Although the curve is distorted, the zero-crossing 1006 still occurs at $\tau/2$, which allows the time shift τ to be determined using the same procedure as used for the case with parallel ultrasonic beams; that is, by finding t when $F(t)=0$, according to well-known principles of the art.

First Embodiment

[0097] Given a correlation speed sensor having unknown tilt angles of its two transducers, it is first necessary, in accordance with the principles of a first embodiment of the present invention, to determine the angle between the ultrasonic beams, such angle denoted in this specification as θ.

[0098] FIGS. 11 and 12 are each a side elevation view of a transducer assembly showing two transducers 101, 102 mounted to a baseplate 100. In FIG. 11, transducers 101, 102 are tilted in such a manner that the ultrasonic beams 103, 104 are tilted away from each other, producing a positive θ as previously described. In FIG. 12, transducers 101, 102 are tilted in such a manner that the ultrasonic beams 103, 104 are tilted toward each other, producing a negative θ as

previously described. FIGS. 11 and 12 also depict contaminant particles 1101, 1102 (FIG. 11) and 1201, 1202 (FIG. 12) that have inadvertently become lodged between baseplate 100 and respective transducers 101, 102 during the manufacturing process, which suggests a possible reason for the tilt of the ultrasonic beams.

[0099] In accordance with the present embodiment, the spacing d_0 (FIGS. 11, 12) between the centers of the transducers' transmitting faces is a predetermined, known value. Two different sampling windows are established, the first, designated "A" (1105) at a predetermined vertical distance y_A from the transducers, and the second, designated "B" (1106) at a predetermined vertical distance y_B from the transducers. Although sampling windows A and B (1105, 1106 in FIGS. 11 and 12) are similar to the already described sampling windows 105, 106 (FIGS. 1, 6, and 7), they are used for a distinctly different purpose in the context of the present embodiment. In particular, sampling windows A and B are established expressly for the purpose of determining the value of θ. Once θ is known, any unknown horizontal distance d_j (as exemplified by distances d_1, d_2 in FIGS. 6 and 7) between the two ultrasonic beams 103, 104 at any predetermined vertical distance from the transducers may be calculated using the simple application of trigonometry.

[0100] The selection of vertical distances y_A, y_B (FIGS. 11, 12) will be influenced by a number of factors. First, it is desirable that y_A and y_B be spaced as far apart from each other as reasonably possible (i.e. maximize $y_B - y_A$), in order to produce sufficient mathematical precision in the calculation of θ. Second, the shallower sampling window A (1105) should not be so shallow that it occurs within the boundary layer (not shown). This is in order to avoid the detection of eddies and currents near the hull that are not representative of the flow of water below the boundary layer. Third, the deeper sampling window B (1106) should not be so deep that it occurs beyond the near field range of the transducers, where spreading of the ultrasonic beams introduces nonlinear effects that are undesirable in a correlation speed sensor application.

[0101] FIGS. 13A and 13B depict a flowchart that describes a process for determining the value of θ for a given instance of a correlation speed sensor according to the principles of the present embodiment. The steps of this process are preferably performed by a software program executing within the microcontroller (200, FIG. 2), with the exception of the first step 1302 which might be performed by a human or by automated test equipment. Alternatively, some or all of the process might be performed by, for example, software executing within a secondary computer during a production test operation, or by other electronic means such as discrete digital electronics. In the following description, reference will be made to the microcontroller 200 executing the process, although it will be understood that the process might in fact be implemented using other means.

[0102] The process of FIGS. 13A and 13B requires operating the correlation speed sensor in the same or similar environment as would be encountered during normal operation of the sensor. That is, the sensor will preferably be either already installed in the vessel in which it will be ultimately operating, or temporarily installed in a test fixture that simulates the eventual operating environment. In particular, conditions that are necessary during execution of this process are: the sensor should be immersed in a fluid medium that provides sonar targets such as suspended particles within sampling windows A and B (1105, 1106 in FIGS. 11 and 12), such sonar targets moving within the ultrasonic beams 103, 104 of transducers 101, 102 along axis of motion 114. According to the principles of the present embodiment, the speed of flow of the particles past the transducers may vary during the course of the process of determining the value of θ; that is, the process of FIGS. 13A-13B does not depend on accurately controlling or knowing the speed of movement of the sensor or of the fluid medium relative to the sensor, except that the range of speeds that occur during this process must be within the normal operating range of the correlation speed sensor. Therefore, it is established that during execution of the process of determining the value of θ as described in the flowchart of FIGS. 13A and 13B, the sensor will already be installed and operating in an environment as so described.

[0103] Referring to FIG. 13A, in step 1302 the predetermined horizontal distance d_0 (FIGS. 11, 12) between the transducers is measured and recorded. In practice, the measurement and recording of d_0 would most likely be performed only once for a given design configuration of a correlation speed sensor, and the value controlled by quality control methods such as statistical process control during the manufacturing process. Alternatively, the measurement and recording of d_0 might be performed as a production step on every unit manufactured, in order to more accurately account for variations in this distance from one unit to the next. The recording of this value would preferably be into non-volatile memory that is accessible to the microcontroller or computer that is performing the remaining steps of the flowchart.

[0104] The determination of the value of θ according to the present embodiment depends on the sampling of echoes from random flowing particles detected by the two transducers in the sensor. Because the number and magnitude of the detected echoes will vary according to the density of particles within the fluid medium, the quality of the resultant value of θ will depend on collecting enough echoes from flowing particles to achieve a statistically favorable result. As such, this is an iterative process that collects and processes data until enough accuracy has been achieved to terminate the iterative loop. Within each iteration, a value θ_{NEW} is determined, which represents the angle between the beams determined based on a set of sample data collected during the iteration. A counter variable K tracks the number of iterations performed during the process. An accumulator variable SUM is maintained which contains the cumulative sum of all of the values of θ_{NEW} over the course of the iterations.

[0105] In step 1304, the values of SUM and K are both initialized to zero, prior to entering the iterative loop.

[0106] Step 1306 invokes a subroutine, "Collect Samples in Two Sampling Windows," which is described on the flowchart depicted in FIG. 14. The execution of this subroutine is ordinarily performed by the microcontroller 200 (FIG. 2).

[0107] Referring to FIG. 14, in step 1402 of the flowchart, a ping counter i is initialized to zero.

[0108] In step 1404, the transducers (101, 102, FIGS. 11, 12, and 201, 202, FIG. 2) are simultaneously energized for a brief interval (for example, 6 cycles at 4.5 MHz, having a total duration of about 1.33 microseconds) to transmit a ping of ultrasonic energy into the fluid medium.

[0109] In step 1406, a time delay occurs while the microcontroller 200 (FIG. 2) waits for the propagation of the ultrasonic energy to traverse vertically through the water from the transducers 101, 102 (FIGS. 11, 12) to the first sampling window (sampling window A, 1105, FIGS. 11, 12) and, assuming one or more echoes occurred from suspended particles within sampling window A, back to the transducers again. The duration of the time delay depends on the predetermined distance y_A from the transducers 101, 102 to sampling window A, and the speed of sound in the fluid medium.

[0110] In step 1408, the microcontroller triggers both A to D converters 206 (FIG. 2) to perform a conversion, thereby sampling the signals from both transducers simultaneously in sampling window A (1105, FIGS. 11, 12). The sample from the first transducer 101 is stored into array variable $S_{1A}[i]$, and the sample from the second transducer 102 is stored into array variable $S_{2A}[i]$. Alternatively, a sequence of a few A to D conversions, such as four for example, can be made consecutively by both A to D converters, and the few respective sample values for each channel summed before storing into array variables $S_{1A}[i]$ and $S_{2A}[i]$. This alternative approach has several benefits: first, this method, commonly known as oversampling, yields more bits of precision, and an improved signal-to-noise ratio. Second, each conversion within the group of consecutive samples is triggered at a slightly different time, which means that the group of samples within the sampling window spans a vertical section of the fluid medium rather than only a single point within the sampling window that a single sample would occupy. Spanning a

vertical section enables more particle targets to be detected as they cross through the ultrasonic beams. Third, some particles in the flow might travel slightly upwards or downwards during the course of their flight between the fore and aft transducer beams. Sampling a vertical span in both beams increases the likelihood that such particles will be detected by both fore and aft transducer beams within the given sampling window, thereby contributing to the cross-correlation.

[0111] In step 1410, a second time delay occurs while the microcontroller waits for the propagation of ultrasonic energy to continue beyond the first sampling window A (1105), to the second sampling window B (1106, FIGS. 11, 12), and, assuming one or more echoes occurred from suspended particles within sampling window B, back to the transducers again. The duration of this second time delay depends on the distance $y_B - y_A$ from sampling window A to sampling window B, as well as the speed of sound in the fluid medium.

[0112] In step 1412, the microcontroller again triggers both A to D converters to perform a conversion, thereby sampling the signals from both transducers simultaneously in sampling window B. The sample from the first transducer 101 is stored in array variable $S_{1B}[i]$, and the sample from the second transducer 102 is stored in array variable $S_{2B}[i]$. As was explained in the description of step 1408, a sequence of a few A to D conversions can be made consecutively by both A to D converters, and the few respective sample values for each channel summed before storing into array variables $S_{1B}[i]$ and $S_{2B}[i]$.

[0113] In step 1414, the ping counter i is incremented by 1.

[0114] In step 1416, a test is performed to determine if the ping counter i has reached a predetermined maximum number of pings N. The value of N in a given system will depend on a number of factors, such as the amount of memory available to store the arrays S_{1A}, S_{2A}, S_{1B}, and S_{2B}, the amount of accuracy desired in the result, and/or the amount of time the end-user might be willing to wait to receive a result. A typical value for N might be, for example, 2850, which

is approximately the number of pings that can occur within a half second when the deeper sampling window B is 5 inches away from the transducers, and the fluid medium is water.

[0115] If the result of the test of step 1416 is "No," meaning that the predetermined maximum number of pings N has not yet been achieved, then the program execution loops back to step 1404, where the process of sample collection continues with the generation of a next ultrasonic ping.

[0116] If the result of the test of step 1416 is "Yes," then samples corresponding to all N pings have been taken and the subroutine described in the flowchart of FIG. 14 has now completed.

[0117] Having completed the subroutine "Collect Samples in Two Sampling Windows," a set of four arrays containing N samples each has been assembled, the four arrays being:

- S_{1A} (samples from the first transducer 101 in sampling window A),
- S_{2A} (samples from the second transducer 102 in sampling window A),
- S_{1B} (samples from the first transducer 101 in sampling window B), and
- S_{2B} (samples from the second transducer 102 in sampling window B),

all four arrays having been collected during the same interval of time.

[0118] Returning to FIG. 13, the program flow continues at step 1308, where autocorrelation and cross-correlation functions are generated using the samples acquired (S_{1A}, S_{2A}) from the first sampling window A at distance y_A from the transducers 101, 102. The functions are generated according to the following relations:

$$AC_{1A}(t) = \sum_{i=0}^{N-1} S_{1A}[i] \times S_{1A}[i+t]$$

$$AC_{2A}(t) = \sum_{i=0}^{N-1} S_{2A}[i] \times S_{2A}[i+t]$$

$$CC_{A}(t) = \sum_{i=0}^{N-1} S_{1A}[i] \times S_{2A}[i+t]$$

[0119] In step 1310, a difference function $F_A(t)$ is generated according to the relation

$$F_A(t) = \frac{AC_{1A}(t) + AC_{2A}(t)}{2} - CC_A(t)$$

and a time shift τ_A is determined by finding t when $F_A(t) = 0$, according to well-known principles of the art.

[0120] In step 1312, the time shift τ_A is tested to determine whether its value falls between predetermined minimum and maximum limits τ_{MIN} and τ_{MAX}. The τ_{MIN} limit is to ensure that the fluid was flowing no faster than a predetermined maximum speed relative to the sensor while the sample data was being collected. At faster speeds, the slopes of the autocorrelation and cross-correlation curves (501, 503 in FIG. 5A, prior art) become steeper, causing the determination of the zero crossing 506 (FIG. 5B, prior art) to be subject to decreased resolution, the resolution being proportional to 1/speed. This decrease in resolution leads to greater uncertainty with respect to the accuracy of the time shift τ_A.

[0121] The τ_{MAX} limit is to ensure that the fluid was flowing no slower than a predetermined minimum speed relative to the sensor while the sample data was being collected. At very slow speeds, e.g. approaching zero, the flow of particles will exhibit more randomness and will not behave in such a way as to produce a good statistical foundation on which to determine an

accurate time shift. Therefore, to achieve a more accurate value for θ, appropriate values should be selected for limits τ_{MIN} and τ_{MAX}.

[0122] If the result of the test of step 1312 is "No," meaning that the flow of fluid relative to the sensor was either too slow or too fast while the sample data was being collected, then the sample data collected during the present iteration is discarded, and the program execution loops back to step 1306, where the collection of sample data is repeated.

[0123] If the result of the test of step 1312 is "Yes," meaning that the speed of flow of fluid relative to the sensor was within appropriate bounds for the satisfactory determination of an angle, then program execution proceeds with step 1314.

[0124] In step 1314, autocorrelation and cross-correlation functions are generated using the samples acquired (S_{1B}, S_{2B}) from the second sampling window B at distance y_B from the transducers 101, 102. The functions are generated according to the following relations:

$$AC_{1B}(t) = \sum_{i=0}^{N-1} S_{1B}[i] \times S_{1B}[i+t]$$

$$AC_{2B}(t) = \sum_{i=0}^{N-1} S_{2B}[i] \times S_{2B}[i+t]$$

$$CC_{B}(t) = \sum_{i=0}^{N-1} S_{1B}[i] \times S_{2B}[i+t]$$

[0125] In step 1316, a difference function $F_B(t)$ is generated according to the relation

$$F_B(t) = \frac{AC_{1B}(t) + AC_{2B}(t)}{2} - CC_B(t)$$

and a time shift τ_B is determined by finding t when $F_B(t) = 0$, according to well-known principles of the art.

[0126] In step 1318, the time shift τ_B is tested to determine whether its value falls between predetermined minimum and maximum limits τ_{MIN} and τ_{MAX}, according to the same considerations as were described above regarding the test of step 1312.

[0127] If the result of the test of step 1318 is "No," meaning that the flow of fluid relative to the sensor was either too slow or too fast while the sample data was being collected, then the sample data collected during the present iteration is discarded, and the program execution loops back to step 1306, where the collection of sample data is repeated.

[0128] If the result of the test of step 1318 is "Yes," meaning that the flow of fluid relative to the sensor was within appropriate bounds for the satisfactory determination of an angle, then program execution proceeds with step 1320.

[0129] In step 1320 (FIG. 13B), the value of $y_B\tau_A - y_A\tau_B$ is calculated and tested to determine whether it is equal to zero. This is to prevent a potential divide-by-zero error from occurring in the subsequent step 1322. If the result of the test is "Yes," meaning that the expression does equal zero, then the subsequent steps in the flowchart are not executed, and program execution loops back to step 1306, where the collection of sample data is repeated.

[0130] If the result of the test of step 1320 is "No," meaning that the result of the expression is nonzero, then program execution proceeds with step 1322.

[0131] In step 1322, a value is calculated for θ_{NEW}, according to the relation

$$\theta_{NEW} = \tan^{-1}\left(\frac{d_0(\tau_B - \tau_A)}{y_B\tau_A - y_A\tau_B}\right)$$

[0132] It is instructive at this point to briefly digress to note that the above calculation for θ_{NEW} depends only on the known predetermined dimensions d_0, y_A, and y_B, and on the two time shifts τ_A and τ_B determined based on sample data acquired within the present iteration of the present process. In particular, an advantage of the present embodiment is that the calculation for θ_{NEW} depends neither on controlling nor knowing the speed of the flow of the fluid relative to the sensor. The process of determining the value of θ can therefore be conducted, for example, by the correlation speed sensor automatically while underway during the first few minutes after installation in a vessel, with no required user interaction.

[0133] Continuing with the flowchart of FIG. 13B, in step 1324, a limit test is performed on the value of θ_{NEW} to ensure its value falls within a reasonable expected range of values. For example, a limit θ_{MAX} might be established at 5 degrees, thereby allowing θ_{NEW} to fall within a range of ±5 degrees.

[0134] If the result of the test of step 1324 is "No," meaning θ_{NEW} falls outside the allowable range of values, then the value is discarded and program execution loops back to step 1306 (FIG. 13A), where the collection of sample data is repeated.

[0135] If the result of the test of step 1324 is "Yes," meaning θ_{NEW} falls within the allowable range of values, then program execution proceeds with step 1326.

[0136] In step 1326, the value of SUM is increased by the present value of θ_{NEW}.

[0137] In step 1328, the iteration counter K is incremented by 1.

[0138] In step 1330, a running average angle between the ultrasonic beams θ_{AVG} is computed by dividing the sum of all θ_{NEW} values by the total number of iterations performed thus far.

[0139] In step 1332, the iteration counter K is compared against a predetermined maximum value K_{MAX}. The value for K_{MAX} should be selected to ensure that enough iterations will occur to allow the calculation of θ_{AVG} to achieve sufficient accuracy. Other methods to ensure accuracy of θ_{AVG} could be employed, such as additionally monitoring the magnitudes and/or standard deviations of the sampled signals over the course of collecting samples, to allow the estimating of particle density to ensure that enough statistical sample data was acquired to make a more informed judgment as to the accuracy of θ_{AVG}.

[0140] If the result of the test of step 1332 is "No," meaning not enough iterations have occurred yet, then program execution loops back to step 1306 (FIG. 13A), where a next iteration is begun.

[0141] If the result of the test of step 1332 is "Yes," meaning that K_{MAX} iterations have occurred, then program execution proceeds with step 1334.

[0142] In step 1334, the final value of θ_{AVG} is stored in variable θ, which now represents the angle between the ultrasonic beams as previously defined. This completes the description of the process of determining the value of θ, in accordance with the present embodiment. The process so described thus constitutes a means for determining an angle between two ultrasonic beams.

[0143] Having determined the value of the angle θ between the ultrasonic beams, the speed of flow of a fluid relative to the sensor may now be determined, in accordance with the principles of the present embodiment of the invention.

[0144] FIG. 15 is a side elevation view of a transducer assembly having tilted ultrasonic beams and a single sampling window 105 at a predetermined distance y_1 from the transducers.

[0145] FIG. 16 depicts a flowchart, "Determine Speed Using One Sampling Window," that describes a process for determining the speed of flow of a fluid relative to a correlation speed sensor according to the principles of the present embodiment. The steps of this process are preferably performed by a software program executing within the microcontroller (200, FIG. 2), but as stated previously, in a given implementation might be executed by other means.

[0146] Referring to FIG. 16 in conjunction with FIG. 15, in step 1602 of the flowchart of FIG. 16, a ping counter i is initialized to zero.

[0147] In step 1604, the transducers (101, 102, FIG. 15) are simultaneously energized for a brief interval (for example, 6 cycles at 4.5 MHz, having a total duration of about 1.33 microseconds) to transmit a ping of ultrasonic energy into the fluid medium.

[0148] In step 1606, a time delay occurs while the microcontroller 200 (FIG. 2) waits for the propagation of the ultrasonic energy to traverse vertically through the water from the transducers 101, 102 to sampling window 105 and, assuming one or more echoes occurred from suspended particles within the sampling window, back to the transducers again. The duration of the time delay depends on the distance y_1 from the transducers 101, 102 to sampling window 105, and the speed of sound in the fluid medium.

[0149] In step 1608, the microcontroller triggers both A to D converters 206 (FIG. 2) to perform a conversion, thereby sampling the signals from both transducers simultaneously in sampling window 105. The sample from the first transducer 101 is stored into array variable $S_1[i]$, and the sample from the second transducer 102 is stored into array variable $S_2[i]$.

[0150] In step 1610, the ping counter i is incremented by 1.

[0151] In step 1612, a test is performed to determine if the ping counter i has reached a predetermined maximum number of pings N. A typical value for N might be, for example, 2850 pings.

[0152] If the result of the test of step 1612 is "No," meaning that the predetermined maximum number of pings N has not yet been achieved, then the program execution loops back to step 1604, where the process of sample collection proceeds with the generation of a next ultrasonic ping.

[0153] If the result of the test of step 1612 is "Yes," then samples corresponding to all N pings have been taken, and program execution proceeds to step 1614.

[0154] In step 1614, autocorrelation and cross-correlation functions are generated using the sample arrays (S_1, S_2) acquired during the execution of steps 1604 to 1612. The functions are generated according to the following relations:

$$AC_1(t) = \sum_{i=0}^{N-1} S_1[i] \times S_1[i+t]$$

$$AC_2(t) = \sum_{i=0}^{N-1} S_2[i] \times S_2[i+t]$$

$$CC(t) = \sum_{i=0}^{N-1} S_1[i] \times S_2[i+t]$$

[0155] In step 1616, a difference function F(t) is generated according to the relation

$$F(t) = \frac{AC_1(t) + AC_2(t)}{2} - CC(t)$$

and a time shift τ is determined by finding t when F(t) = 0, according to well-known principles of the art.

[0156] In step 1618, the distance d_1 (FIG. 15) is calculated according to the relation

$$d_1 = d_0 + y_1 \tan\theta$$

using the predetermined dimensions d_0 and y_1, and the angle θ that was determined earlier using the process described in the flowchart of FIGS. 13A and 13B. This distance d_1 represents the horizontal distance between the ultrasonic beams 103, 104 at the vertical distance y_1 between the transducers and the sampling window 105.

[0157] In step 1620, the speed is calculated according to the relation

$$\text{speed} = \frac{d_1}{\tau}$$

using the distance d_1 that was calculated in step 1618, and the time shift τ that was determined in step 1616.

[0158] This completes the description of the process of determining the speed of flow of a fluid relative to a correlation speed sensor, using a single sampling window, in accordance with the first embodiment.

[0159] It is noted that the processes of determining the value of θ, and determining the speed of flow of the fluid, may occur concurrently in a given application, wherein sample data acquired within sampling windows A and B used for the determining of θ is also used in the determining of the speed. For example, on each startup of the correlation speed sensor after applying power, θ can be initially assumed to be zero. As the sensor begins collecting sample data, the speed is determined using an assumed value of zero for θ. The same sample data used to determine the speed is then used to determine a new value for θ. Over the course of iterating the determination of both speed and θ from the same sets of sample data, the accuracy of the speed reading will gradually improve since the value of θ will be improving. This method would constitute an automatic self-calibration of the sensor that is performed during normal operation.

[0160] I have thus shown a novel method for more accurately determining a distance d_1 between the centers of the two non-parallel ultrasonic beams, at an arbitrary vertical distance y_1 from the transmitting surfaces of the transducers, and thereby also more accurately determining the speed of flow of a fluid relative to the sensor. This has been shown to be achieved without change to the physical configuration of the transducers, baseplate, or other mechanical aspects of a correlation speed sensor as employed in the prior art. The determining of the angle θ between the ultrasonic beams, and the distance d_1 between the beams at the depth y_1 of the sampling window, may be performed with the sensor in situ, with no need for a separate calibration step or interaction with the user. Sensors manufactured with varying degrees of tilt of their transducer elements may thereby be brought into general agreement with one another with regard to their reported speed values under equivalent operating conditions.

[0161] Other embodiments of the invention will now be described. Each of the remaining described embodiments is similar to the first embodiment, but with certain details changed. As such, the remaining embodiments will be described more briefly, noting only the differences from the first embodiment.

Second Embodiment

[0162] A second embodiment is similar to the first embodiment, but employs a modified method for determining the angle θ between the ultrasonic beams.

[0163] FIGS. 17A and 17B depict a flowchart that describes a process for determining the value of θ for a given instance of a correlation speed sensor according to the principles of the second embodiment. The process as described in the flowchart of FIGS. 17A and 17B replaces the process of FIGS. 13A and 13B that was presented in the description of the first embodiment. The steps of this process are preferably performed by a software program executing within the microcontroller (200, FIG. 2), but as stated previously, in a given implementation might be executed by other means.

[0164] In the present embodiment, the process of determining the value of the angle θ between the beams must occur with the correlation speed sensor operating in a controlled environment. In particular, the sensor should be immersed in a fluid medium that provides sonar targets such as suspended particles traveling at a controlled and known speed v within a single sampling window A (1105 in FIGS. 11 and 12). For example, a test apparatus can be constructed that provides such an environment. It is noted that sampling window B (1106 in FIGS. 11 and 12) is not used in the present embodiment.
According to the principles of the present embodiment, the speed of flow v of the particles past the transducers must be known, and must not vary during the course of the process of determining the value of θ. Therefore, it is established that during execution of the process of

determining the value of θ as described in the flowchart of FIGS. 17A and 17B, the sensor will already be installed and operating in an environment as so described.

[0165] Referring to FIG. 17A, in step 1702 the predetermined horizontal distance d_0 between the transducers is measured and recorded with the same considerations as described for step 1302 of FIG. 13A.

[0166] Step 1704 initializes the values of accumulator variable SUM, and counter variable K, both to zero, prior to entering an iterative loop.

[0167] Step 1706 invokes a subroutine, "Collect Samples in a Single Sampling Window," which is described on the flowchart depicted in FIG. 18.

[0168] Referring to FIG. 18, in step 1802 of the flowchart, a ping counter i is initialized to zero.

[0169] In step 1804, the transducers (101, 102, FIGS. 11, 12, and 201, 202, FIG. 2) are simultaneously energized for a brief interval to transmit a ping of ultrasonic energy into the fluid medium.

[0170] In step 1806, a time delay occurs while the microcontroller 200 (FIG. 2) waits for the propagation of the ultrasonic energy to traverse vertically through the water from the transducers 101, 102 (FIGS. 11, 12) to the sampling window (sampling window A, 1105, FIGS. 11, 12) and, assuming one or more echoes occurred from suspended particles within sampling window A, back to the transducers again. The duration of the time delay depends on the distance y_A from the transducers 101, 102 to sampling window A, and the speed of sound in the fluid medium.

[0171] In step 1808, the microcontroller triggers both A to D converters 206 (FIG. 2) to perform a conversion, thereby sampling the signals from both transducers simultaneously in

sampling window A (1105). The sample from the first transducer 101 is stored into array variable $S_{1A}[i]$, and the sample from the second transducer 102 is stored into array variable $S_{2A}[i]$. As was explained in the description of step 1408 in FIG. 14, a sequence of a few A to D conversions, such as four for example, can alternatively be made consecutively by both A to D converters, and the few respective sample values for each channel summed before storing into array variables $S_{1A}[i]$ and $S_{2A}[i]$.

[0172] In step 1814, the ping counter i is incremented by 1.

[0173] In step 1816, a test is performed to determine if the ping counter i has reached a predetermined maximum number of samples N. The considerations in determining an appropriate value for N are the same as were described for step 1416 of FIG. 14.

[0174] If the result of the test of step 1816 is "No," meaning that the predetermined maximum number of pings N has not yet been achieved, then the program execution loops back to step 1804, where the process of sample collection continues with the generation of a next ultrasonic ping.

[0175] If the result of the test of step 1816 is "Yes," then samples corresponding to all N pings have been taken and the subroutine described in the flowchart of FIG. 18 has now completed.

[0176] Having now completed the subroutine "Collect Samples in a Single Sampling Window," a set of two arrays containing N samples each has been assembled, the two arrays being:

- S_{1A} (samples from the first transducer 101 in sampling window A),
- S_{2A} (samples from the second transducer 102 in sampling window A),

both arrays having been collected during the same interval of time.

[0177] Returning to FIG. 17, the program flow continues at step 1708, where autocorrelation and cross-correlation functions are generated using the samples acquired (S_{1A}, S_{2A}) from sampling window A at distance y_A from the transducers 101, 102. The functions are generated according to the following relations:

$$AC_{1A}(t) = \sum_{i=0}^{N-1} S_{1A}[i] \times S_{1A}[i+t]$$

$$AC_{2A}(t) = \sum_{i=0}^{N-1} S_{2A}[i] \times S_{2A}[i+t]$$

$$CC_{A}(t) = \sum_{i=0}^{N-1} S_{1A}[i] \times S_{2A}[i+t]$$

[0178] In step 1710, a difference function $F_A(t)$ is generated according to the relation

$$F_A(t) = \frac{AC_{1A}(t) + AC_{2A}(t)}{2} - CC_A(t)$$

and a time shift τ_A is determined by finding t when $F_A(t) = 0$, according to well-known principles of the art.

[0179] In step 1712, the time shift τ_A is tested to determine whether its value falls between predetermined minimum and maximum limits τ_{MIN} and τ_{MAX}, according to the same considerations as were described regarding the test of step 1312 in the flowchart of FIG. 13A.

[0180] If the result of the test of step 1712 is "No," meaning that the flow of fluid relative to the sensor was either too slow or too fast while the sample data was being collected, then the sample data collected during the present iteration is discarded, and the program execution loops back to step 1706, where the collection of sample data is repeated.

[0181] If the result of the test of step 1712 is "Yes," meaning that the speed of flow of fluid relative to the sensor was within appropriate bounds for the satisfactory determination of an angle, then program execution proceeds with step 1714 in FIG. 17B.

[0182] Referring to FIG. 17B, in step 1714, a value is calculated for θ_{NEW}, according to the relation

$$\theta_{NEW} = \tan^{-1}\left(\frac{v\tau_A - d_0}{y_A}\right)$$

where v represents the known speed of flow of the fluid relative to the correlation speed sensor as provided in the controlled environment; d_0 and y_A are known predetermined dimensions as shown in FIGS. 11 and 12; and τ_A is the time shift determined in step 1710.

[0183] In step 1716, a limit test is performed on the value of θ_{NEW} to ensure its value falls within a reasonable expected range of values. For example, a limit θ_{MAX} might be established at 5 degrees, thereby allowing θ_{NEW} to fall within a range of ±5 degrees.

[0184] If the result of the test of step 1716 is "No," meaning θ_{NEW} falls outside the allowable range of values, then the value is discarded and program execution loops back to step 1706 (FIG. 17A), where the collection of sample data is repeated.

[0185] If the result of the test of step 1716 is "Yes," meaning θ_{NEW} falls within the allowable range of values, then program execution proceeds with step 1718.

[0186] In step 1718, the value of SUM is increased by the present value of θ_{NEW}.

[0187] In step 1720, the iteration counter K is incremented by 1.

[0188] In step 1722, a running average angle between the ultrasonic beams θ_{AVG} is computed by dividing the sum of all θ_{NEW} values by the total number of iterations performed thus far.

[0189] In step 1724, the iteration counter K is compared against a maximum value K_{MAX}. The value for K_{MAX} should be selected to ensure that enough iterations will occur to allow the calculation of θ_{AVG} to achieve sufficient accuracy. If the result of the test of step 1724 is "No," meaning not enough iterations have occurred yet, then program execution loops back to step 1706 (FIG. 17A), where a next iteration is begun.

[0190] If the result of the test of step 1724 is "Yes," meaning that K_{MAX} iterations have occurred, then program execution proceeds with step 1726.

[0191] In step 1726, the final value of θ_{AVG} is stored in variable θ, which now represents the angle between the ultrasonic beams as previously defined. This completes the description of the process of determining the value of θ, in accordance with the second embodiment. The process so described thus constitutes a means for determining an angle between two ultrasonic beams.

[0192] It is noted that the process of determining the value of θ in accordance with the second embodiment presents both advantages and disadvantages when compared with the process of determining the value of θ in accordance with the first embodiment. In particular, an advantage of the second embodiment is that only two arrays, S_{1A} and S_{2A} need to be populated, whereas the

first embodiment requires the four arrays, S_{1A}, S_{2A}, S_{1B}, and S_{2B}. This advantage can be significant if a correlation speed sensor has a limited memory resource for storing the array data when performing the process for determining the value of θ. On the other hand, an obvious disadvantage to the second embodiment is that a controlled environment must be provided having a known speed of flow of the fluid in which the sensor must be immersed.

Third Embodiment

[0193] A third embodiment is similar to the first and second embodiments, but in this case the method for determining the angle θ between the ultrasonic beams begins with the assumption that the distance d_0 between the transmitting surfaces of the transducers is unknown. The third embodiment would be applicable in a situation where manufacturing deviations affect not only the tilt angle of the ultrasonic beams, but potentially the spacing between the transducer elements, as well. Therefore, in the third embodiment, the process of determining the value of θ includes additional steps required to determine the value of d_0.

[0194] FIGS. 19A, 19B, and 19C depict a flowchart that describes a process for determining the values of θ and d_0 for a given instance of a correlation speed sensor according to the principles of the present embodiment. The process as described in the flowchart of FIGS. 19A-19C replaces the process of FIGS. 13A-13B that was presented in the description of the first embodiment. The steps of this process are preferably performed by a software program executing within the microcontroller (200, FIG. 2), but as stated previously, in a given implementation might be executed by other means.

[0195] The process of FIGS. 19A-19C, according to the principles of the present embodiment, must occur with the correlation speed sensor operating in a controlled environment. In particular, the sensor should be immersed in a fluid medium that provides sonar targets such as suspended particles traveling at a controlled and known speed v within two sampling windows A

and B (1105, 1106 in FIGS. 11 and 12). For example, a test apparatus can be constructed that provides such an environment. According to the principles of the present embodiment, the speed of flow v of the particles past the transducers must be known, and must not vary during the course of execution of the process of Figs 19A-19C. Therefore, it is established that during execution of the process of determining the values of θ and d_0 as described in the flowchart of FIGS. 19A-19C, the sensor will already be installed and operating in an environment as so described.

[0196] Referring to FIG. 19A, step 1902 initializes the values of angle accumulator variable ASUM, distance accumulator variable DSUM, and counter variable K, all to zero, prior to entering an iterative loop.

[0197] Step 1904 invokes the subroutine, "Collect Samples in Two Sampling Windows," which was described earlier in conjunction with the flowchart of FIG. 14. The subroutine will not be described again here, except to remind the reader that upon return from the subroutine, a set of four arrays containing N samples each will have been assembled, the four arrays being:

- S_{1A} (samples from the first transducer 101 in sampling window A),
- S_{2A} (samples from the second transducer 102 in sampling window A),
- S_{1B} (samples from the first transducer 101 in sampling window B), and
- S_{2B} (samples from the second transducer 102 in sampling window B),

all four arrays having been collected during the same interval of time.

[0198] Steps 1906 through 1916 are identical to steps 1308 to 1318 of the flowchart of FIG. 13A; in summary, these steps lead to the establishment of the two time shifts τ_A and τ_B, and will not otherwise be described here.

[0199] Referring to FIG. 19B, in step 1918, a value is calculated for θ_{NEW}, according to the relation

$$\theta_{NEW} = \tan^{-1}\left(v\left(\frac{\tau_B - \tau_A}{y_B - y_A}\right)\right)$$

where v represents the known speed of flow of the fluid relative to the correlation speed sensor as provided in the controlled environment; y_A and y_B are known predetermined dimensions as shown in FIGS. 11 and 12; and τ_A and τ_B are the time shifts determined in steps 1908 and 1914, respectively.

[0200] In step 1920, a limit test is performed on the value of θ_{NEW} to ensure its value falls within a reasonable expected range of values. For example, a limit θ_{MAX} might be established at 5 degrees, thereby allowing θ_{NEW} to fall within a range of ±5 degrees.

[0201] If the result of the test of step 1920 is "No," meaning θ_{NEW} falls outside the allowable range of values, then the value is discarded and program execution loops back to step 1904 (FIG. 19A), where the collection of sample data is repeated.

[0202] If the result of the test of step 1920 is "Yes," meaning θ_{NEW} falls within the allowable range of values, then program execution proceeds with step 1922.

[0203] In step 1922, a value is calculated for d_{0NEW}, according to the relation

$$d_{0NEW} = \frac{v(\tau_A + \tau_B) - (y_A + y_B)\tan\theta_{NEW}}{2}$$

[0204] In step 1924, a limit test is performed on the value of d_{0NEW} to ensure its value falls within a reasonable expected range of values. For example, assuming a nominal design value of

0.44 inch spacing between the transducer elements, d_{MAX} might be established at 0.5 inches, and d_{MIN} might be established at 0.41 inches.

[0205] If the result of the test of step 1924 is "No," meaning d_{0NEW} falls outside the allowable range of values, then the value is discarded and program execution loops back to step 1904 (FIG. 19A), where the collection of sample data is repeated.

[0206] If the result of the test of step 1924 is "Yes," meaning d_{0NEW} falls within the allowable range of values, then program execution proceeds with step 1926 in FIG. 19C.

[0207] Referring to FIG. 19C, in step 1926, the value of the angular accumulator variable ASUM is increased by the present value of θ_{NEW}.

[0208] In step 1928, the value of the distance accumulator variable DSUM is increased by the present value of d_{0NEW}.

[0209] In step 1930, the iteration counter K is incremented by 1.

[0210] In step 1932, a running average angle between the ultrasonic beams θ_{AVG} is computed by dividing the sum of all accumulated θ_{NEW} values thus far by the total number of iterations performed thus far.

[0211] In step 1934, a running average distance between the transducers d_{0AVG} is computed by dividing the sum of all accumulated d_{0NEW} values thus far by the total number of iterations performed thus far.

[0212] In step 1936, the iteration counter K is compared against a maximum value K_{MAX}. The value for K_{MAX} should be selected to ensure that enough iterations will occur to allow the

calculations of θ_{AVG} and d_{0AVG} to achieve sufficient accuracy. If the result of the test of step 1936 is "No," meaning not enough iterations have occurred yet, then program execution loops back to step 1904 (FIG. 19A), where a next iteration is begun.

[0213] If the result of the test of step 1936 is "Yes," meaning that K_{MAX} iterations have occurred, then program execution proceeds with step 1938.

[0214] In step 1938, the final values of θ_{AVG} and d_{0AVG} are stored in variables θ and d_0, respectively. This completes the description of the process of determining the values of θ and d_0, in accordance with the third embodiment. The process so described thus constitutes a means for determining an angle between two ultrasonic beams, and a means for determining a distance between two transducers.

[0215] It is noted that the process of determining the values of θ and d_0 in accordance with the third embodiment presents both advantages and disadvantages when compared with the process of determining the value of θ in accordance with the first embodiment. In particular, an advantage of the third embodiment is that the dimension d_0 does not need to be carefully controlled in manufacturing, since the value will be determined during the same procedure that determines the value of θ. On the other hand, an obvious disadvantage of the third embodiment is that a controlled environment must be provided having a known speed of flow of the fluid in which the sensor must be immersed.

[0216] At this point, it is recommended that the reader keep FIG. 20 available for frequent reference during the descriptions of the fourth and fifth embodiments.

Fourth Embodiment

[0217] A fourth embodiment is similar to the first embodiment, but employs a modified method for determining the speed that uses a plurality of sampling windows.

[0218] FIG. 20 is a side elevation view of a transducer assembly having tilted ultrasonic beams and three sampling windows 2005, 2006, 2007 at respective predetermined distances y_1, y_2, y_3 from transducers 101, 102, and having respective unknown distances d_1, d_2, d_3 between ultrasonic beams 103, 104 within the respective sampling windows 2005, 2006, 2007. In the context of the present embodiment, the sampling windows 2005, 2006, 2007 in FIG. 20 are to be regarded as exemplifying any number of sampling windows in a given application. In the description that follows, the sampling windows shall be numbered from 1 to a total number of sampling windows M. The j^{th} sampling window shall be assigned a predetermined vertical distance y_j from the transducers. The unknown horizontal distance between the ultrasonic beams 103, 104 at the depth of the j^{th} sampling window shall be denoted d_j. Therefore, in FIG. 20, sampling windows 2005, 2006, 2007 represent a first, second, and third sampling window, respectively, out of a total of M sampling windows. In the fourth embodiment, M may have any value greater than zero, although if M is 1, the method reduces to that of the first embodiment.

[0219] FIGS. 21A and 21B depict a flowchart, "Determine Speed Using M Sampling Windows," that describes a process for determining the speed of flow of a fluid relative to a correlation speed sensor according to the principles of the present embodiment. The process as described in the flowchart of FIGS. 21A-21B replaces the process of FIG. 16 of the first embodiment. The steps of this process are preferably performed by a software program executing within the microcontroller (200, FIG. 2), but as stated previously, in a given implementation might be executed by other means.

[0220] Referring to FIG. 21A in conjunction with FIG. 20, in step 2102 of the flowchart of FIG. 21A, an accumulator variable SUM is initialized to zero.

[0221] In step 2104, a ping counter variable i is initialized to zero.

[0222] In step 2106, a sampling window index variable j is initialized to 1.

[0223] In step 2108, the transducers (101, 102, FIG. 20) are simultaneously energized for a brief interval to transmit a ping of ultrasonic energy into the fluid medium.

[0224] For the purpose of explaining step 2110, a value $y_0 = 0$ shall hereby be defined that represents the vertical position within the ultrasonic beams 103, 104 corresponding to the transmitting surfaces of transducers 101, 102.

[0225] In step 2110, a time delay DELAY(j) occurs while the microcontroller 200 (FIG. 2) waits for the propagation of the ultrasonic energy to traverse vertically through the water from the point y_{j-1} to the j^{th} sampling window at distance y_j from the transducers, and, assuming one or more echoes occurred from suspended particles within the j^{th} sampling window, back to point y_{j-1}. The duration of the time delay depends on the distance $y_j - y_{j-1}$, and the speed of sound in the fluid medium.

[0226] In step 2112, the microcontroller 200 (FIG. 2) triggers both A to D converters 206 (FIG. 2) to perform a conversion, thereby sampling the signals from both transducers simultaneously in the j^{th} sampling window. The sample from the first transducer 101 is stored into array variable $S_1[j, i]$, and the sample from the second transducer 102 is stored into array variable $S_2[j, i]$.

[0227] In step 2114, the sampling window index j is incremented by 1.

[0228] In step 2116, a test is performed to determine if the sampling window index variable j has exceeded the total number of sampling windows M.

[0229] If the result of the test of step 2116 is "No," meaning that the sampling window index variable j has not yet exceeded the total number of sampling windows M, then the program execution loops back to step 2110, where another delay is initiated while the ultrasonic energy proceeds to the next sampling window.

[0230] If the result of the test of step 2116 is "Yes," then all M sampling windows have been sampled in conjunction with the most recent ultrasonic ping, and program execution proceeds to step 2118.

[0231] In step 2118, the ping counter i is incremented by 1.

[0232] In step 2120, a test is performed to determine if the ping counter i has reached a predetermined maximum number of pings N. A typical value for N might be, for example, 2850 samples.

[0233] If the result of the test of step 2120 is "No," meaning that the predetermined maximum number of pings N has not yet been achieved, then the program execution loops back to step 2106, where the process of sample collection proceeds with the re-initialization of sampling window index variable j, and the generation of a next ultrasonic ping (step 2108).

[0234] If the result of the test of step 2120 is "Yes," then samples corresponding to all N pings have been taken, and program execution proceeds to step 2122 in FIG. 21B.

[0235] Referring to FIG. 21B, in steps 2122 through 2136, the sample data acquired during the previous steps 2104 through 2120 is processed, for each sampling window in succession.

[0236] In step 2122, the sampling window index j is re-initialized to 1.

[0237] In step 2124, autocorrelation and cross-correlation functions for the j^{th} sampling window are generated using the samples acquired (S_1, S_2) during the execution of steps 2104 to 2120. The functions are generated according to the following relations:

$$AC_{1j}(t) = \sum_{i=0}^{N-1} S_1[j,i] \times S_1[j,i+t]$$

$$AC_{2j}(t) = \sum_{i=0}^{N-1} S_2[j,i] \times S_2[j,i+t]$$

$$CC_j(t) = \sum_{i=0}^{N-1} S_1[j,i] \times S_2[j,i+t]$$

[0238] In step 2126, a difference function $F_j(t)$ is generated according to the relation

$$F_j(t) = \frac{AC_{1j}(t) + AC_{2j}(t)}{2} - CC_j(t)$$

and a time shift τ_j is determined by finding t when $F_j(t) = 0$, according to well-known principles of the art.

[0239] In step 2128, the unknown distance d_j is calculated according to the relation

$$d_j = d_0 + y_j \tan\theta$$

using the predetermined dimensions d_0 and y_j, and the angle θ that was determined using the process described in the flowchart of FIGS. 13A and 13B of the first embodiment. This distance

d_j represents the horizontal distance between the ultrasonic beams within the j^{th} sampling window, as exemplified in FIG. 20 by distances d_1, d_2, and d_3 within sampling windows 1, 2, and 3.

[0240] In step 2130 (FIG. 21B), the value d_j / τ_j is calculated, which represents the speed determined using only the samples collected within the j^{th} sampling window. This value is added to accumulator variable SUM.

[0241] In step 2132, the sampling window index j is incremented by 1.

[0242] In step 2134, a test is performed to determine if the sampling window index variable j has exceeded the total number of sampling windows M.

[0243] If the result of the test of step 2134 is "No," meaning that the sampling window index variable j has not yet exceeded the total number of sampling windows M, then the program execution loops back to step 2124, where processing of the sample data continues with the generation of autocorrelation and cross-correlation functions for the next sampling window.

[0244] If the result of the test of step 2134 is "Yes," then the sample data for all M sampling windows has been processed, and program execution proceeds to step 2136.

[0245] In step 2136, a final speed is calculated by taking the average of the speeds accumulated for all sampling windows, i.e. speed = SUM / M.

[0246] This completes the description of the process of determining the speed of flow of a fluid relative to a correlation speed sensor, using a plurality of sampling windows, in accordance with the fourth embodiment.

[0247] It will be instructive to briefly examine the correlation functions generated within the above process. FIG. 22A depicts a graph showing autocorrelation and cross-correlation functions generated according to the process of FIGS. 21A-21B, and corresponding to the correlation speed sensor configuration depicted in FIG. 20. Curves 2202, 2203, and 2204 represent the cross-correlation functions $CC_1(t)$, $CC_2(t)$, and $CC_3(t)$, respectively, corresponding to signals received from reflective particles traversing through sampling windows 1, 2, and 3 (FIG. 20), respectively. Note that the cross-correlation curves 2202, 2203, 2204 are shifted to the right from their ideal position (cf. curve 503 in prior art FIG. 5A) by different amounts. This is as a result of the varying distances d_1, d_2, d_3 (FIG. 20) between the ultrasonic beams 103, 104. The varying amounts of shift of the cross-correlation curves therefore causes the resulting respective time shifts τ_1, τ_2, τ_3 to differ accordingly. Curve 2201 (FIG. 22A) represents the autocorrelation curves for all three sampling windows. A single curve is drawn because the autocorrelation functions for all sampling windows are theoretically identical.

[0248] FIG. 22B depicts a graph showing the difference functions derived from the autocorrelation and cross-correlation curves of FIG. 22A. Curves 2205, 2206, and 2207 represent the difference functions $F_1(t)$, $F_2(t)$, and $F_3(t)$, respectively, generated in step 2126 of the flowchart of FIG. 21B. Zero-crossings 2208, 2209, and 2210 correspond to the three different time shifts τ_1, τ_2, and τ_3, respectively. Although the time shifts are different for each sampling window as a result of the tilted ultrasonic beams, it is possible to derive the correct speed from each sampling window by associating each time shift with its corresponding distance d_1, d_2, d_3 determined in step 2128 (FIG. 21B).

[0249] It is noted that the process of determining the speed of flow of a fluid in accordance with the fourth embodiment presents both advantages and disadvantages when compared with the corresponding process in accordance with the first embodiment. In particular, an advantage of the fourth embodiment is that a plurality of sampling windows at a range of depths is used, whereas the first embodiment employed only a single sampling window. This is advantageous

because, in general, the overall signal-to-noise ratio of the system is improved upon the detection of an increased number of echoes from reflective particles. Noting that reflective particles appear within the ultrasonic beams at random, the use of multiple sampling windows provides more data with which to determine speed, which can result in improved accuracy when compared with an application that employs only a single sampling window. On the other hand, a significant disadvantage to the fourth embodiment is that enough memory must be available to store the sample arrays for all sampling windows.

Fifth Embodiment

[0250] A fifth embodiment is similar to the fourth embodiment, in that the speed is determined based on samples collected from one or more sampling windows, but the fifth embodiment holds the advantage of requiring less memory to store the sample arrays. To summarize the difference between the approaches of the fourth and fifth embodiments, in the fourth embodiment a separate difference function $F_j(t)$ is generated for each sampling window j, whereas in the fifth embodiment a single composite difference function F(t) is generated that combines rate-converted sample data from all sampling windows.

[0251] In accordance with the principles of the fifth embodiment, a sample rate conversion algorithm is applied to the samples as they are received, thus resampling the data "on the fly," which has the intended effect of compressing or expanding the discrete signal waveforms in the time domain. The question as to whether the discrete waveforms are to be compressed or expanded depends on whether the ultrasonic beams are tilted apart, or toward each other, respectively. The purpose of employing sample rate conversion is to adjust the discrete signal waveforms for each sampling window so that the autocorrelation and cross-correlation functions will yield a difference function having a zero crossing in the same position it would have held if the ultrasonic beams were parallel in the first place. The amount of compression or expansion to apply to sample data acquired in a j^{th} sampling window depends on the angle θ between the

ultrasonic beams, and the vertical distance y_j from the transducers to the sampling window. The time shift τ derived from the difference function F(t) will correspond with the actual distance d_0 between the transducer elements.

[0252] Referring again to FIG. 20, the sampling windows 2005, 2006, 2007 in the context of the fifth embodiment are to be regarded as exemplifying any number of sampling windows in a given application. In the description that follows, the sampling windows shall be numbered from 1 to a total number of sampling windows M. The j^{th} sampling window shall be assigned a predetermined vertical distance y_j from the transducers. Therefore, in FIG. 20, sampling windows 2005, 2006, 2007 represent a first, second, and third sampling window, respectively, out of a total of M sampling windows. In the present embodiment, M may have any value greater than zero.

[0253] FIG. 23 depicts a flowchart, "Determine Speed Using M Sampling Windows," that describes a process for determining the speed of flow of a fluid relative to a correlation speed sensor according to the principles of the present embodiment. The process as described in the flowchart of FIG. 23 replaces the process of FIG. 16 of the first embodiment. The steps of this process are preferably performed by a software program executing within the microcontroller (200, FIG. 2), but as stated previously, in a given implementation might be executed by other means.

[0254] Referring to FIG. 23, in step 2302 of the flowchart, a subroutine, "Collect Samples, Performing Sample Rate Conversion and Time Compression/Expansion" is invoked.

[0255] FIG. 24 is a block diagram illustrating the general functionality of the subroutine referred to in step 2302 of the flowchart of FIG. 23. It is recommended that the reader keep FIG. 24 (as well as FIG. 20) available for frequent reference during the remaining description of the fifth embodiment.

[0256] Summarizing the subroutine of FIG. 24, block 2402 represents a Sample Collection process wherein samples from the fore and aft transducers (101, 102, respectively, in FIG. 20) are collected in M sampling windows. The Sample Collection process 2402 is depicted in FIG. 24 as collecting samples from three exemplary sampling windows, numbered 1, 2, and 3, corresponding to the sampling windows 2005, 2006, and 2007, respectively, in FIG. 20. Therefore, in the example scenario of Figs. 20 and 24, M=3. The stream of fore and aft samples 2404 (FIG. 24) from the three sampling windows of the Sample Collection process 2402 are fed into the input FIFOs 2408 of three respective Sample Rate Conversion processes 2406. The outputs 2410 of the Sample Rate Conversion processes 2406 are rate-converted sample streams that are fed into the output FIFOs 2412. The Combine Samples process 2416 synchronously removes the rate-converted samples 2414 from the three FIFOs 2412, and combines them into a single fore/aft sample stream 2418 that is then stored in memory buffer 2420. It is therefore seen that the subroutine of FIG. 24 is composed of several processes executing simultaneously to produce a single set of samples that is derived from multiple sampling windows. The processes of FIG. 24 will now be described in detail.

[0257] FIGS. 25A and 25B depict a flowchart, "Sample Collection," that describes the process of the Sample Collection block 2402 of FIG. 24.

[0258] Referring to FIG. 25A, in step 2502, a time increment variable t_{INC} is initialized to a value of 1 / ping rate. That is, t_{INC} contains a value corresponding to the amount of time between consecutive pings of the transducers. t_{INC} may be represented in any convenient units of time having sufficient resolution; for example if 2850 samples are collected in ½ second, then a suggested unit of time for t_{INC} would be nanoseconds (nS). The ping rate is also the rate at which samples are acquired from the A to D converters; therefore t_{INC} also refers to the amount of time between consecutive samples within a given sampling window. The ping rate shall also be referred to in this description as the raw sample rate.

[0259] In step 2504, a time variable t is initialized to zero. Variable t will be used to keep track of total elapsed time, for the purpose of time-stamping samples. t should have the same units as t_{INC}.

[0260] In step 2506, a ping counter variable i is initialized to zero.

[0261] In step 2508, a sample window index variable j is initialized to 1.

[0262] In step 2510, the transducers (101, 102, FIG. 20) are simultaneously energized for a brief interval to transmit a ping of ultrasonic energy into the fluid medium.

[0263] In step 2512, a time delay DELAY(j) occurs while the microcontroller 200 (FIG. 2) waits for the propagation of the ultrasonic energy to traverse vertically through the water from the point y_{j-1} to the j^{th} sampling window at distance y_j from the transducers, and, assuming one or more echoes occurred from suspended particles within the j^{th} sampling window, back to point y_{j-1}. The duration of the time delay depends on the distance $y_j - y_{j-1}$, and the speed of sound in the fluid medium. As was the case in the fourth embodiment, the value y_0 shall be understood as having a value of zero.

[0264] In step 2514, the microcontroller triggers both A to D converters 206 (FIG. 2) to perform a conversion, thereby sampling the signals from both transducers simultaneously in the j^{th} sampling window. A sample object variable S_{RAW} is instantiated, containing the sample S_1 from the first transducer 101 (FIG. 20), the sample S_2 from the second transducer 102, and a time stamp member variable t into which the current contents of the elapsed time variable t are copied.

[0265] Referring to FIG. 25A in conjunction with FIG. 24, in step 2516, the sample object variable S_{RAW} is added to the input FIFO (first-in, first-out buffer) 2408 (FIG. 24) of the Sample Rate Conversion (SRC) process block 2406 (FIG. 24) corresponding to the j^{th} sampling window.

[0266] In step 2518 of FIG. 25A, the sampling window index j is incremented by 1.

[0267] In step 2520, a test is performed to determine if the sampling window index variable j has exceeded the total number of sampling windows M.

[0268] If the result of the test of step 2520 is "No," meaning that the sampling window index variable j has not yet exceeded the total number of sampling windows M, then the program execution loops back to step 2512, where another delay is initiated while the ultrasonic energy proceeds to the next sampling window.

[0269] If the result of the test of step 2520 is "Yes," then all M sampling windows have been sampled in conjunction with the most recent ultrasonic ping, and program execution proceeds to step 2522 in FIG. 25B.

[0270] Referring to FIG. 25B, in step 2522 the elapsed time variable t is incremented by the value of the time increment variable t_{INC}.

[0271] In step 2524, the ping counter i is incremented by 1.

[0272] In step 2526, a test is performed to determine if the ping counter i has reached a predetermined maximum number of pings N. A typical value for N might be, for example, 2850 samples.

[0273] If the result of the test of step 2526 is "No," meaning that the predetermined maximum number of pings N has not yet been achieved, then the program execution loops back to step 2508, where the process of sample collection proceeds with the re-initialization of the sampling window index j to 1, followed by the generation of a next ultrasonic ping.

[0274] If the result of the test of step 2526 is "Yes," then samples corresponding to all N pings have been taken, and the Sample Collection process of FIGS. 25A-25B is now complete.

[0275] Returning to FIG. 24, it is seen that the Sample Collection process 2402 provides a stream of samples 2404 to the input FIFO 2408 of each of the Sample Rate Conversion processes 2406. There is established one Sample Rate Conversion process 2406 for each of the M sampling windows, as exemplified by the three Sample Rate Conversion process blocks 2406 shown in FIG. 24.

[0276] The Sample Rate Conversion process 2406 of FIG. 24 is described in detail in the flowchart of FIGS. 26A and 26B.

[0277] Referring to FIG. 26A, in step 2602, a time increment variable t_{INC} is initialized to a value of 1 / ping rate. This is the same value as was defined in step 2502 of FIG. 25A, but is re-declared here since the value is also used in the context of the present process. In the present process, t_{INC} is understood to be the rate at which the raw samples are received in the input FIFO 2408 (FIG. 24).

[0278] In step 2604, a second time increment variable t_{RCINCj} is initialized according to the relation

$$t_{RCINCj} = t_{INC} \times \frac{d_0}{d_0 + y_j \tan\theta}$$

where t_{INC} is the raw sample rate defined in step 2602, d_0 is the known horizontal distance between the transducer elements as shown in FIG. 20, y_j is the predetermined vertical distance from the transmitting surfaces of the transducers to the j^{th} sampling window as exemplified by y_1, y_2, and y_3 in FIG. 20, and θ is the angle between the ultrasonic beams 103, 104 that was determined using the process described in the flowchart of FIGS. 13A and 13B of the first embodiment. It is seen that each running Sample Rate Conversion process 2406 (FIG. 24) corresponding to each unique sampling window j will have a corresponding unique value for t_{RCINCj}. t_{RCINCj} represents the time between consecutive output samples produced within the context of the present Sample Rate Conversion process.

[0279] In step 2606, a value t_{RCj} is initialized to zero. t_{RCj} represents the anticipated time at which a next output sample, within the context of the present Sample Rate Conversion process, will occur.

[0280] In step 2608, a raw sample object is retrieved from input FIFO 2408 (FIG. 24) and is assigned to a variable named S_{IN}. The purpose of S_{IN} is to contain the most recently acquired input sample.

[0281] In step 2610, a new output sample object S_{OUT} is instantiated, and the sample data S_1, S_2 from the input sample S_{IN} are copied into S_{OUT}. It is noted that unlike the raw input samples retrieved from the input FIFO, the output samples are not time-stamped.

[0282] In step 2612, the sample object S_{OUT} is added to the output FIFO 2412 (FIG. 24) corresponding to the j^{th} sampling window. The sample object S_{OUT} thus added to the output FIFO represents a first sample in a stream of output samples.

[0283] In step 2614, the value t_{RCj} is incremented by the value of the time increment variable t_{RCINCj}.

[0284] Referring to FIG. 26B, in step 2616 the input FIFO 2408 (FIG. 24), and the Sample Collection process 2402 (FIG. 24), are both queried to determine if any more raw samples are (or will be) available in the input FIFO.

[0285] If the result of the query of step 2616 is "No," meaning all raw samples have already been processed, then the Sample Rate Conversion process is now completed.

[0286] If the result of the query of step 2616 is "Yes," meaning that another raw sample is (or will be) available in the input FIFO 2408, then execution proceeds to step 2618.

[0287] In step 2618, the contents of the most recently acquired input sample S_{IN} are assigned to a sample object variable S_{PREV}. While as already stated, S_{IN} represents the most recently acquired input sample; S_{PREV} represents the previously acquired input sample. The assignment thus declares that the contents of S_{IN} are no longer considered to be the most recently acquired sample, and are now considered to be the previously acquired input sample. As a consequence of the assignment of step 2618, the former contents of S_{PREV} are discarded.

[0288] In step 2620, a next raw sample object is retrieved from input FIFO 2408 (FIG. 24) and is assigned to variable S_{IN}, discarding the previous contents of S_{IN}. If the input FIFO is empty upon entering step 2620, then the Sample Rate Conversion process will wait for a next raw sample object to be added to the FIFO by the Sample Collection process.

[0289] In step 2622, the time stamp member variable t of the most recently acquired input sample S_{IN} is compared with the contents of t_{RCj}. If the comparison determines that the time

stamp of the sample (i.e. $S_{IN}.t$) occurred earlier than t_{RCj}, then program execution loops back to step 2616 in order to retrieve a next sample from the input FIFO.

[0290] If the comparison of step 2622 determines that the time stamp of the sample occurred at the same time as, or later than, t_{RCj}, then program execution proceeds with step 2624.

[0291] In step 2624, a new output sample object S_{OUT} is instantiated, and the values of its member variables S_1, S_2 are synthesized using the data from the input samples S_{IN} and S_{PREV}. The method of synthesis is to interpolate the magnitude of each output sample from its two nearest enclosing consecutive input samples S_{IN} and S_{PREV}. The formulas for interpolation of the fore and aft output samples, respectively, are

$$S_{OUT}.S_1 = \frac{(S_{IN}.S_1 \times (t_{RCj} - S_{PREV}.t)) + ((S_{PREV}.S_1 \times (S_{IN}.t - t_{RCj}))}{t_{INC}}$$

and

$$S_{OUT}.S_2 = \frac{(S_{IN}.S_2 \times (t_{RCj} - S_{PREV}.t)) + ((S_{PREV}.S_2 \times (S_{IN}.t - t_{RCj}))}{t_{INC}}$$

[0292] In step 2626, the sample object S_{OUT} is added to the output FIFO 2412 (FIG. 24) corresponding to the j^{th} sampling window.

[0293] In step 2628, the value t_{RCj} is incremented by the value of the time increment variable t_{RCINCj}. Process execution then loops back to step 2622, where $S_{IN}.t$ is compared with the new value of t_{RCj} to determine whether to create a new output sample falling between the present S_{IN} and S_{PREV} input samples, or to check for a new sample in the input FIFO.

[0294] The Sample Rate Conversion process thus described continues until, in step 2616, it is determined that there are no further input samples to be processed, at which time the process is completed.

[0295] Summarizing the block diagram of FIG. 24 described thus far, it is seen that a Sample Collection process 2402 provides streams of raw samples 2404 from a fore and an aft transducer, collected in M sampling windows, to the input FIFOs 2408 of M Sample Rate Conversion processes 2406, where M=3 in the example of FIG. 24. Each of the M Sample Rate Conversion processes 2406 in turn provides a stream of rate-converted samples 2410 to a corresponding output FIFO 2412.

[0296] Referring again to FIG. 20, on the left side of the figure are shown three particles 2008, 2009, 2010 suspended in the water in a hypothetical configuration, each particle aligned one directly above the next, and each positioned so as to be detected by respective sampling windows 2005, 2006, 2007 as the transducers 101, 102 pass over the particles. This hypothetical scenario is presented in order to illustrate the resultant behavior of the processes of FIG. 24.

[0297] In accordance with the present embodiment, FIG. 28A is a plot of raw samples collected over time from two transducers 101, 102 (FIG. 20) in a total of three sampling windows 2005, 2006, 2007 (FIG. 20), corresponding to the hypothetical scenario of FIG. 20 in which three reflective particles 2008, 2009, 2010 simultaneously pass through the three sampling windows. FIG. 28A should be studied in conjunction with FIG. 20. The horizontal axis of FIG. 28A represents time, and the vertical axis represents relative signal amplitude. Discrete signal waveforms 2801, 2802 are sampled from the fore and aft transducers, respectively, in the first sampling window 2005 (FIG. 20); waveforms 2803, 2804 are sampled from the fore and aft transducers, respectively, in the second sampling window 2006 (FIG. 20); and waveforms 2805, 2806 are sampled from the fore and aft transducers, respectively, in the third sampling window 2007 (FIG. 20).

[0298] Referring to FIG. 28A, in region 2808 of discrete signal waveforms 2801, 2802, the first particle 2008 (FIG. 20) approaches the first ultrasonic beam 103 (FIG. 20) from the fore transducer 101 (FIG. 20). Because the particle has not yet reached the beam, it is not detected. In region 2810 (FIG. 28A), the particle 2008 (FIG. 20) has crossed into the first ultrasonic beam 103 and is now detected by the fore transducer 101 for a total of 20 consecutive samples as the particle traverses through the beam. The detection of particle 2008 is evidenced by the increased amplitude of the signal within region 2810 (FIG. 28A). In region 2812, the particle has exited the first ultrasonic beam 103, and, because the ultrasonic beams 103, 104 as shown in FIG. 20 are tilted apart from one another, the particle 2008 goes undetected by either transducer for several samples as it approaches the second ultrasonic beam 104. In region 2814 (FIG. 28A), the particle 2008 has crossed into the second ultrasonic beam 104 and is now detected by the aft transducer 102 for a total of 20 consecutive samples. In region 2816, the particle has exited the second beam and is now moving away from the sensor.

[0299] On further inspection of FIG. 28A, it is seen that while the first particle 2008 (FIG. 20) was traversing through the first sampling window 2005 (FIG. 20), resulting in the discrete signal waveforms 2801, 2802; the second and third particles 2009, 2010 (FIG. 20) were at the same time traversing through the respective second and third sampling windows 2006, 2007 (FIG. 20), resulting in the discrete signal waveforms 2803-2806. Since each ping of the transducers results in raw samples being created for both transducers in all sampling windows, it is seen in FIG. 28A that the raw sample rates for all sampling windows are the same; that is, the time t_{INC} between consecutive raw samples is the same for all sampling windows. As was seen in the flowchart of FIG. 25A, this time is equal to 1 / ping rate.

[0300] Because the ultrasonic beams 103, 104 in FIG. 20 are tilted relative to each other, the horizontal distances d_1, d_2, and d_3 between the ultrasonic beams in the three sampling windows are all different. Therefore, the discrete signal waveforms shown in FIG. 28A corresponding to

the three sampling windows indicate the detection of their corresponding respective particles at different times. For example, on inspection of waveform 2805, corresponding to the fore transducer in the third sampling window, it is seen that the region in which its corresponding particle is detected starts on an earlier sample than the corresponding regions for the fore transducer in the first and second sampling windows. This is to be expected, since, as shown in FIG. 20, particle 2010 will encounter the ultrasonic beam 103 before either of particles 2008 or 2009.

[0301] FIG. 28A has been drawn in such a way that the vertical spacing between the discrete signal waveforms of the three sampling windows is proportional to the actual distances between the sampling windows ($y_3 - y_2$) and ($y_2 - y_1$). Lines 2818 and 2820 are drawn through the centers of the regions in which the particles were detected, to illustrate how the tilted ultrasonic beams affect the discrete signal waveforms 2801-2806.

[0302] Referring to FIG. 24, it is noted that the discrete signal waveforms of FIG. 28A are a depiction of the raw sample streams 2404 provided by the Sample Collection process 2402 to the input FIFOs 2408 of the Sample Rate Conversion processes 2406.

[0303] Continuing with the hypothetical scenario of FIG. 20, it is seen that FIG. 28B is a plot of rate-converted samples generated over time by the Sample Rate Conversion processes 2406 of FIG. 24. The rate-converted discrete sample waveforms 2821-2826 (FIG. 28B) are a depiction of the sample streams 2410 (FIG. 24) provided by the Sample Rate Conversion processes 2406 (FIG. 24) to the output FIFOs 2412 (FIG. 24). The time axis of FIG. 28B is drawn to the same scale as the time axis of FIG. 28A. Sample waveforms 2821, 2822 represent the rate-converted samples for the fore and aft channels, respectively, in the first sampling window 2005 (FIG. 20); waveforms 2823, 2824 represent the rate-converted samples for the fore and aft channels, respectively, in the second sampling window 2006 (FIG. 20); and waveforms 2825, 2826

represent the rate-converted samples for the fore and aft channels, respectively, in the third sampling window 2007 (FIG. 20).

[0304] It is noted in FIG. 28B that the sample rates are different for the three sampling windows; that is, the time increments between consecutive rate-converted samples in the first, second, and third sampling windows are t_{RCINC1}, t_{RCINC2}, and t_{RCINC3}, respectively. Close inspection of the waveforms of FIG. 28B will reveal that, for example, the spacing in the horizontal time axis between consecutive samples in sampling window 3 is wider than the spacing between samples in sampling windows 1 and 2. Therefore, in a given span of time, fewer rate-converted samples are produced for sampling window 3 than for either of sampling windows 1 or 2.

[0305] It is further noted when comparing the sample waveforms in FIG. 28A against the corresponding waveforms in FIG. 28B that the individual rate-converted samples of FIG. 28B are shown as being spaced further apart on the horizontal time axis than the raw samples of FIG. 28A. This is because in the example being presented, the ultrasonic beams are tilted apart from each other. If the ultrasonic beams were tilted toward one another, then the formula for t_{RCINCj} as presented in step 2604 of FIG. 26A would cause the rate-converted samples to occur more frequently than the raw samples.

[0306] It is readily seen on comparison of FIGS. 28A and 28B that the overall shapes of the discrete waveforms remain largely intact after having performed the Sample Rate Conversion process. For example, consider lines 2828, 2830 in FIG. 28B, in comparison with lines 2818, 2820 in FIG. 28A. Both sets of lines have been drawn through the centers of the regions in which the particles were detected for all sampling windows; and it is seen that the positions and mutual angles between the lines are unchanged after performing the Sample Rate Conversion process.

[0307] Returning to the block diagram of FIG. 24, and considering the differing sample rates for the rate-converted sample waveforms illustrated in FIG. 28B, it is noted that the Sample Rate Conversion processes 2406 add samples to the output FIFOs 2412 at different rates for different sampling windows. In contrast, although samples are added to FIFOs 2412 at different times and at different rates, the FIFOs are emptied in unison, at a rate equivalent to the original raw sample rate t_{INC}. This is illustrated in FIG. 28C, which is a plot of rate-converted samples 2414 (FIG. 24) as they are removed from the FIFOs 2412 (FIG. 24), prior to being combined in the Combine Samples process 2416 (FIG. 24). The time axis of FIG. 28C is drawn to the same scale as the time axes of FIGS. 28A and 28B.

[0308] The sample waveforms 2841-2846 of FIG. 28C are a depiction of the sample streams 2414 (FIG. 24) as they exit the FIFOs 2412 (FIG. 24). Because the samples are removed from the FIFOs at a different rate than the rates at which they were added, this results in the corresponding discrete waveforms being either compressed or expanded in time, in comparison to their original forms when added to the FIFOs. Rate-converted samples that have been compressed or expanded in time shall be collectively referred to in the following description as having been time-stretched.

[0309] Referring to FIG. 28C in conjunction with FIG. 20, waveforms 2841, 2842 represent time-stretched samples for the fore and aft channels, respectively, in the first sampling window 2005 (FIG. 20); waveforms 2843, 2844 represent the time-stretched samples for the fore and aft channels, respectively, in the second sampling window 2006 (FIG. 20); and waveforms 2845, 2846 represent the time-stretched samples for the fore and aft channels, respectively, in the third sampling window 2007 (FIG. 20).

[0310] The time-stretching of the samples can be better understood by comparing FIG. 28B, which depicts the sample streams 2410 (FIG. 24) as they enter the FIFOs 2412 (FIG. 24), with FIG. 28C, which depicts the sample streams 2414 (FIG. 24) as they exit the FIFOs 2412. It is

noted that the number of samples in each discrete waveform of FIG. 28C is the same as the number of samples in the corresponding discrete waveform of FIG. 28B. Likewise, the ordering of the samples, and the amplitudes of the samples, remain unchanged between the two figures. For example, the sequence of samples in the discrete waveform 2841 of FIG. 28C is identical to the sequence of samples shown in the discrete waveform 2821 of FIG. 28B; both waveforms representing samples corresponding to the fore channel in the first sampling window. The data set, therefore, is unchanged between the two figures. The only difference between FIGS. 28B and 28C is that the positions of the samples on the time axis have been adjusted in FIG. 28C so as to synchronize all M sample streams to the common sample rate t_{INC}.

[0311] Performing sample rate conversion, followed by time stretching, consequently re-aligns the discrete sample waveforms so that the signals in each sampling window from the aft transducer lag behind the signals in the corresponding sampling window in the fore transducer, by an amount of time equivalent to the expected time shift if the ultrasonic beams had been parallel in the first place. This effect can be seen by comparing lines 2848, 2850 in FIG. 28C, with lines 2828, 2830 in FIG. 28B. Both sets of lines have been drawn through the centers of the regions in which the particles were detected for all sampling windows. In FIG. 28B, the lines 2828 and 2830 are not parallel because, simply stated, the ultrasonic beams (103, 104, FIG. 20) in this example are not parallel. But in FIG. 28C, lines 2848 and 2850 are seen to be parallel, because the discrete sample waveforms have been adjusted by the processes of sample rate conversion and time stretching for the very purpose of parallelization. It is additionally noted in FIG. 28C that the distance 2852 on the time axis between lines 2848 and 2850 represents the time shift that would be expected between the raw fore and aft signals if the ultrasonic beams had been parallel in the first place.

[0312] It is noted that the example presented herein, based on the premise that the ultrasonic beams 103, 104 (FIG. 20) are tilted apart, results in a smaller total number of time-stretched, rate-converted samples in a given period of time than the number of raw samples originally

collected in the Sample Collection process 2402 (FIG. 24). This may be easily seen by comparing FIG. 28C with FIG. 28A, which both use the same time reference t_{INC}. The number of samples in FIG. 28C, representing the results of the time-stretching process, is clearly smaller than the number of samples of FIG. 28A, which represents the original raw sample data. If, however, the ultrasonic beams 103, 104 (FIG. 20) are tilted toward each other, then the formula for t_{RCINCj} as presented in step 2604 of FIG. 26A would cause the Sample Rate Conversion processes 2406 (FIG. 24) to produce a larger total number of rate-converted samples in a given period of time than the number of raw samples originally collected in the Sample Collection process 2402 (FIG. 24).

[0313] It will be instructive at this point to digress briefly and consider the effect of sample rate conversion and time stretching on the autocorrelation and cross-correlation functions. Although in the present embodiment the autocorrelations and cross-correlations are not computed based solely on the samples acquired within an individual sampling window (as they were in the fourth embodiment), one can consider what the functions would look like if they in fact were. Referring once again to FIG. 22A, we recall that curves 2202, 2203, and 2204 represent cross-correlation functions corresponding to raw samples from sampling windows 1, 2, and 3, respectively. In the context of the present example in the present embodiment, cross-correlation curve 2202 corresponds to the discrete raw sample waveforms 2801, 2802 in FIG. 28A; cross-correlation curve 2203 corresponds to waveforms 2803, 2804 in FIG. 28A; and cross-correlation curve 2204 corresponds to waveforms 2805, 2806 in FIG. 28A. As noted previously, the cross-correlation curves of FIG. 22 are shifted to the right from their ideal position (cf. curve 503 in FIG. 5A) by differing amounts as a result of the increased distances d_1, d_2, d_3 between the ultrasonic beams 103, 104 (FIG. 20).

[0314] FIG. 29A depicts a graph showing theoretical curves that would be produced if autocorrelation and cross-correlation functions were calculated using the time-stretched sample waveforms of FIG. 28C. Once again, within the present embodiment these individual functions

are not actually calculated, but the curves are presented for instructional purposes. Curves 2901, 2904 are the autocorrelation and cross-correlation, respectively, corresponding to the time-stretched sample waveforms 2841, 2842 (FIG. 28C); curves 2902, 2905 are the autocorrelation and cross-correlation, respectively, corresponding to waveforms 2843, 2844; and curves 2903, 2906 are the autocorrelation and cross-correlation, respectively, corresponding to waveforms 2845, 2846. Comparing FIG. 22A with FIG. 29A, it is seen that the processes of sample rate conversion and time stretching serve to bring the peaks of the cross-correlation curves into alignment with one another, which is the desired result. As a side-effect, the overall shapes of the autocorrelation and cross-correlation curves are also time-stretched, causing the individual curves in FIG. 29A to vary in width. Comparing FIG. 29A with the ideal case presented in FIG. 5A, both figures having been drawn to the same scale, it is seen that the time shift τ in FIG. 29A has been brought into agreement with the τ of FIG. 5A corresponding to parallel ultrasonic beams, as a consequence of the processes of sample rate conversion and time stretching.

[0315] Returning to the block diagram of FIG. 24, it is seen that all sample streams 2414 are combined in the Combine Samples process block 2416 to produce a single, combined sample stream 2418. The process of combining the samples is described in detail in the flowchart of FIG. 27.

[0316] Referring to FIG. 27, in step 2702, a sample counter i_{OUT} is initialized to zero.

[0317] In step 2704, a sample object is retrieved from each of the M FIFOs 2412 (FIG. 24); the sample object from the FIFO corresponding to the j^{th} sampling window being denoted S_j. Since the previously-described Sample Rate Conversion process 2406 (FIG. 24) results in each FIFO 2412 being filled with a different number of rate-converted sample objects for the different sampling windows within a given time frame, it is necessary to reconcile this difference. The method of reconciliation differs depending on whether the ultrasonic beams 103, 104 (FIG. 20) are tilted apart or tilted toward each other. If the ultrasonic beams are tilted apart, as shown in

FIG. 20, then the FIFO corresponding to the shallowest sampling window (2005 in FIG. 20) will contain the largest number of sample objects, as seen in FIG. 28C where discrete sample waveforms 2841, 2842 correspond to the shallowest sampling window. In this case, the FIFOs for the remaining sampling windows are padded at the end of their corresponding streams with dummy sample objects $S_{DUMMY} = \{S_1=0, S_2=0\}$, to bring the total number of samples for each sampling window to be the same as the total number of samples for the shallowest sampling window. Therefore, upon retrieving sample objects in step 2704 (FIG. 27) from the M FIFOs 2412 (FIG. 24), some of the sample objects retrieved will be dummy sample objects. If, however, the ultrasonic beams are tilted toward each other, then the FIFO corresponding to the shallowest sampling window will contain the smallest number of sample objects. In this case, the sample streams for the remaining sample windows are truncated (that is, sample objects in some of the FIFOs 2412 are discarded), in order to bring the total number of samples for each sampling window to be the same as the total number of samples for the shallowest sampling window. Alternatively, if memory resources are sufficient, in the case where the ultrasonic beams are tilted toward each other it would instead be possible to employ padding with dummy sample objects as used in the case for ultrasonic beams tilted apart, except that the FIFOs 2412 corresponding to shallower sampling windows will in this case be padded to bring the total number of samples for each sampling window to be the same as the total number of samples for the deepest sampling window.

[0318] In step 2706 (FIG. 27), two values are calculated and stored in arrays S_{COMB1} and S_{COMB2} in buffer 2420 (FIG. 24), according to the following formulas:

$$S_{COMB1}[i_{OUT}] = \sum_{j=1}^{M} S_j . S_1$$

$$S_{COMB2}[i_{OUT}] = \sum_{j=1}^{M} S_j . S_2$$

[0319] The first value, $S_{COMB1}[i_{OUT}]$ is the sum of the time-compressed, rate-converted samples from the fore transducer that were retrieved in step 2704 from the FIFOs 2412 (FIG. 24) for all sampling windows. The second value, $S_{COMB2}[i_{OUT}]$ is the corresponding sum for the aft transducer.

[0320] In step 2708, the sample counter i_{OUT} is incremented by 1.

[0321] In step 2710, the FIFOs 2412 (FIG. 24), and the Sample Rate Conversion processes 2406 (FIG. 24), are queried to determine if any more samples are (or will be) available in FIFOs 2412.

[0322] If the result of the query of step 2710 is "Yes," meaning that samples are (or will be) available in FIFOs 2412, then execution loops back to step 2704, where a next set of samples is retrieved from FIFOs 2412.

[0323] If the result of the query of step 2710 is "No," meaning all samples have already been processed, then execution proceeds with step 2712.

[0324] In step 2712, a variable N_{OUT} is assigned the final value of the sample counter i_{OUT}, and the Combine Samples process is now completed. N_{OUT} therefore contains the total number of samples stored in arrays S_{COMB1} and S_{COMB2} at the completion of the Combine Samples process.

[0325] Returning to FIG. 24, the entire block diagram may thus be summarized as follows. Sample Collection process 2402 provides streams of raw samples 2404 from a fore and an aft

transducer, collected in M sampling windows, to the input FIFOs 2408 of M Sample Rate Conversion processes 2406, where M=3 in the example of FIG. 24. Each of the M Sample Rate Conversion processes 2406 in turn provides a stream of rate-converted samples 2410 to a corresponding output FIFO 2412. The Combine Samples process 2416 retrieves the samples from FIFOs 2412 synchronously and in unison at a rate equivalent to the original raw sample rate, thus causing the sample streams 2414, as they are retrieved, to be time-stretched. The Combine Samples process 2416 furthermore pads or truncates the sample streams as necessary to bring the number of samples from all sample streams in agreement, prior to combining the samples from all sampling streams into a single fore/aft sample stream 2418 that is stored in arrays in buffer 2420.

[0326] It is noted that the processes shown in FIG. 24 of Sample Collection (2402), Sample Rate Conversion (2406), and Combine Samples (2416), as described in the flowcharts of FIGS. 25A-25B, 26A-26B, and 27, respectively, all occur concurrently. While samples are being collected in the Sample Collection process 2402 and added to the FIFOs 2408, the Sample Rate Conversion 2406 and Combine Samples 2416 processes are concurrently performing their operations on the already-retrieved samples as well. As will be well understood by those skilled in the art, the subroutine of FIG. 24 may be implemented as multiple concurrent processes running within a real-time operating system (RTOS) environment, but in practice would most likely execute more efficiently if it were instead coded as a single process managing the flow of samples from Sample Collection, through Sample Rate Conversion, and finally the combining of the samples, all of these being activities that occur within a single subroutine in a single process in real time as new samples are collected.

[0327] FIG. 28D is a plot showing the results of the Combine Samples process 2416 (FIG. 24) as applied to the time-stretched samples of FIG. 28C. Discrete sample waveform 2861 (FIG. 28D) represents the summation of sample waveforms 2841, 2843, 2845 (FIG. 28C) according to the process described in the flowchart of FIG. 27, to produce the combined sample array S_{COMB1}

for the fore channel. Likewise, discrete sample waveform 2862 (FIG. 28D) represents the summation of sample waveforms 2842, 2844, 2846 (FIG. 28C), to produce the combined sample array S_{COMB2} for the aft channel. Close inspection of FIG. 28D will reveal that discrete aft sample waveform 2862 is a time-shifted replica of discrete fore sample waveform 2861. The time shift 2864 is the same as the time shift 2852 of FIG. 28C, and is what would be expected between the raw fore and aft signals if the ultrasonic beams had been parallel in the first place.

[0328] Returning to FIG. 23, it is seen that step 2302, "Collect Samples, Performing Sample Rate Conversion and Time Compression/Expansion" has now been described in detail, and execution continues with step 2304.

[0329] In step 2304, autocorrelation and cross-correlation functions are generated using the samples acquired (S_{COMB1}, S_{COMB2}) during step 2302. The functions are generated according to the following relations:

$$AC_1(t) = \sum_{i_{OUT}=0}^{N_{OUT}-1} S_{COMB1}[i_{OUT}] \times S_{COMB1}[i_{OUT} + t]$$

$$AC_2(t) = \sum_{i_{OUT}=0}^{N_{OUT}-1} S_{COMB2}[i_{OUT}] \times S_{COMB2}[i_{OUT} + t]$$

$$CC(t) = \sum_{i_{OUT}=0}^{N_{OUT}-1} S_{COMB1}[i_{OUT}] \times S_{COMB2}[i_{OUT} + t]$$

[0330] In step 2306, a difference function F(t) is generated according to the relation

$$F(t) = \frac{AC_1(t) + AC_2(t)}{2} - CC(t)$$

and a time shift τ is determined by finding t when F(t) = 0, according to well-known principles of the art.

[0331] FIG. 29B depicts a graph showing a difference function F(t) 2907 derived from the sum of the autocorrelation and cross-correlation curves of FIG. 29A, and normalized to the magnitudes of those curves. Curve 2907 represents the shape of F(t) that would be produced from samples combined according to the Combine Samples process, where ultrasonic beams 103, 104 (FIG. 20) are tilted away from each other. Zero crossing 2908 occurs at $\tau/2$.

[0332] Continuing with the flowchart of FIG. 23, in step 2308, the speed is calculated according to the relation

$$\text{speed} = \frac{d_0}{\tau}$$

using the predetermined distance d_0 between the transducer elements 101, 102 (FIG. 20) and the time shift τ that was determined in step 2306.

[0333] This completes the description of the process of determining the speed of flow of a fluid relative to a correlation speed sensor, using one or more sampling windows, in accordance with the fifth embodiment.

[0334] It is noted that the process of determining the speed of flow of a fluid in accordance with the fifth embodiment presents both advantages and disadvantages when compared with the corresponding process in accordance with the fourth embodiment. In particular, as previously

mentioned, an advantage of the fifth embodiment is that less memory is required to store the sample arrays. On the other hand, a disadvantage to the fifth embodiment is the considerable amount of additional signal processing complexity required to perform the sample rate conversion and time stretching processes.

[0335] From the foregoing and as mentioned above, it will be observed that numerous variations and modifications may be effected without departing from the spirit and scope of the novel concept of the invention. It is to be understood that no limitation with respect to the specific methods illustrated herein is intended or should be inferred, and that within the scope of the appended claims, the invention may be practiced otherwise than as specifically described.

I claim:

1. A method for determining a relative speed of a fluid with respect to a sensor, comprising:
    a. providing said sensor, including:
        i. a first ultrasonic transducer, having a first ultrasonic beam and receiving a first signal, and
        ii. a second ultrasonic transducer, having a second ultrasonic beam and receiving a second signal whose varying magnitude is similar to that of said signal of said first transducer but shifted in time,
    b. providing a first means for determining a transducer distance between said first and second ultrasonic transducers,
    c. providing a second means for determining an angle between said first and second ultrasonic beams,
    d. establishing at least one sampling window to monitor said first and second signals originating within said first and second ultrasonic beams at about a predetermined depth from said first and second ultrasonic transducers, each said at least one sampling window positioned at a different predetermined depth than all other said at least one sampling window,
    e. sampling said first and second signals within each said at least one sampling window, to create a sample set corresponding to that sampling window, and
    f. determining said relative speed of said fluid based on:
        i. said sample sets corresponding to all said at least one sampling window,
        ii. said predetermined depths corresponding to all said at least one sampling window,
        iii. said transducer distance, and
        iv. said angle,

whereby a more accurate value for said relative speed of said fluid with respect to said sensor may be determined because said transducer distance and said angle between said ultrasonic beams are accounted for in the method.

2. The method of claim 1, wherein said determining of said relative speed of said fluid comprises:
    a. for each said at least one sampling window:
        i. calculating a beam distance between said first and second ultrasonic beams, based on said transducer distance, said angle, and said predetermined depth,
        ii. generating a discrete mathematical function based on said sample set, and
        iii. determining a time shift between said first and second signals based on said discrete mathematical function, and
    b. calculating said relative speed of said fluid based on
        i. said beam distances corresponding to all said at least one sampling window, and
        ii. said time shifts corresponding to all said at least one sampling window.

3. The method of claim 2, wherein said calculating of said relative speed of said fluid comprises:
    a. for each said at least one sampling window, calculating a speed value based on said beam distance and said time shift, and
    b. computing an average of said speed values corresponding to all said at least one sampling window.

4. The method of claim 1, wherein said determining of said relative speed of said fluid comprises:

a. for each said at least one sampling window, performing sample rate conversion on said sample set to correct said sample set according to said angle, said transducer distance, and said predetermined depth, to create a rate-converted sample set,
b. generating a discrete mathematical function based on said rate-converted sample sets corresponding to all said at least one sampling window,
c. determining a time shift between said first and second signals based on said discrete mathematical function, and
d. calculating said relative speed of said fluid based on said transducer distance and said time shift.

5. The method of claim 1, wherein:
    a. said first means comprises directly measuring said transducer distance between said first and second ultrasonic transducers, and
    b. said second means comprises:
        i. establishing a first sampling window A to monitor said first and second signals originating within said first and second ultrasonic beams at about a first predetermined depth y_A from said first and second ultrasonic transducers,
        ii. establishing a second sampling window B to monitor said first and second signals originating within said first and second ultrasonic beams at about a second predetermined depth y_B from said first and second ultrasonic transducers,
        iii. sampling said first and second signals within said first sampling window A, to generate a first discrete mathematical function,
        iv. sampling said first and second signals within said second sampling window B, to generate a second discrete mathematical function,

v. determining a first time shift between said first and second signals based on said first discrete mathematical function,
vi. determining a second time shift between said first and second signals based on said second discrete mathematical function, and
vii. calculating said angle based on said first and second time shifts, said first predetermined depth y_A, said second predetermined depth y_B, and said transducer distance.

6. The method of claim 1, wherein:
   a. said first means comprises directly measuring said transducer distance between said first and second ultrasonic transducers, and
   b. said second means comprises:
      i. providing an environment in which reflective targets move at a known fixed speed through said first and second ultrasonic beams,
      ii. establishing a certain sampling window to monitor said first and second signals originating within said first and second ultrasonic beams at about a certain predetermined depth from said first and second ultrasonic transducers,
      iii. sampling said first and second signals within said certain sampling window, to generate a discrete mathematical function,
      iv. determining a time shift between said first and second signals based on said discrete mathematical function, and
      v. calculating said angle between said first and second ultrasonic beams based on said time shift, said certain predetermined depth, said transducer distance, and said known fixed speed of said reflective targets.

7. The method of claim 1, wherein said first and second means comprise:

a. providing an environment in which reflective targets move at a known fixed speed through said first and second ultrasonic beams,
b. establishing a first sampling window A to monitor said first and second signals originating within said first and second ultrasonic beams at about a first predetermined depth y_A from said first and second ultrasonic transducers,
c. establishing a second sampling window B to monitor said first and second signals originating within said first and second ultrasonic beams at about a second predetermined depth y_B from said first and second ultrasonic transducers,
d. sampling said first and second signals within said first sampling window A, to generate a first discrete mathematical function,
e. sampling said first and second signals within said second sampling window B, to generate a second discrete mathematical function,
f. determining a first time shift between said first and second signals based on said first discrete mathematical function,
g. determining a second time shift between said first and second signals based on said second discrete mathematical function,
h. calculating said angle based on said first and second time shifts, said first predetermined depth y_A, said second predetermined depth y_B, and said known fixed speed of said reflective targets, and
i. calculating said transducer distance based on said first and second time shifts, said first predetermined depth y_A, said second predetermined depth y_B, said known fixed speed of said reflective targets, and said angle.

8. A method for determining an angle, comprising:
    a. providing a first ultrasonic transducer, having a first ultrasonic beam and receiving a first signal,
    b. providing a second ultrasonic transducer at a predetermined distance from said first ultrasonic transducer, having a second ultrasonic beam and receiving a

second signal whose varying magnitude is similar to that of said signal of said first transducer but shifted in time,

c. establishing a first sampling window A to monitor said first and second signals originating within said first and second ultrasonic beams at about a first predetermined depth y_A from said first and second ultrasonic transducers,
d. establishing a second sampling window B to monitor said first and second signals originating within said first and second ultrasonic beams at about a second predetermined depth y_B from said first and second ultrasonic transducers,
e. sampling said first and second signals within said first sampling window A, to generate a first discrete mathematical function,
f. sampling said first and second signals within said second sampling window B, to generate a second discrete mathematical function,
g. determining a first time shift between said first and second signals based on said first discrete mathematical function,
h. determining a second time shift between said first and second signals based on said second discrete mathematical function, and
i. calculating said angle based on said first and second time shifts, said first predetermined depth y_A, said second predetermined depth y_B, and said predetermined distance.

9. A method as in claim 8, further comprising:
    a. establishing at least one sampling window C to monitor said first and second signals originating within said first and second ultrasonic beams at about a predetermined depth y_C from said first and second ultrasonic transducers, each said at least one sampling window C positioned at a different predetermined depth y_C than all other said at least one sampling window C,
    b. sampling said first and second signals within each said at least one sampling window C, to create a sample set corresponding to that sampling window C, and

c. determining a relative speed based on:
    i. said sample sets corresponding to all said at least one sampling window,
    ii. said predetermined depths corresponding to all said at least one sampling window y_C,
    iii. said predetermined distance, and
    iv. said angle.

10. The method of claim 9, wherein said determining of said relative speed comprises:
    a. for each said at least one sampling window:
        i. calculating a beam distance between said first and second ultrasonic beams, based on said transducer distance, said angle, and said predetermined depth,
        ii. generating a discrete mathematical function based on said sample set, and
        iii. determining a time shift between said first and second signals based on said discrete mathematical function, and
    b. calculating said relative speed based on:
        i. said beam distances corresponding to all said at least one sampling window, and
        ii. said time shifts corresponding to all said at least one sampling window.

11. The method of claim 10, wherein said calculating of said relative speed comprises:
    a. for each said at least one sampling window, calculating a speed value based on said beam distance and said time shift, and
    b. computing an average of said speed values corresponding to all said at least one sampling window.

12. The method of claim 9, wherein said determining of said relative speed comprises:

a. for each said at least one sampling window, performing sample rate conversion on said sample set to correct said sample set according to said angle, said predetermined distance, and said predetermined depth, to create a rate-converted sample set,
b. generating a discrete mathematical function based on said rate-converted sample sets corresponding to all said at least one sampling window,
c. determining a time shift between said first and second signals based on said discrete mathematical function, and
d. calculating said relative speed based on said predetermined distance and said time shift.

13. A method for determining an angle, comprising:
a. providing a first ultrasonic transducer, having a first ultrasonic beam and receiving a first signal,
b. providing a second ultrasonic transducer at a predetermined distance from said first ultrasonic transducer, having a second ultrasonic beam and receiving a second signal whose varying magnitude is similar to that of said signal of said first transducer but shifted in time,
c. providing an environment in which reflective targets move at a known fixed speed through said first and second ultrasonic beams,
d. establishing a certain sampling window to monitor said first and second signals originating within said first and second ultrasonic beams at about a certain predetermined depth from said first and second ultrasonic transducers,
e. sampling said first and second signals within said certain sampling window, to generate a discrete mathematical function,
f. determining a time shift between said first and second signals based on said discrete mathematical function, and

g. calculating said angle based on said time shift, said certain predetermined depth, said predetermined distance, and said known fixed speed of said reflective targets.

14. A method as in claim 13, further comprising:
    a. establishing at least one sampling window to monitor said first and second signals originating within said first and second ultrasonic beams at about a predetermined depth from said first and second ultrasonic transducers, each said at least one sampling window positioned at a different predetermined depth than all other said at least one sampling window,
    b. sampling said first and second signals within each said at least one sampling window, to create a sample set corresponding to that sampling window, and
    c. determining a relative speed based on:
        i. said sample sets corresponding to all said at least one sampling window,
        ii. said predetermined depths corresponding to all said at least one sampling window,
        iii. said predetermined distance, and
        iv. said angle.

15. A method for determining an angle and a distance between a first ultrasonic transducer and a second ultrasonic transducer, comprising:
    a. providing said first ultrasonic transducer, having a first ultrasonic beam and receiving a first signal,
    b. providing said second ultrasonic transducer, having a second ultrasonic beam and receiving a second signal whose varying magnitude is similar to that of said signal of said first transducer but shifted in time,
    c. providing an environment in which reflective targets move at a known fixed speed through said first and second ultrasonic beams,

d. establishing a first sampling window A to monitor said first and second signals originating within said first and second ultrasonic beams at about a first predetermined depth y_A from said first and second ultrasonic transducers,
e. establishing a second sampling window B to monitor said first and second signals originating within said first and second ultrasonic beams at about a second predetermined depth y_B from said first and second ultrasonic transducers,
f. sampling said first and second signals within said first sampling window A, to generate a first discrete mathematical function,
g. sampling said first and second signals within said second sampling window B, to generate a second discrete mathematical function,
h. determining a first time shift between said first and second signals based on said first discrete mathematical function,
i. determining a second time shift between said first and second signals based on said second discrete mathematical function,
j. calculating said angle based on said first and second time shifts, said first predetermined depth y_A, said second predetermined depth y_B, and said known fixed speed of said reflective targets, and
k. calculating said distance between said first and second ultrasonic transducers based on said first and second time shifts, said first predetermined depth y_A, said second predetermined depth y_B, said known fixed speed of said reflective targets, and said angle.

16. A method as in claim 15, further comprising:

a. establishing at least one sampling window C to monitor said first and second signals originating within said first and second ultrasonic beams at about a predetermined depth y_C from said first and second ultrasonic transducers, each said at least one sampling window C positioned at a different predetermined depth y_C than all other said at least one sampling window C,

b. sampling said first and second signals within each said at least one sampling window C, to create a sample set corresponding to that sampling window C, and
c. determining a relative speed based on:
    i. said sample sets corresponding to all said at least one sampling window C,
    ii. said predetermined depths y_C corresponding to all said at least one sampling window C,
    iii. said predetermined distance, and
    iv. said angle.

17. A sensor, comprising:
    a. a first ultrasonic transducer, having a first ultrasonic beam and receiving a first signal,
    b. a second ultrasonic transducer at a predetermined distance from said first ultrasonic transducer, having a second ultrasonic beam and receiving a second signal whose varying magnitude is similar to that of said signal of said first transducer but shifted in time,
    c. a sampling circuit that:
        i. samples said first and second signals within a first sampling window A to create a first sample set, said first sampling window A monitoring signals originating within said first and second ultrasonic beams at about a first predetermined depth y_A from said first and second ultrasonic transducers, and
        ii. samples said first and second signals within a second sampling window B to create a second sample set, said second sampling window B monitoring signals originating within said first and second ultrasonic beams at about a second predetermined depth y_B from said first and second ultrasonic transducers, and
    d. a processing circuit that:

i. generates a first discrete mathematical function based on said first sample set,
ii. generates a second discrete mathematical function based on said second sample set,
iii. determines a first time shift between said first and second signals based on said first discrete mathematical function,
iv. determines a second time shift between said first and second signals based on said second discrete mathematical function, and
v. calculates an angle between said first and second ultrasonic beams based on said first and second time shifts, said first predetermined depth y_A, said second predetermined depth y_B, and said predetermined distance.

18. The sensor of claim 17, wherein said processing circuit additionally determines a speed of flow of a fluid based on:
    a. at least one sample set selected from the group consisting of said first sample set and said second sample set,
    b. at least one predetermined depth selected from the group consisting of said first predetermined depth y_A and said second predetermined depth y_B,
    c. said predetermined distance, and
    d. said angle.

19. The sensor of claim 17, wherein said sampling circuit additionally samples said first and second signals within at least one sampling window other than said sampling windows A or B, to create a sample set corresponding to that sampling window, each said at least one sampling window monitoring signals originating within said first and second ultrasonic beams at about a predetermined depth from said first and second ultrasonic transducers, and positioned at a different predetermined depth than all other said at least one sampling window.

20. The sensor of claim 19 wherein said processing circuit additionally:
    a. for each said at least one sampling window:
        i. generates a discrete mathematical function based on said sample set, and
        ii. determines a time shift between said first and second signals based on said discrete mathematical function, and
    b. determines a speed of flow of a fluid based on:
        i. said time shifts corresponding to all said at least one sampling window,
        ii. said predetermined depths corresponding to all said at least one sampling window,
        iii. said predetermined distance, and
        iv. said angle.

21. The sensor of claim 19 wherein said processing circuit additionally:
    a. for each said at least one sampling window, performs sample rate conversion on said sample set to correct said sample set according to said angle, said predetermined distance, and said predetermined depth, to create a rate-converted sample set,
    b. generates a discrete mathematical function based on said rate-converted sample sets corresponding to all said at least one sampling window,
    c. determines a time shift between said first and second signals based on said discrete mathematical function, and
    d. calculates a relative speed based on said predetermined distance and said time shift.

ABSTRACT: One embodiment of a method for improving the accuracy of a correlation speed sensor. Two identical ultrasonic transducers are positioned at a known spacing. The ultrasonic beams of the two transducers are nearly, but not quite, parallel. Echoes from random particles traversing through the two beams are correlated to determine a time shift, from which the speed of the flow of water relative to the sensor is determined. The degree to which the beams are non-parallel causes a corresponding error in the time shift, which results in an error in the reported speed value. By performing correlations on sets of data received from the transducers in two different sampling windows, two different time shifts may be determined, corresponding to two different known vertical distances from the transducers. The angle between the ultrasonic beams may then be determined, which allows the determination of the horizontal distance between the ultrasonic beams in all sampling windows. The reported speed value may then be corrected accordingly. Other embodiments are described and shown.

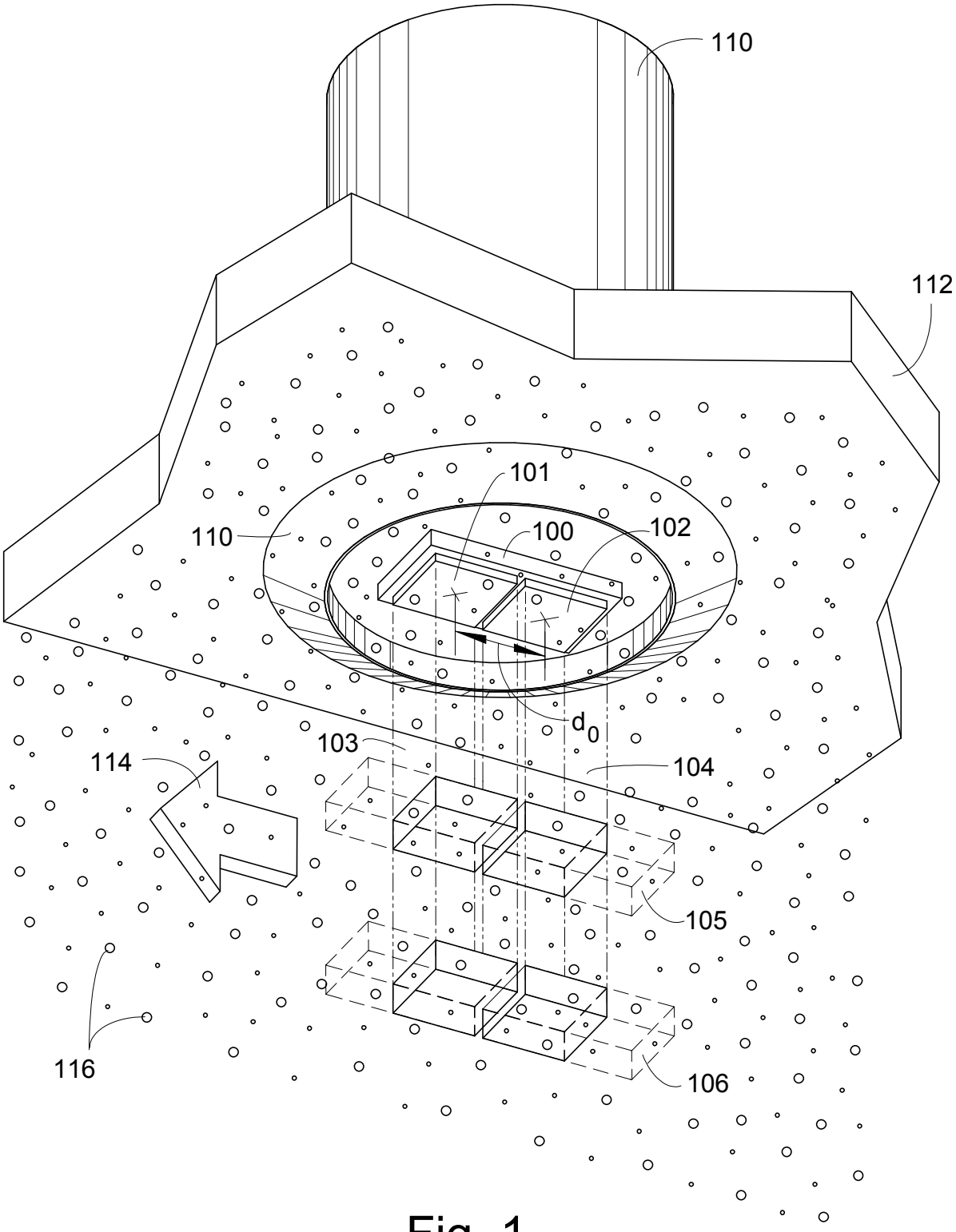

Fig. 1
PRIOR ART

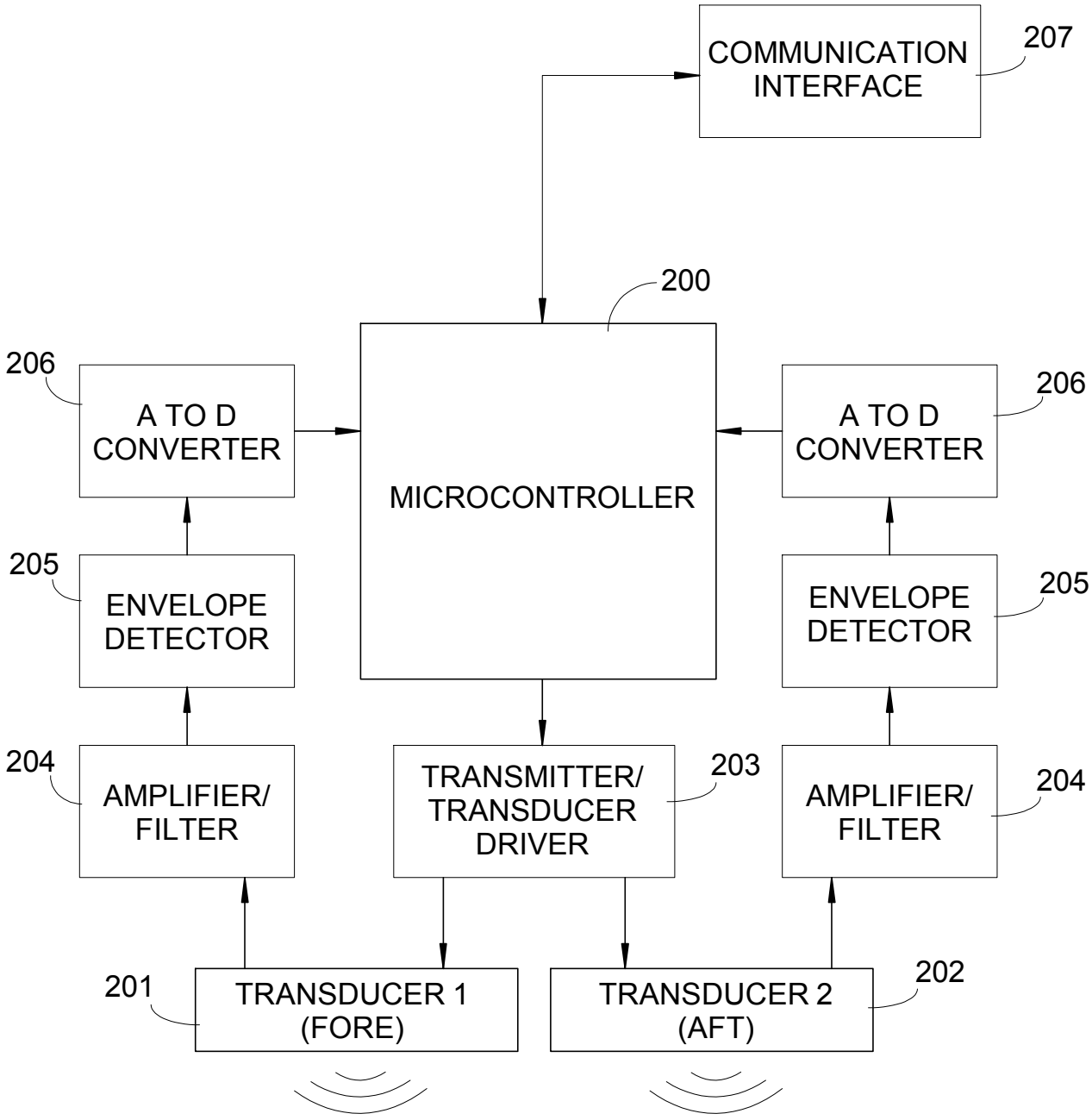

Fig. 2

PRIOR ART

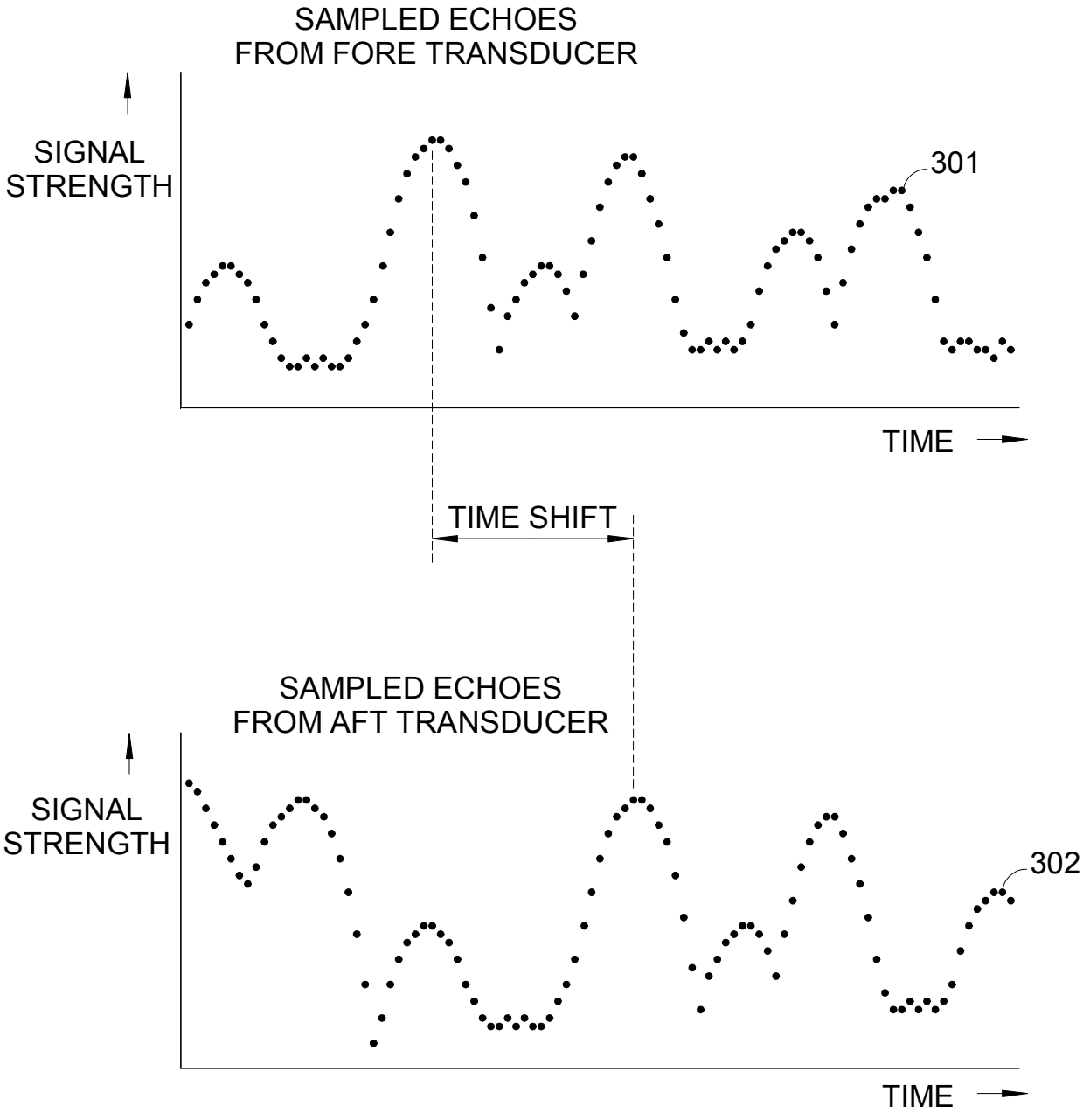

Fig. 3

PRIOR ART

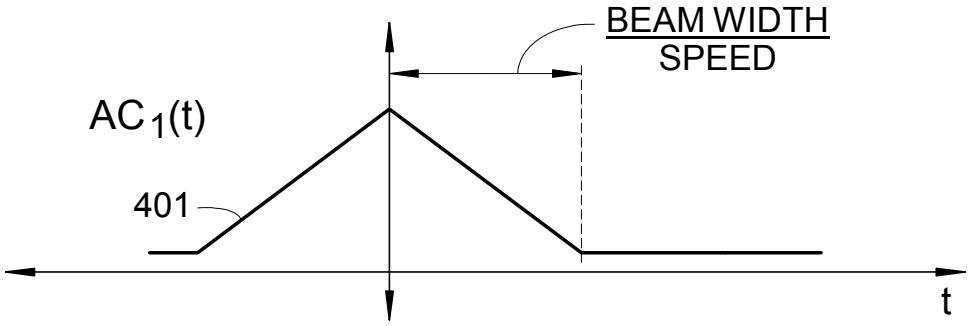

Fig. 4A
PRIOR ART

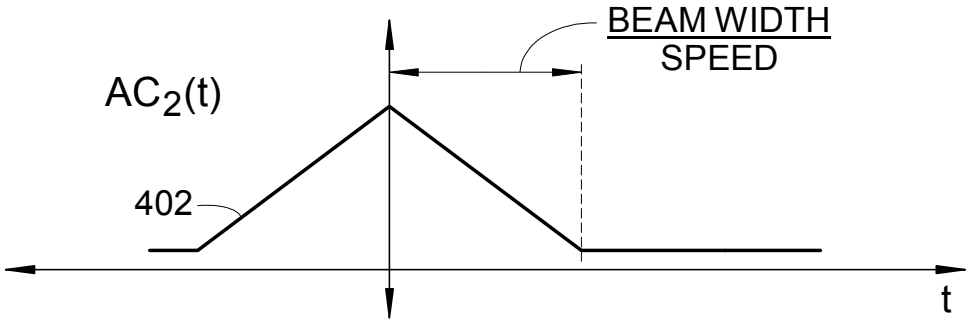

Fig. 4B
PRIOR ART

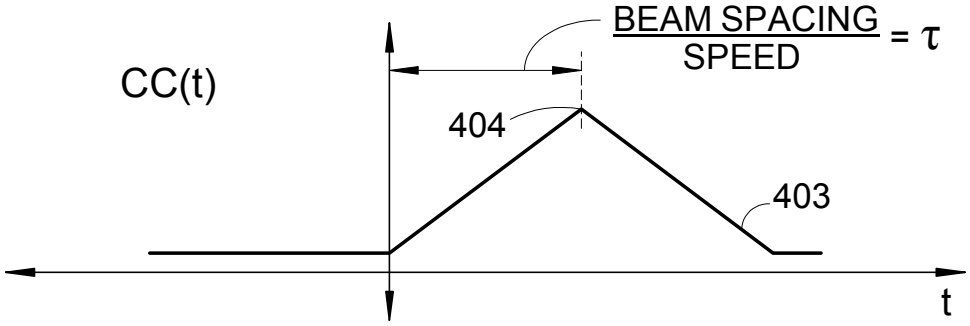

Fig. 4C
PRIOR ART

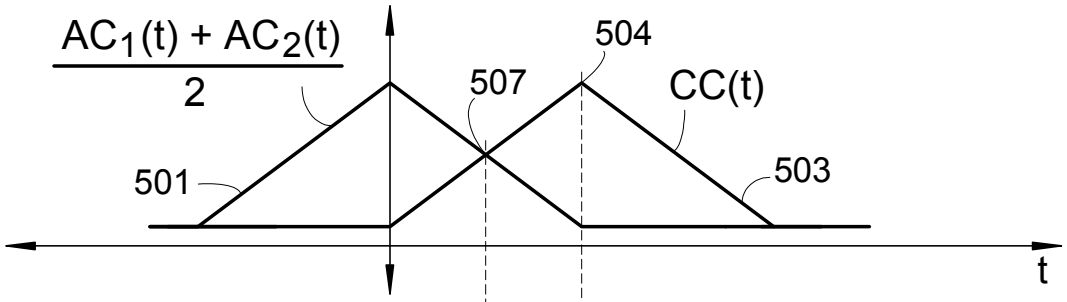

Fig. 5A
PRIOR ART

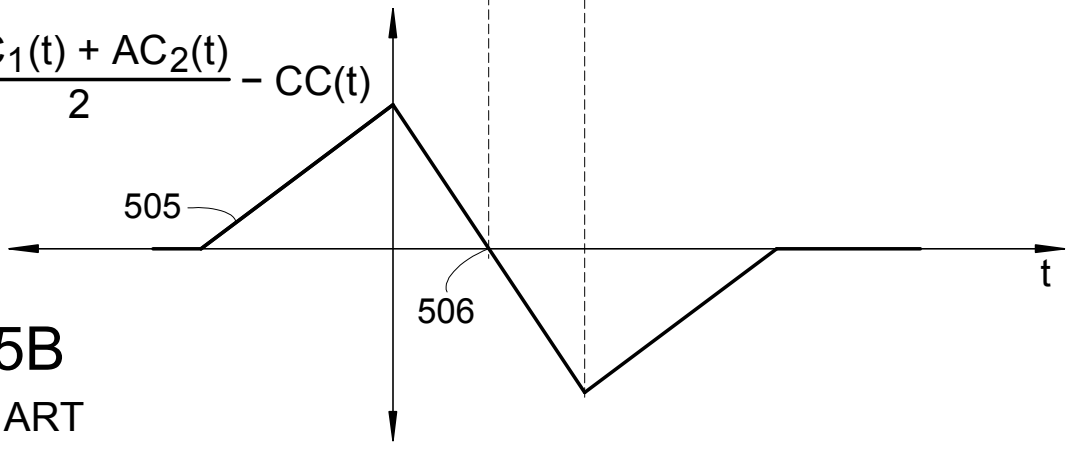

Fig. 5B
PRIOR ART

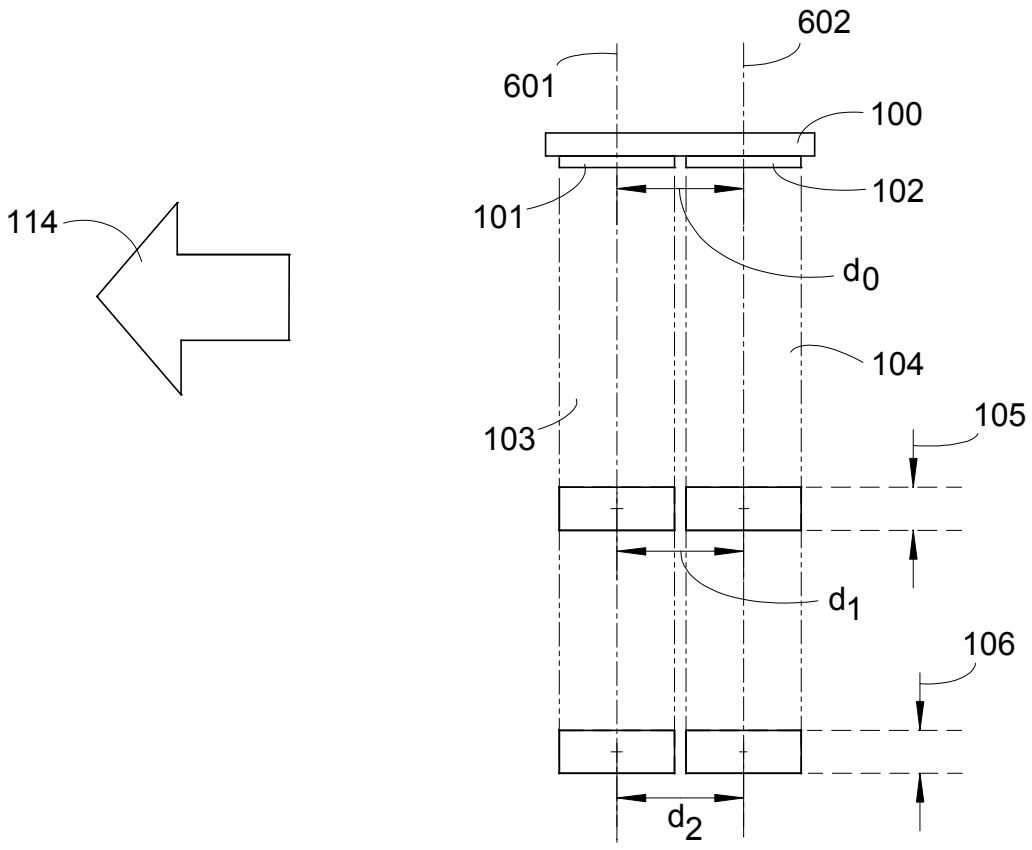

Fig. 6

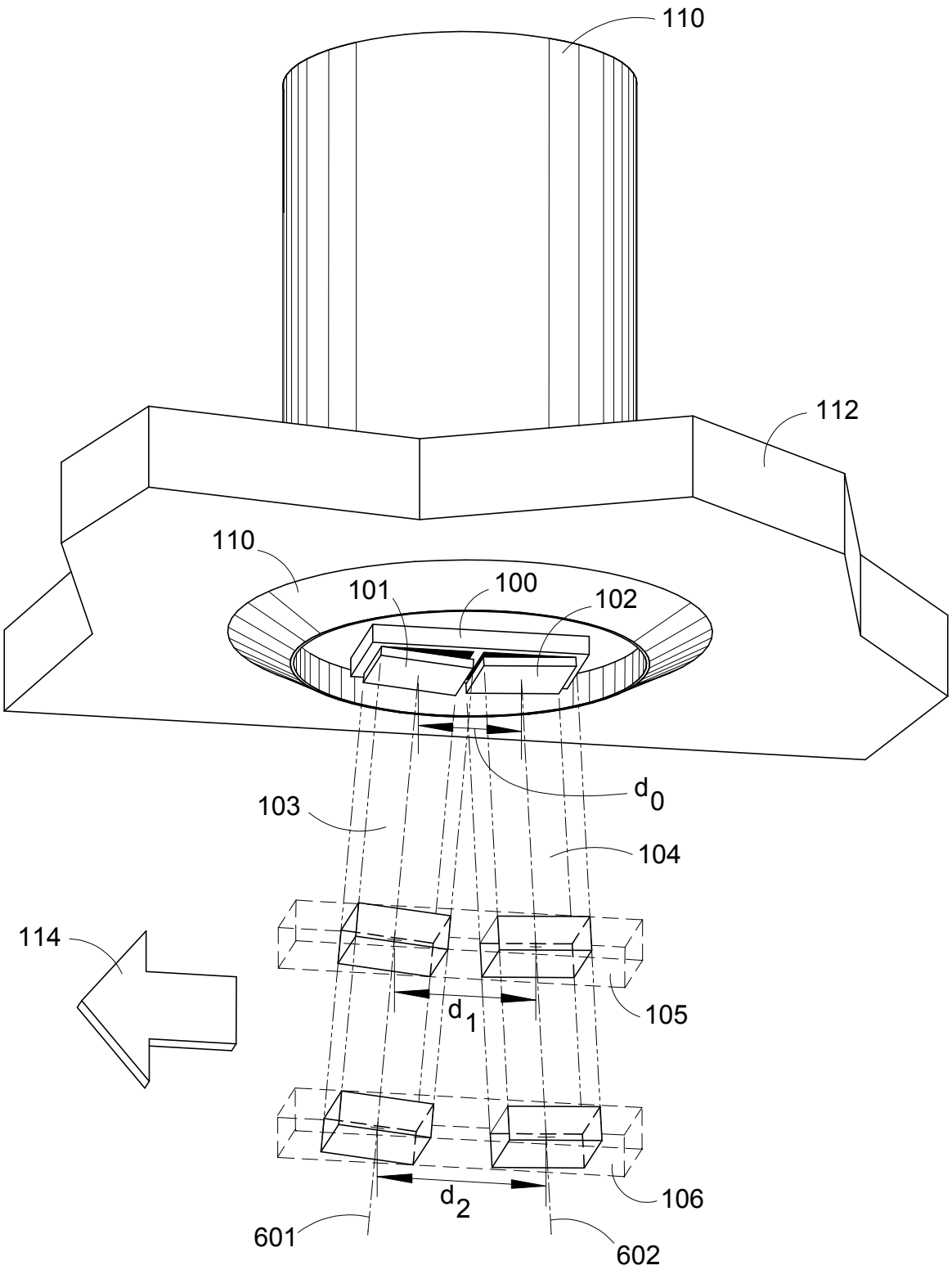

Fig. 7

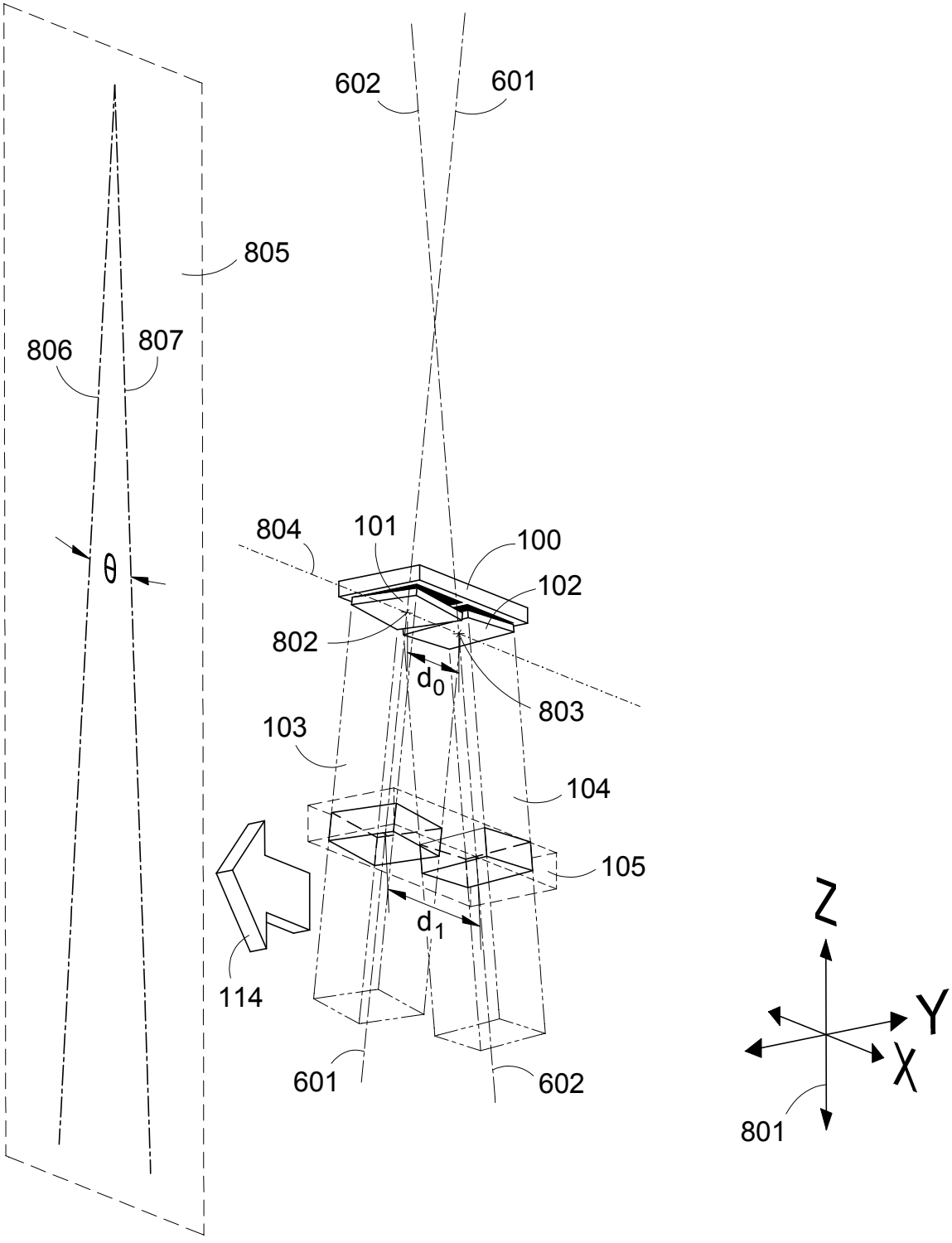
602
601
805
806
807
θ
804
101
100
102
802
d_0
803
103
104
105
d_1
114
601
602
Z
Y
X
801

Fig. 8A

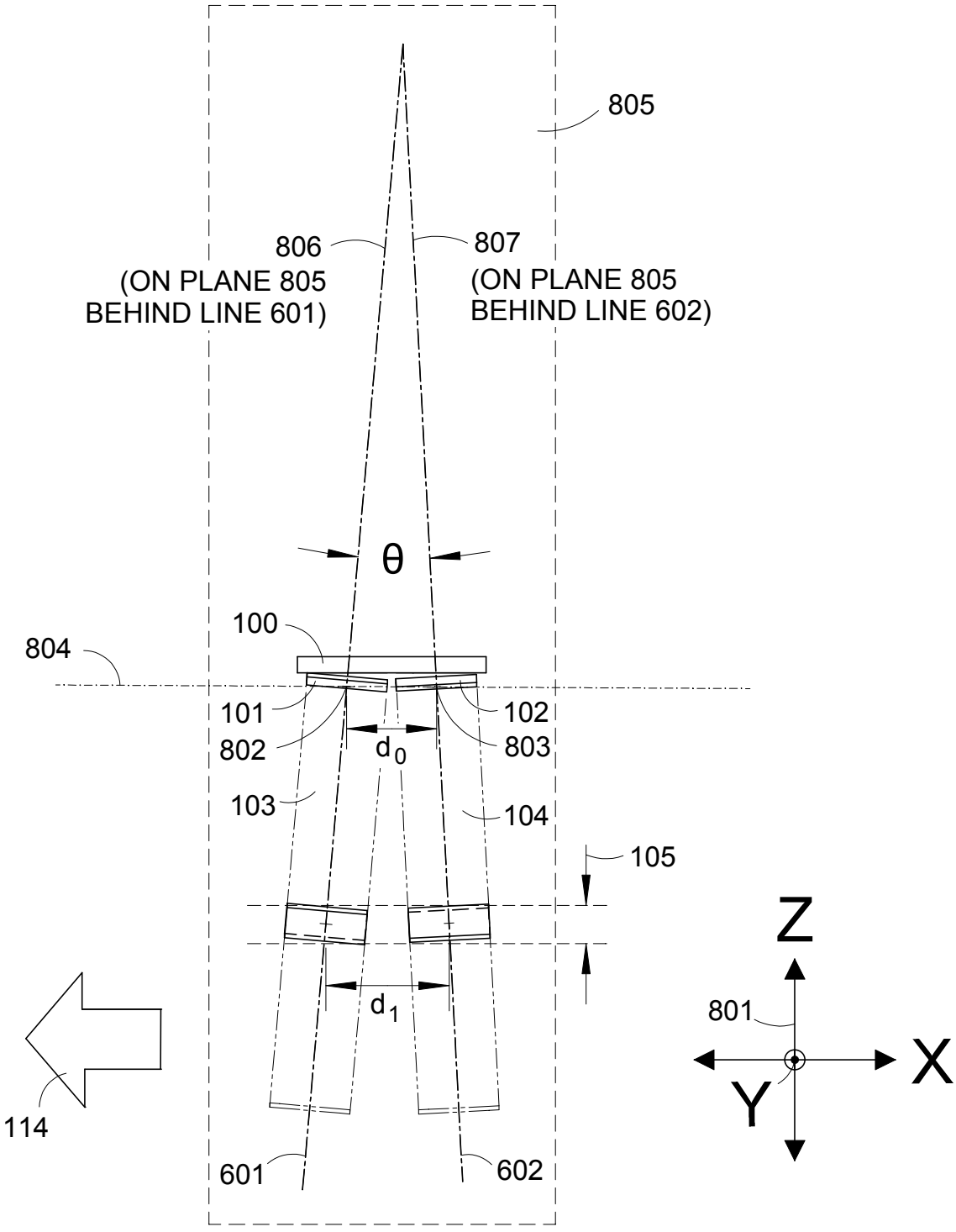
805
806
(ON PLANE 805
BEHIND LINE 601)
807
(ON PLANE 805
BEHIND LINE 602)
θ
100
804
101
802
102
803
d_0
103
104
105
d_1
114
601
602
Z
801
X
Y

Fig. 8B

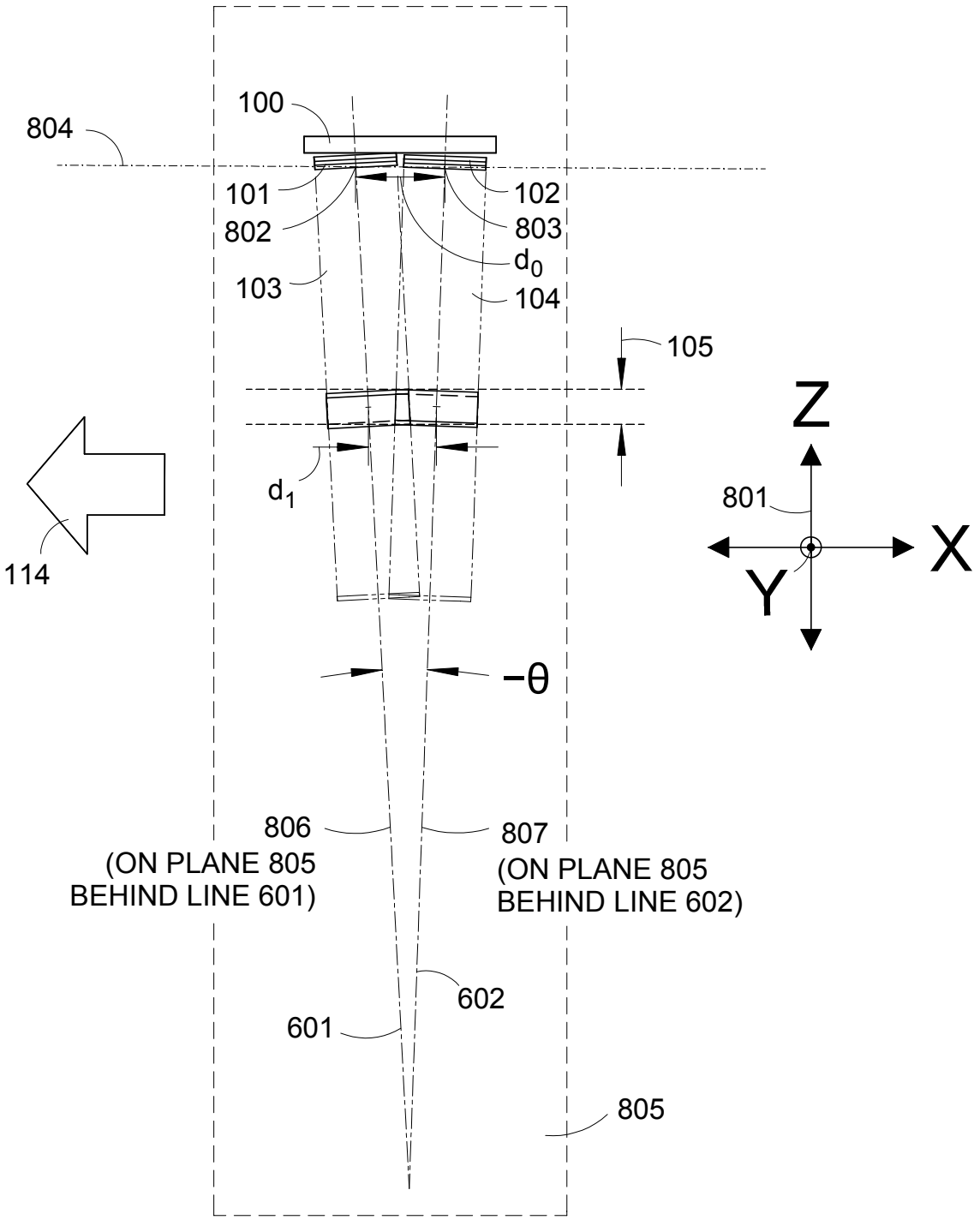
804
100
101
102
802
803
d_0
103
104
105
d_1
114
Z
801
X
Y
$-\theta$
806
(ON PLANE 805
BEHIND LINE 601)
807
(ON PLANE 805
BEHIND LINE 602)
602
601
805

Fig. 8C

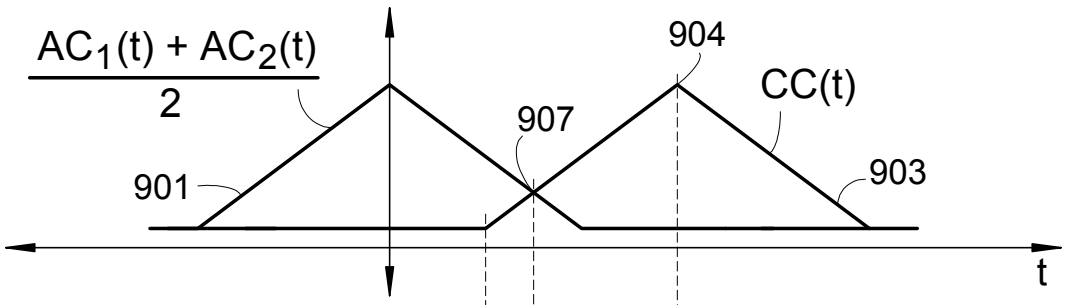
$\frac{AC_1(t) + AC_2(t)}{2}$
904
CC(t)
907
901
903
t

Fig. 9A

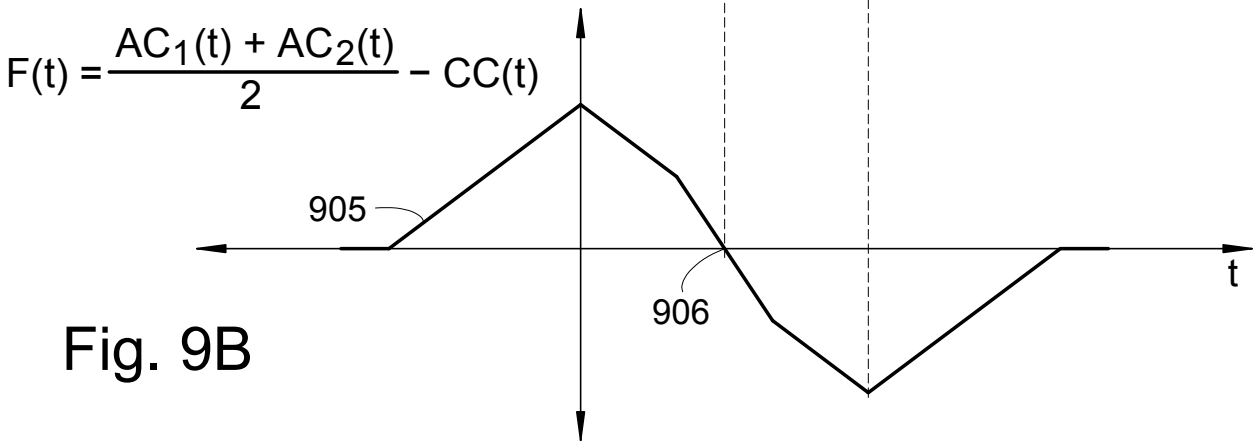
$F(t) = \frac{AC_1(t) + AC_2(t)}{2} - CC(t)$
905
906
t

Fig. 9B

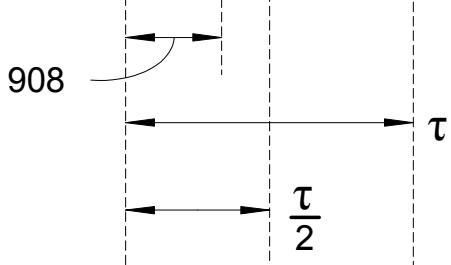
908
τ
$\frac{\tau}{2}$

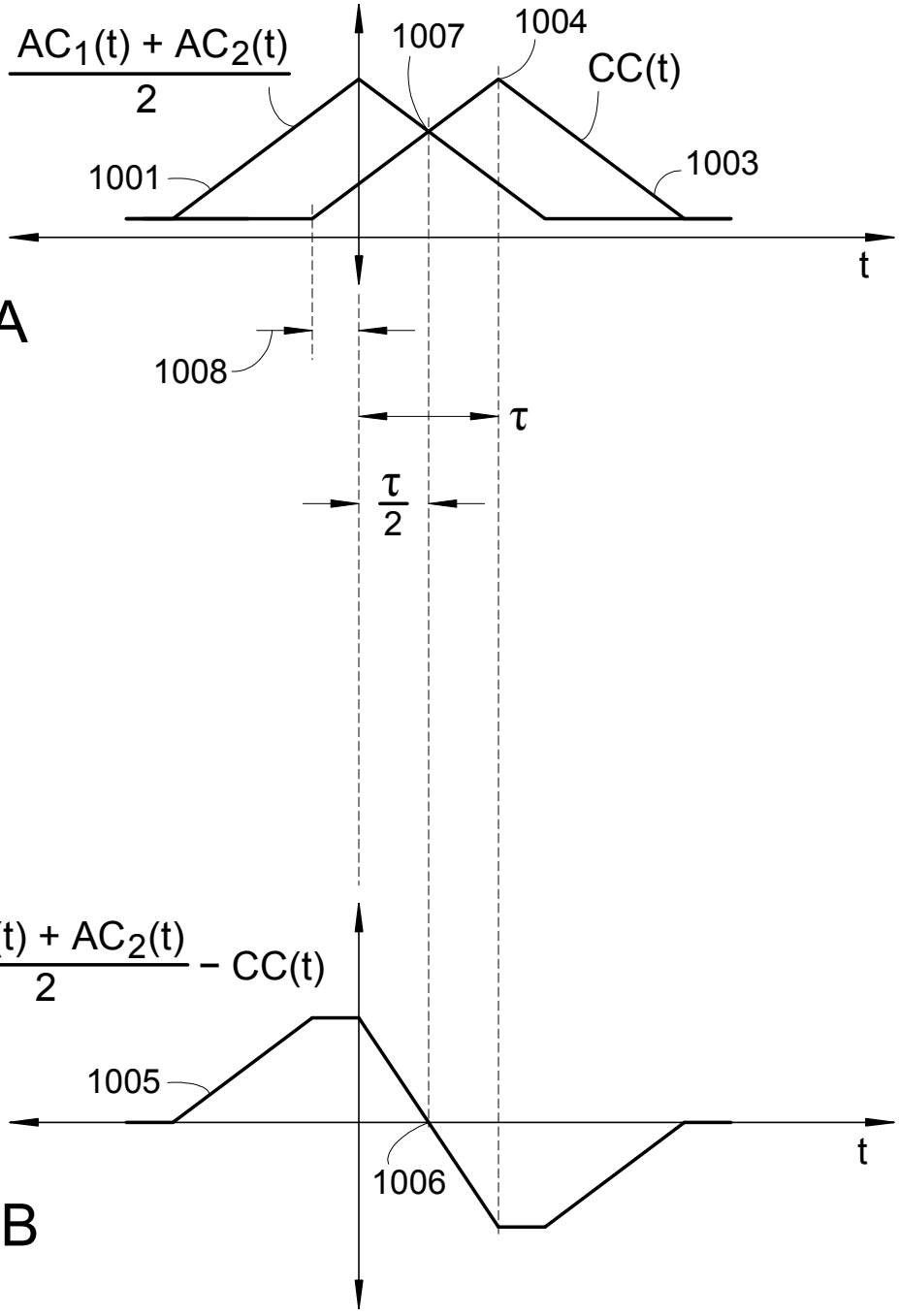

Fig. 10A

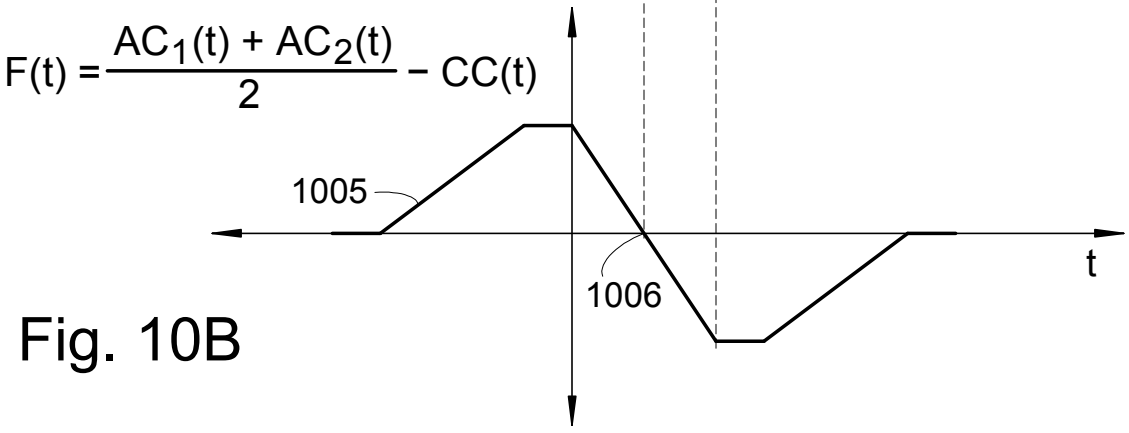

Fig. 10B

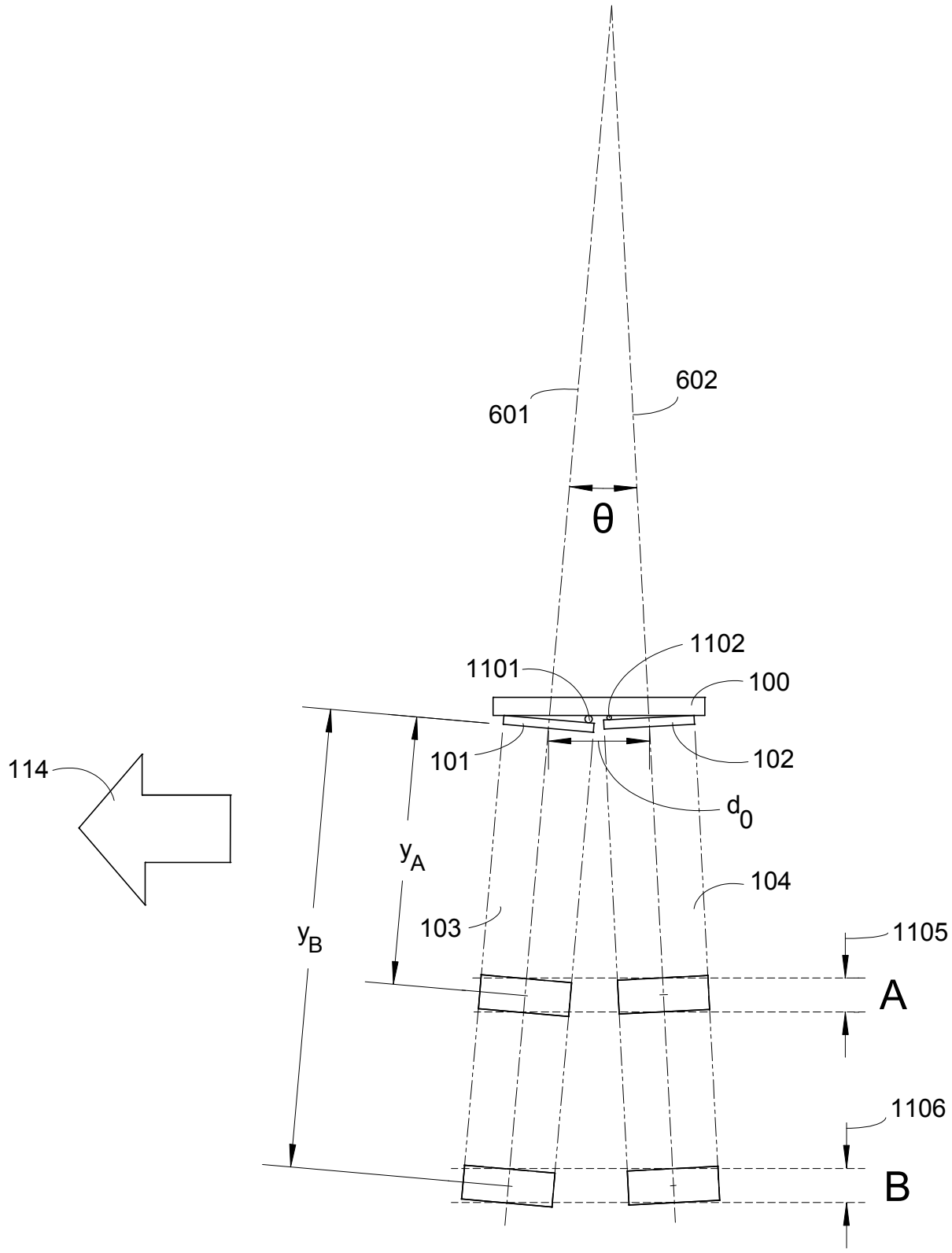

Fig. 11

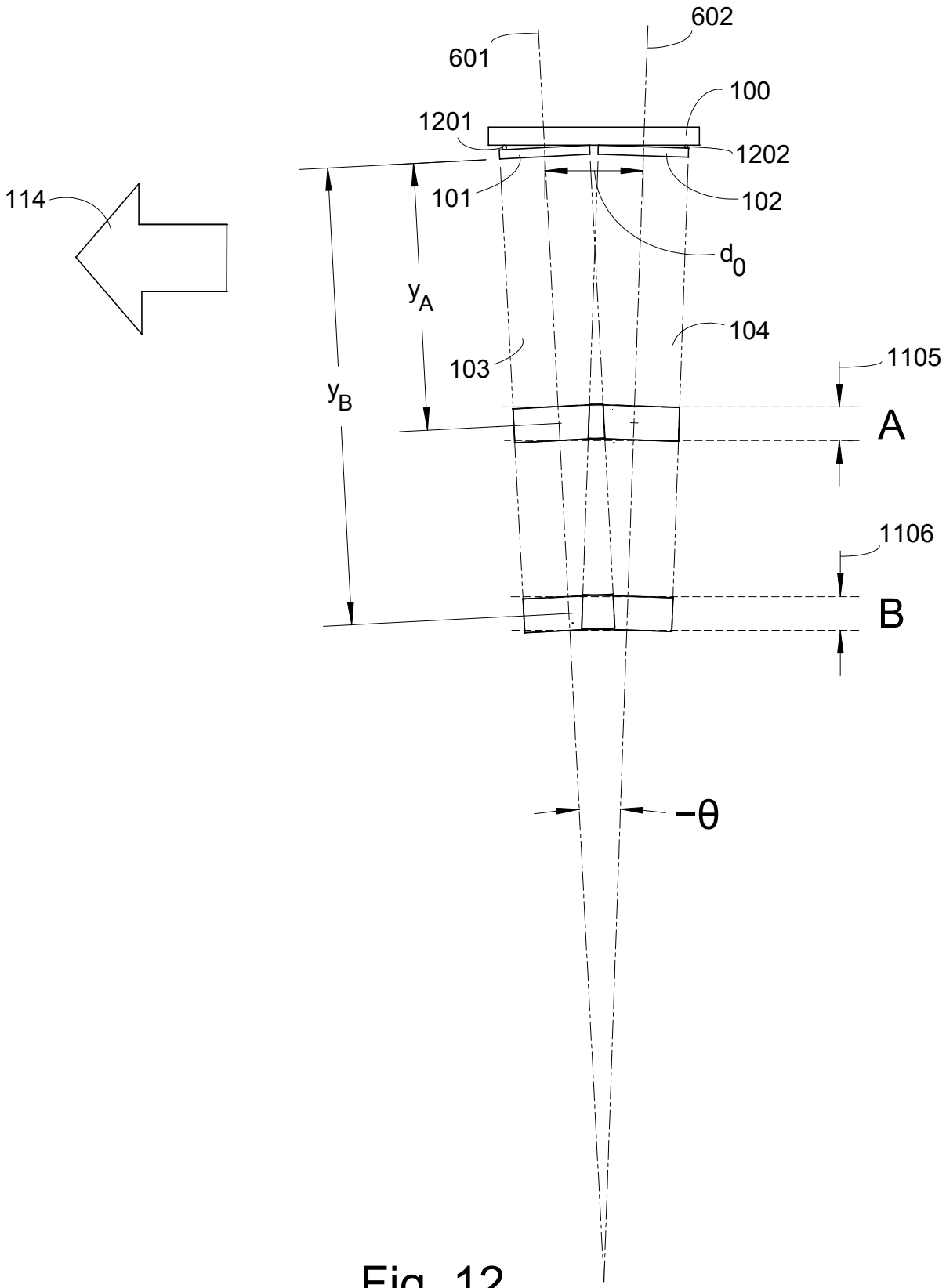

Fig. 12

Fig. 13A

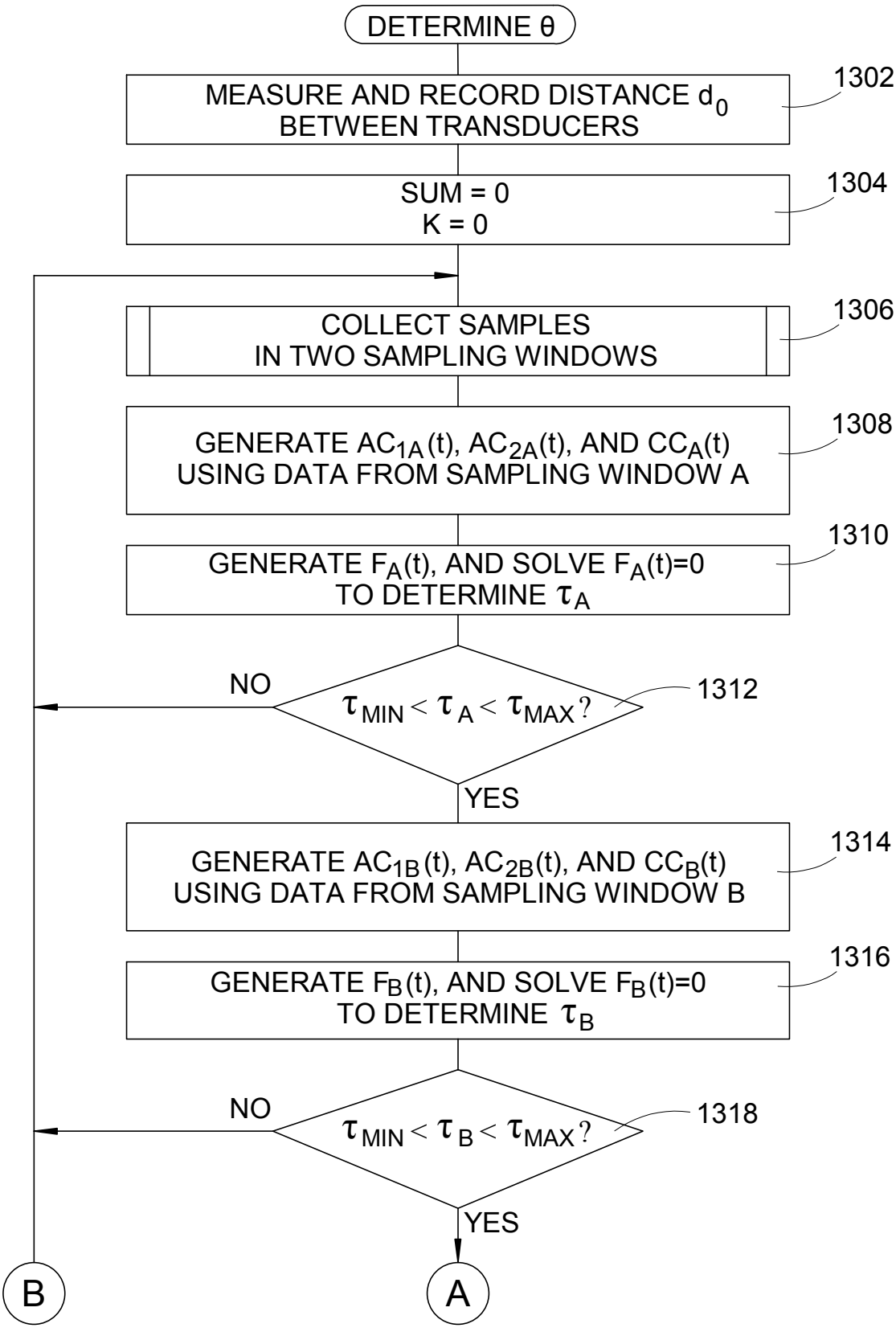
DETERMINE θ
MEASURE AND RECORD DISTANCE d_0 BETWEEN TRANSDUCERS
1302
SUM = 0
K = 0
1304
COLLECT SAMPLES IN TWO SAMPLING WINDOWS
1306
GENERATE $AC_{1A}(t)$, $AC_{2A}(t)$, AND $CC_A(t)$ USING DATA FROM SAMPLING WINDOW A
1308
GENERATE $F_A(t)$, AND SOLVE $F_A(t)=0$ TO DETERMINE τ_A
1310
$\tau_{MIN} < \tau_A < \tau_{MAX}$?
1312
NO
YES
GENERATE $AC_{1B}(t)$, $AC_{2B}(t)$, AND $CC_B(t)$ USING DATA FROM SAMPLING WINDOW B
1314
GENERATE $F_B(t)$, AND SOLVE $F_B(t)=0$ TO DETERMINE τ_B
1316
$\tau_{MIN} < \tau_B < \tau_{MAX}$?
1318
NO
YES
B
A

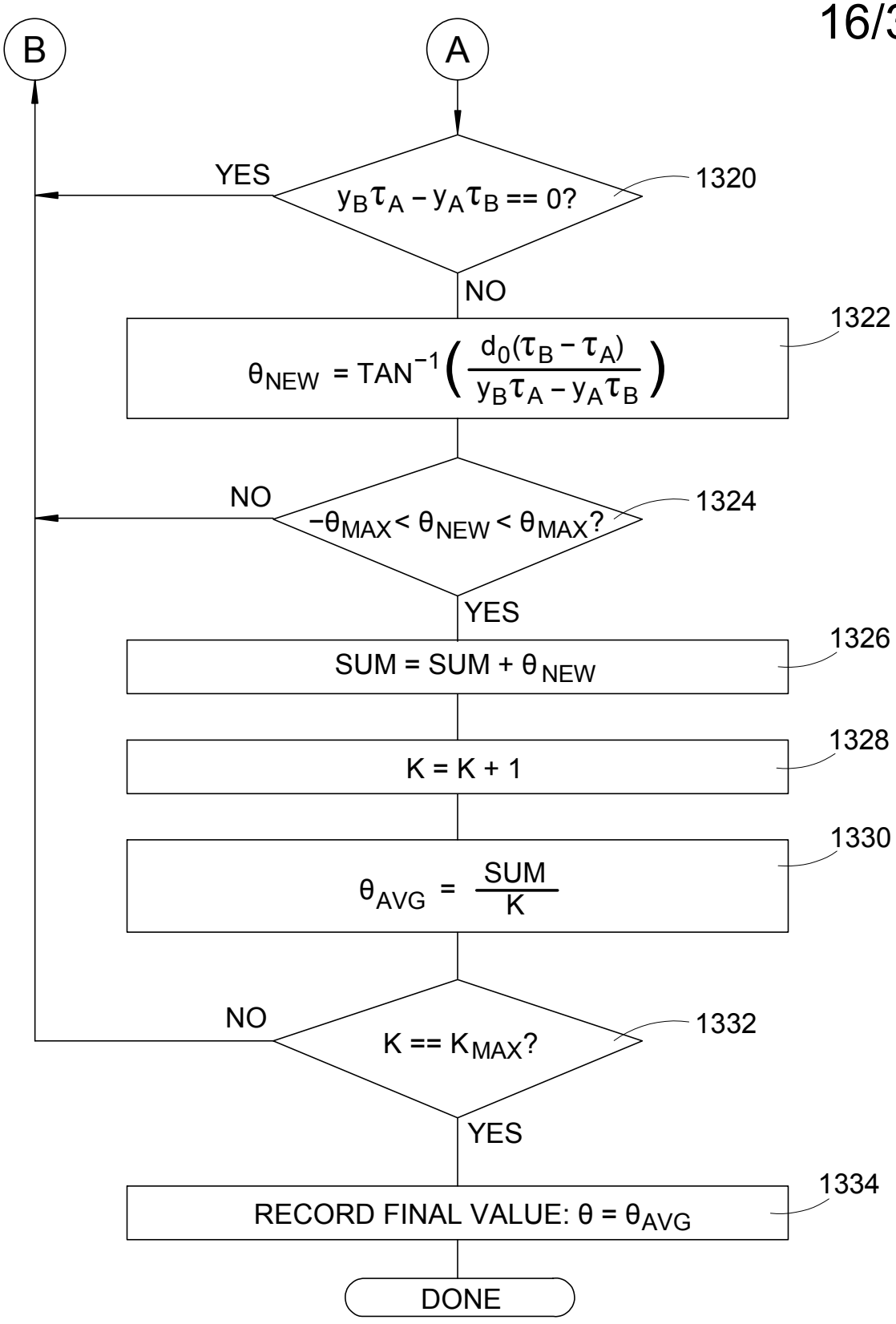
B
A
YES
$y_B\tau_A - y_A\tau_B == 0?$
1320
NO
$\theta_{NEW} = TAN^{-1}\left(\frac{d_0(\tau_B - \tau_A)}{y_B\tau_A - y_A\tau_B}\right)$
1322
NO
$-\theta_{MAX} < \theta_{NEW} < \theta_{MAX}?$
1324
YES
SUM = SUM + θ_{NEW}
1326
K = K + 1
1328
$\theta_{AVG} = \frac{SUM}{K}$
1330
NO
K == K_{MAX}?
1332
YES
RECORD FINAL VALUE: $\theta = \theta_{AVG}$
1334
DONE

Fig. 13B

Fig. 14

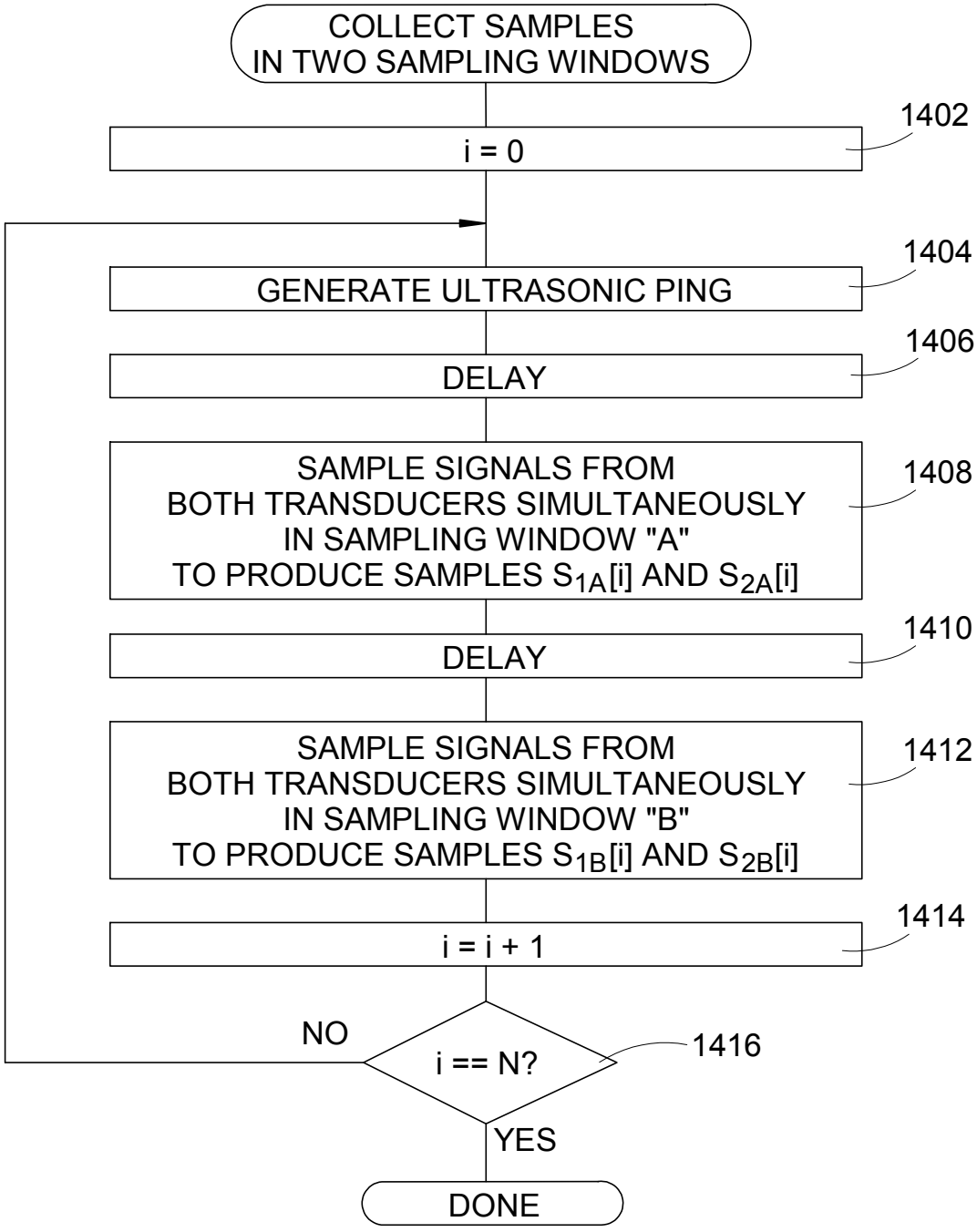
COLLECT SAMPLES
IN TWO SAMPLING WINDOWS
1402
i = 0
1404
GENERATE ULTRASONIC PING
1406
DELAY
1408
SAMPLE SIGNALS FROM
BOTH TRANSDUCERS SIMULTANEOUSLY
IN SAMPLING WINDOW "A"
TO PRODUCE SAMPLES $S_{1A}[i]$ AND $S_{2A}[i]$
1410
DELAY
1412
SAMPLE SIGNALS FROM
BOTH TRANSDUCERS SIMULTANEOUSLY
IN SAMPLING WINDOW "B"
TO PRODUCE SAMPLES $S_{1B}[i]$ AND $S_{2B}[i]$
1414
i = i + 1
NO
i == N?
1416
YES
DONE

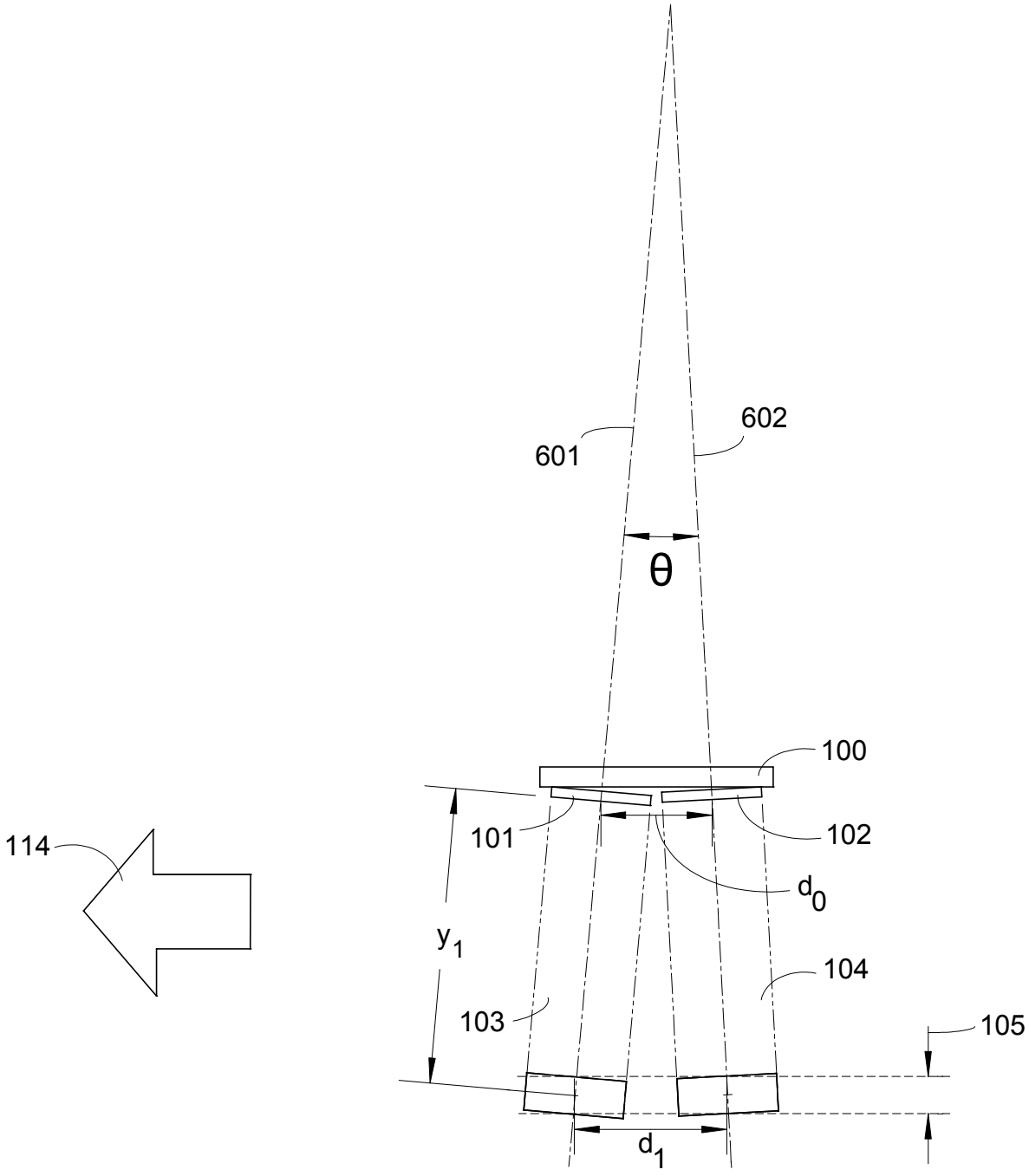

Fig. 15

Fig. 16

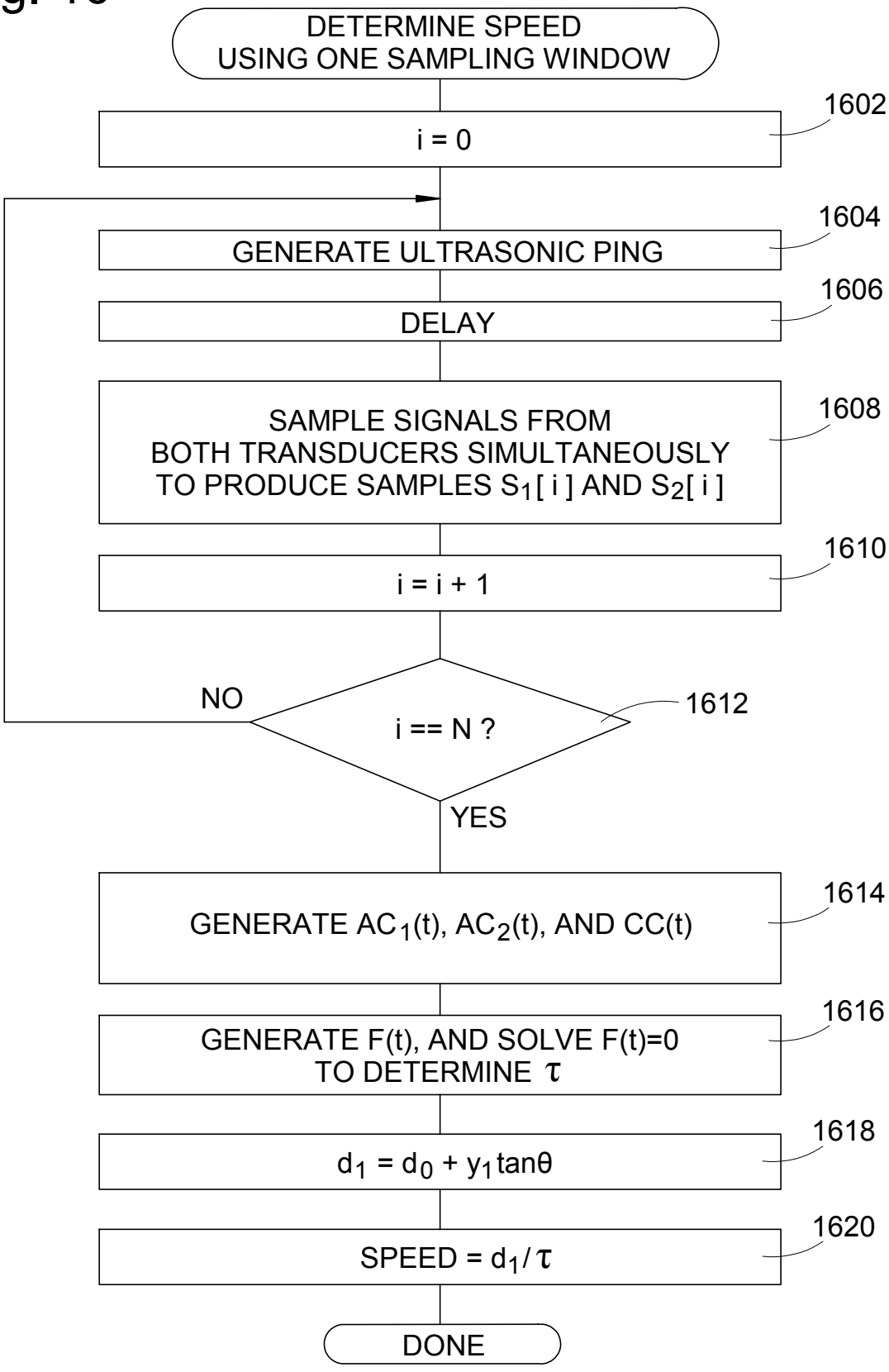
DETERMINE SPEED
USING ONE SAMPLING WINDOW
1602
i = 0
1604
GENERATE ULTRASONIC PING
1606
DELAY
1608
SAMPLE SIGNALS FROM
BOTH TRANSDUCERS SIMULTANEOUSLY
TO PRODUCE SAMPLES S1[i] AND S2[i]
1610
i = i + 1
NO
i == N ?
1612
YES
1614
GENERATE AC1(t), AC2(t), AND CC(t)
1616
GENERATE F(t), AND SOLVE F(t)=0
TO DETERMINE τ
1618
d1 = d0 + y1 tanθ
1620
SPEED = d1 / τ
DONE

Fig. 17A

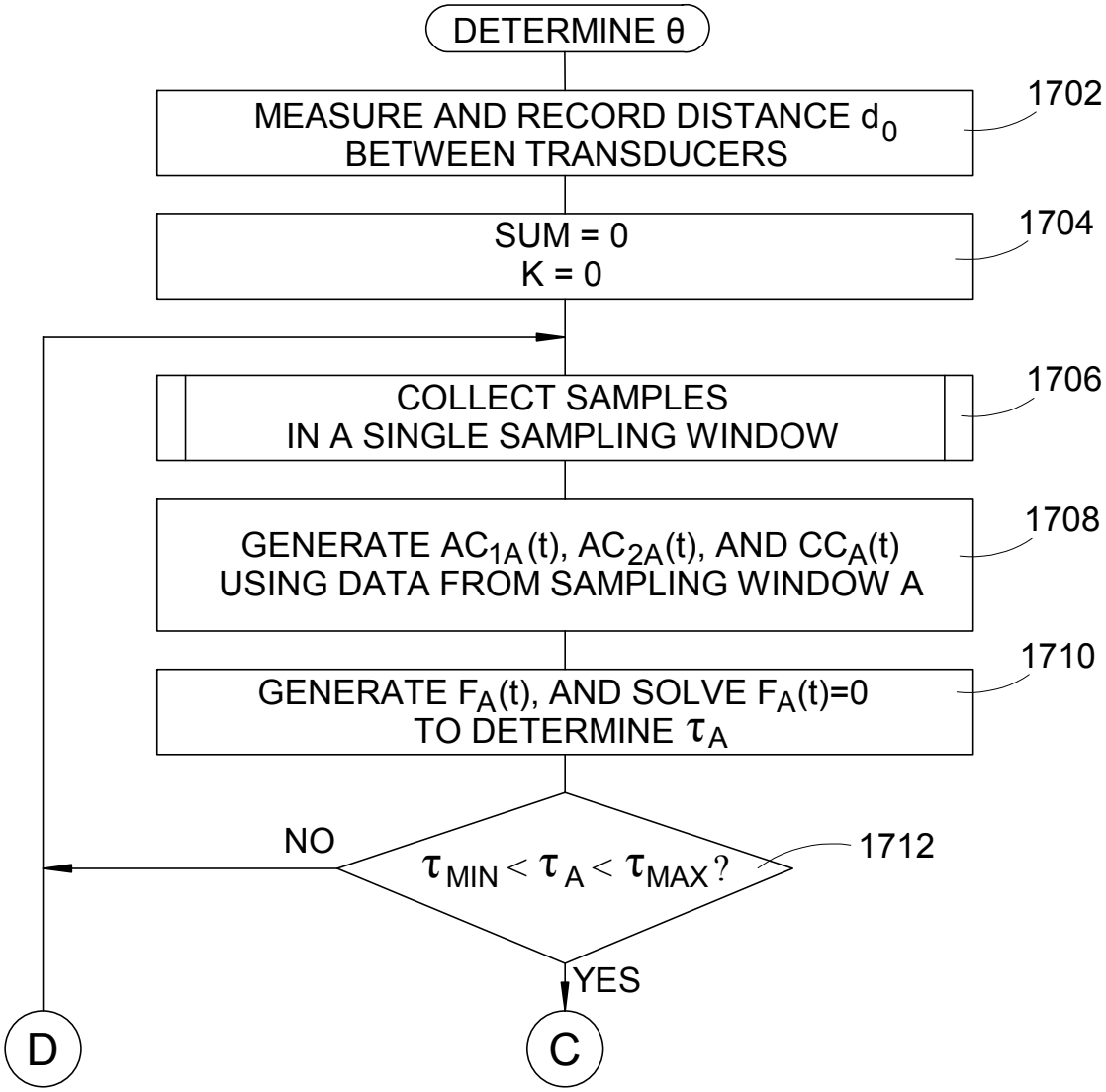
DETERMINE θ
MEASURE AND RECORD DISTANCE d_0 BETWEEN TRANSDUCERS
1702
SUM = 0
K = 0
1704
COLLECT SAMPLES IN A SINGLE SAMPLING WINDOW
1706
GENERATE $AC_{1A}(t)$, $AC_{2A}(t)$, AND $CC_A(t)$ USING DATA FROM SAMPLING WINDOW A
1708
GENERATE $F_A(t)$, AND SOLVE $F_A(t)=0$ TO DETERMINE τ_A
1710
$\tau_{MIN} < \tau_A < \tau_{MAX}$?
1712
NO
YES
D
C

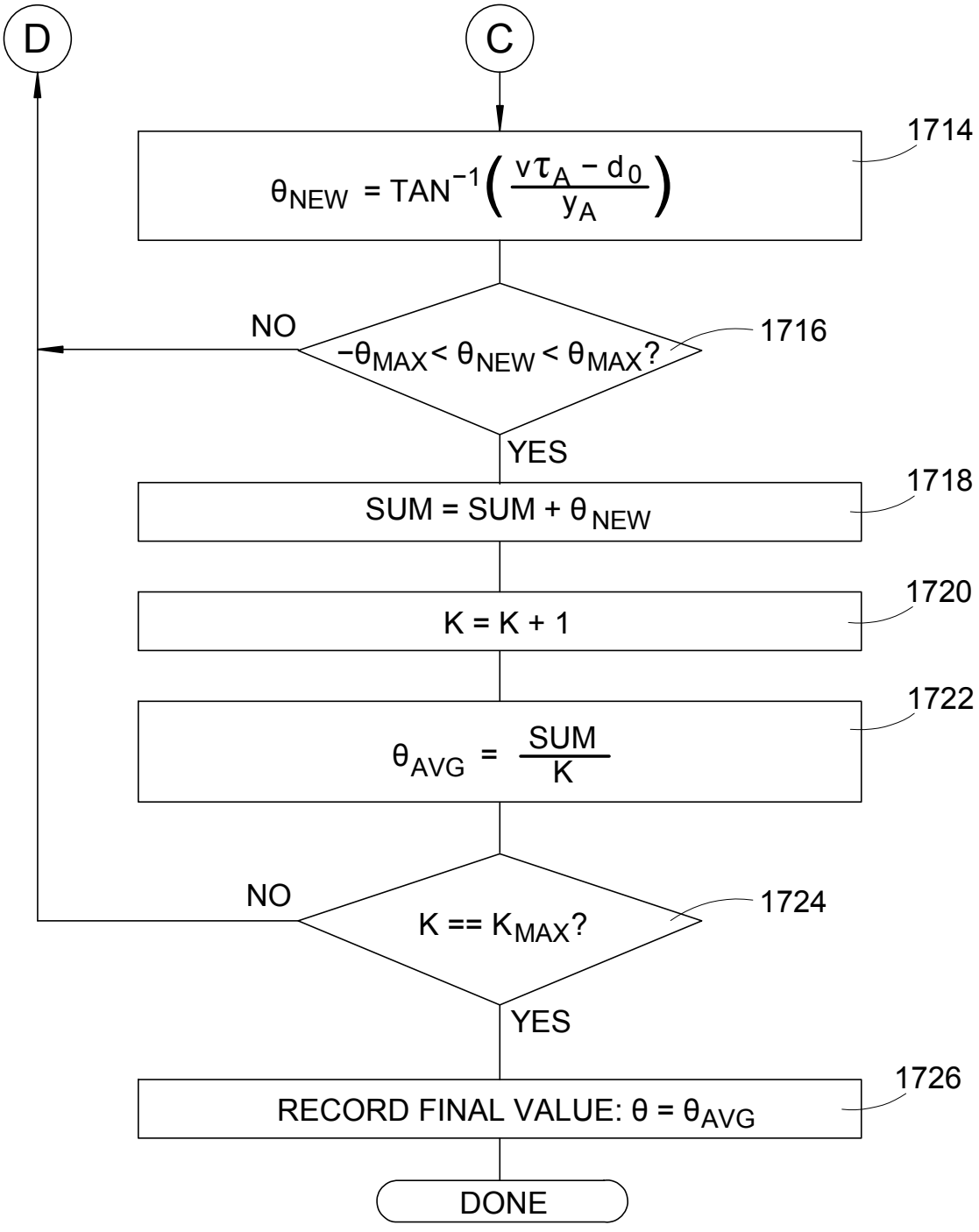
D
C
1714
$\theta_{NEW} = TAN^{-1}\left(\frac{v\tau_A - d_0}{y_A}\right)$
NO
$-\theta_{MAX} < \theta_{NEW} < \theta_{MAX}$?
1716
YES
1718
SUM = SUM + θ_{NEW}
1720
K = K + 1
1722
$\theta_{AVG} = \frac{SUM}{K}$
NO
K == K_{MAX}?
1724
YES
1726
RECORD FINAL VALUE: $\theta = \theta_{AVG}$
DONE

Fig. 17B

Fig. 18

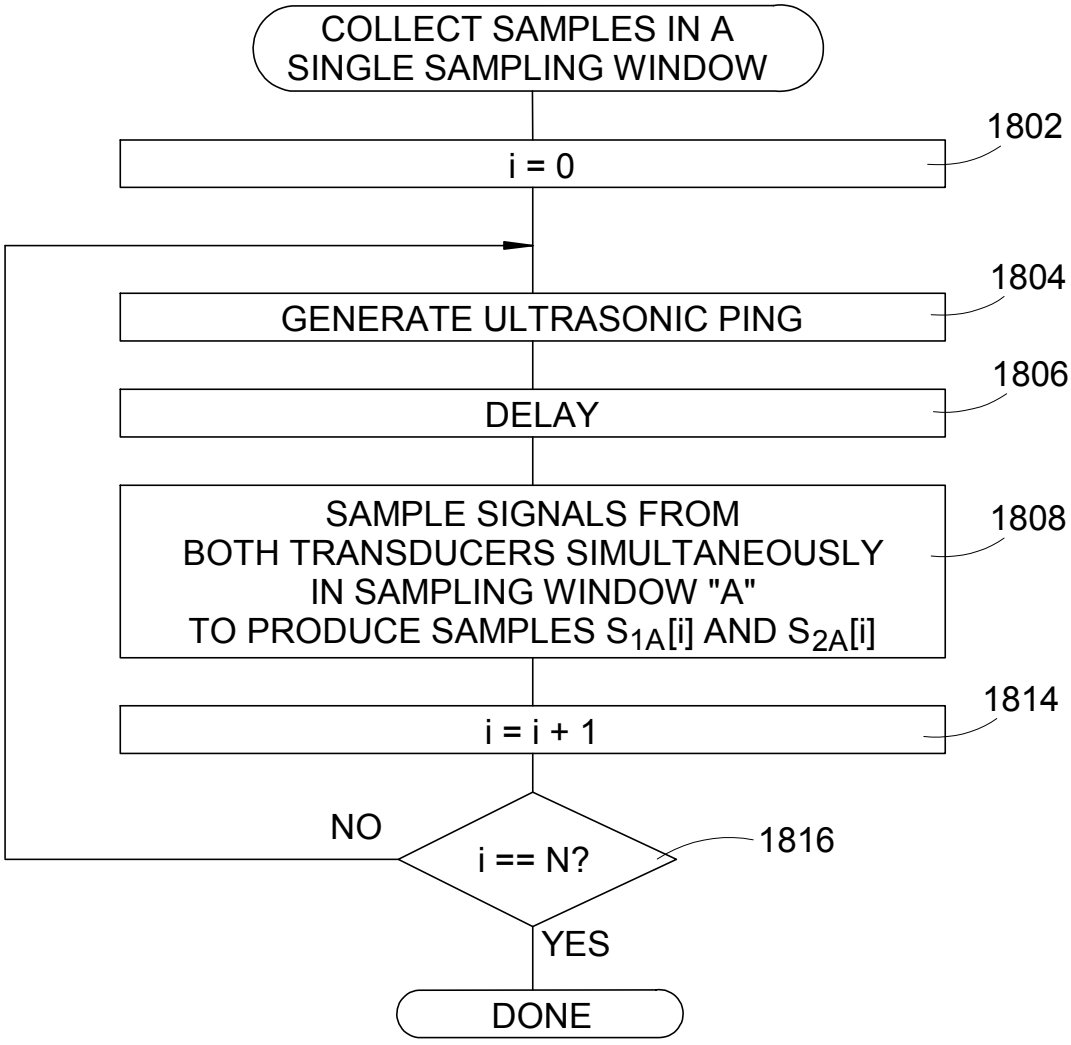
COLLECT SAMPLES IN A SINGLE SAMPLING WINDOW
1802
i = 0
1804
GENERATE ULTRASONIC PING
1806
DELAY
SAMPLE SIGNALS FROM BOTH TRANSDUCERS SIMULTANEOUSLY IN SAMPLING WINDOW "A" TO PRODUCE SAMPLES $S_{1A}[i]$ AND $S_{2A}[i]$
1808
1814
i = i + 1
NO
i == N?
1816
YES
DONE

Fig. 19A

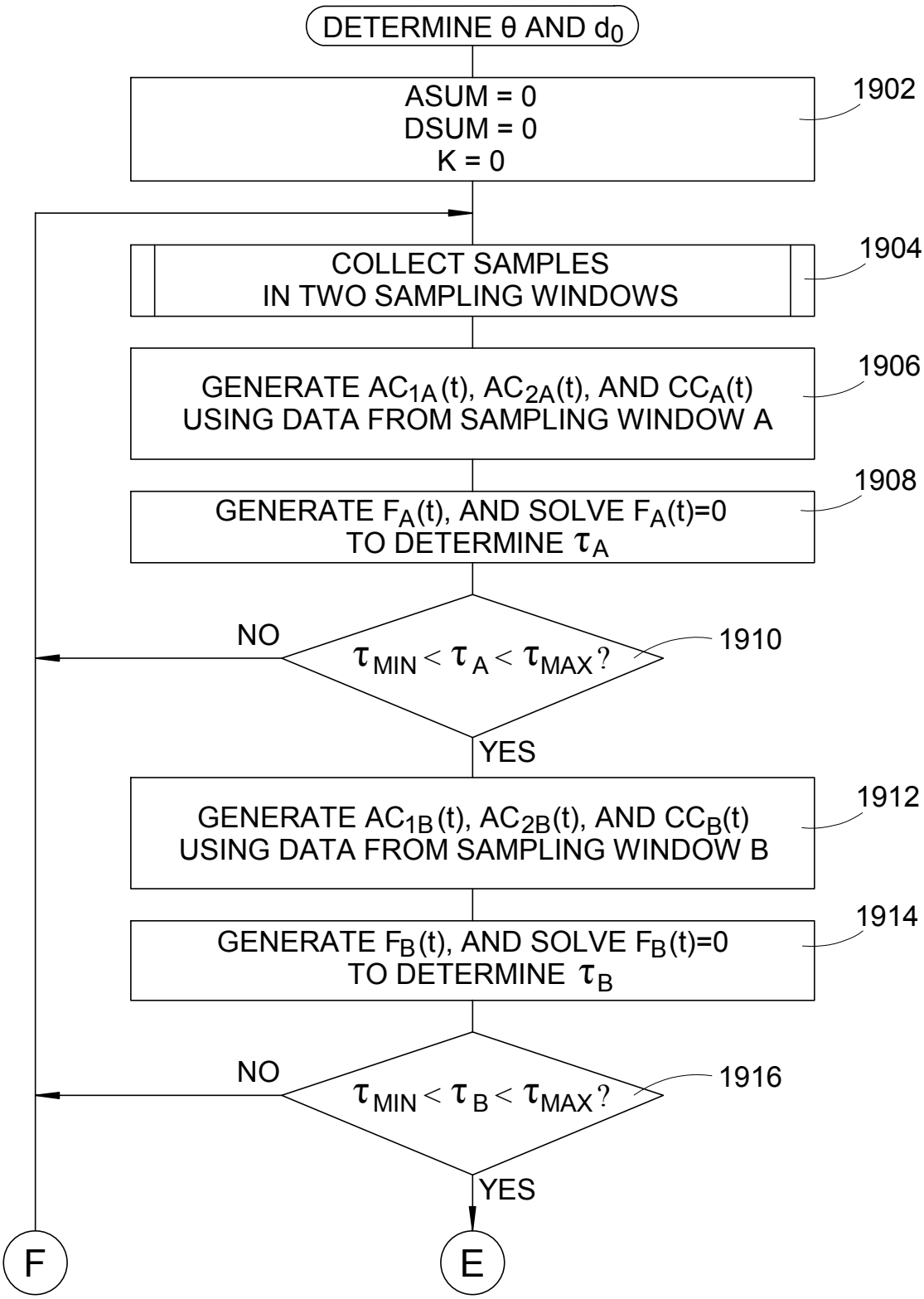
DETERMINE θ AND d_0
ASUM = 0
DSUM = 0
K = 0
1902
COLLECT SAMPLES
IN TWO SAMPLING WINDOWS
1904
GENERATE $AC_{1A}(t)$, $AC_{2A}(t)$, AND $CC_A(t)$
USING DATA FROM SAMPLING WINDOW A
1906
GENERATE $F_A(t)$, AND SOLVE $F_A(t)=0$
TO DETERMINE τ_A
1908
NO
$\tau_{MIN} < \tau_A < \tau_{MAX}$?
1910
YES
GENERATE $AC_{1B}(t)$, $AC_{2B}(t)$, AND $CC_B(t)$
USING DATA FROM SAMPLING WINDOW B
1912
GENERATE $F_B(t)$, AND SOLVE $F_B(t)=0$
TO DETERMINE τ_B
1914
NO
$\tau_{MIN} < \tau_B < \tau_{MAX}$?
1916
YES
F
E

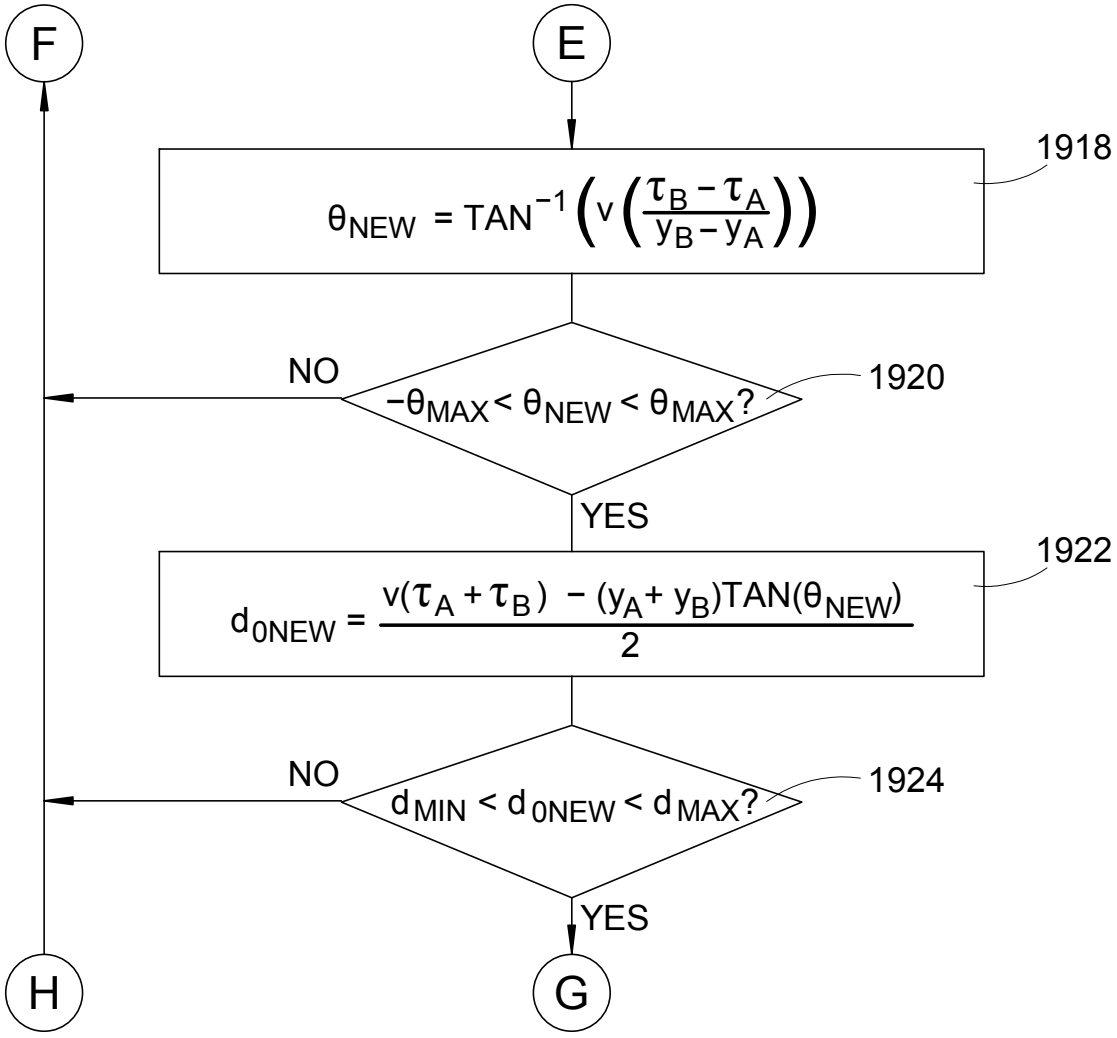
F
E
1918
$\theta_{NEW} = TAN^{-1}\left(v\left(\frac{\tau_B - \tau_A}{y_B - y_A}\right)\right)$
NO
$-\theta_{MAX} < \theta_{NEW} < \theta_{MAX}$?
1920
YES
1922
$d_{0NEW} = \frac{v(\tau_A + \tau_B) - (y_A + y_B)TAN(\theta_{NEW})}{2}$
NO
$d_{MIN} < d_{0NEW} < d_{MAX}$?
1924
YES
H
G

Fig. 19B

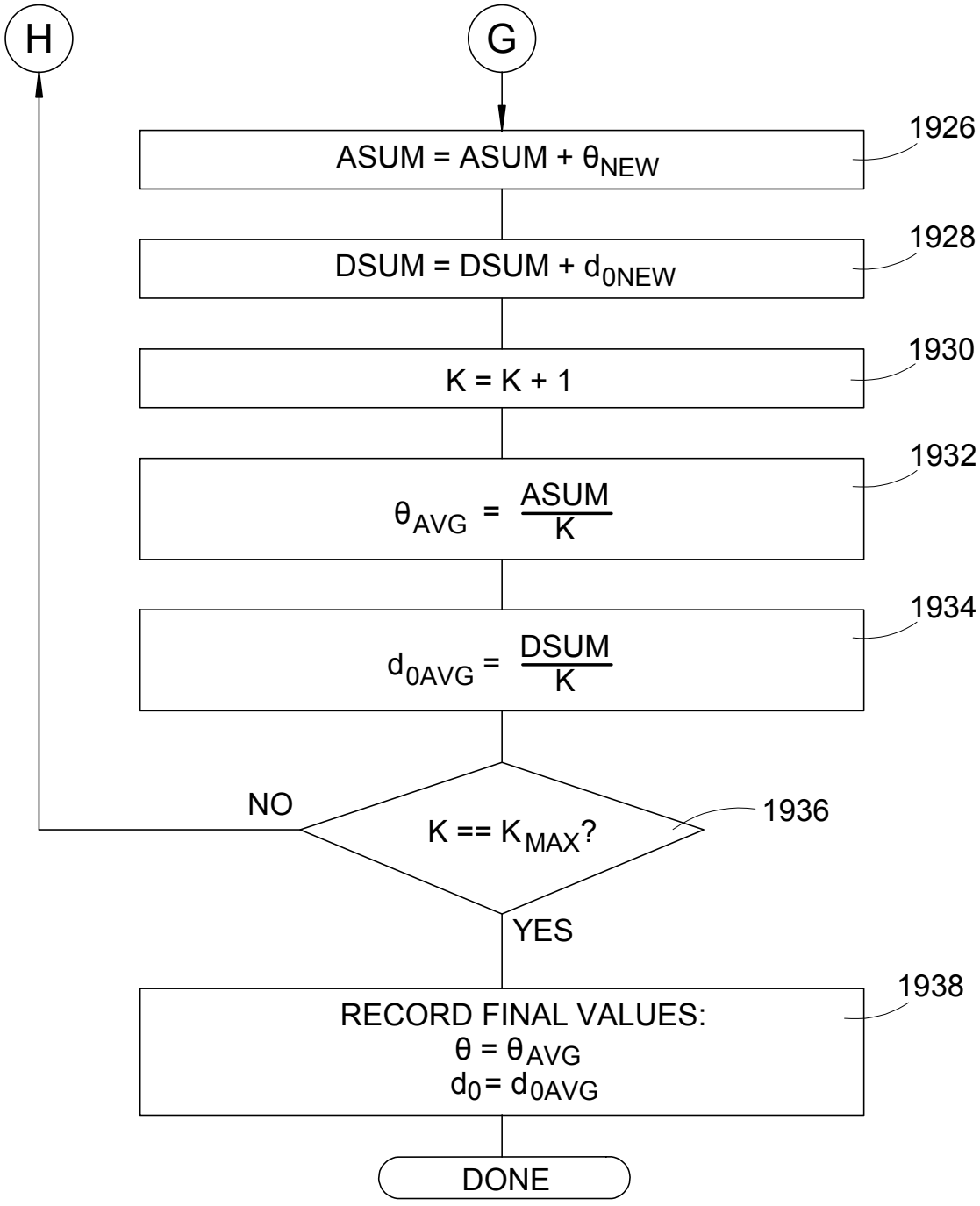
H
G
ASUM = ASUM + θ_{NEW}
1926
DSUM = DSUM + d_{0NEW}
1928
K = K + 1
1930
$\theta_{AVG} = \frac{ASUM}{K}$
1932
$d_{0AVG} = \frac{DSUM}{K}$
1934
NO
K == K_{MAX}?
1936
YES
RECORD FINAL VALUES:
$\theta = \theta_{AVG}$
$d_0 = d_{0AVG}$
1938
DONE

Fig. 19C

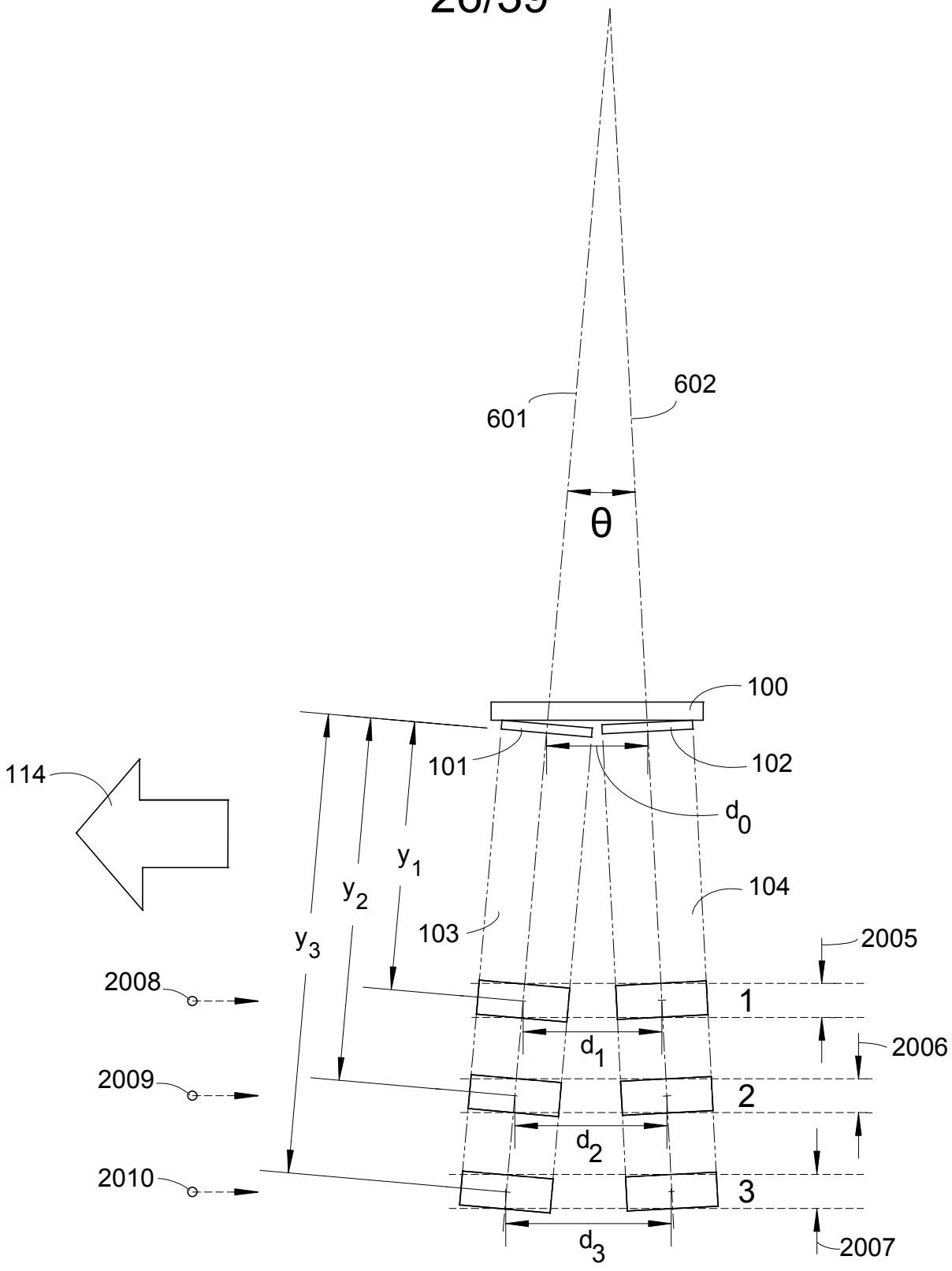
601
602
θ
100
101
102
114
d_0
y_1
y_2
y_3
104
103
2005
2008
1
d_1
2006
2009
2
d_2
2010
3
d_3
2007

Fig. 20

Fig. 21A

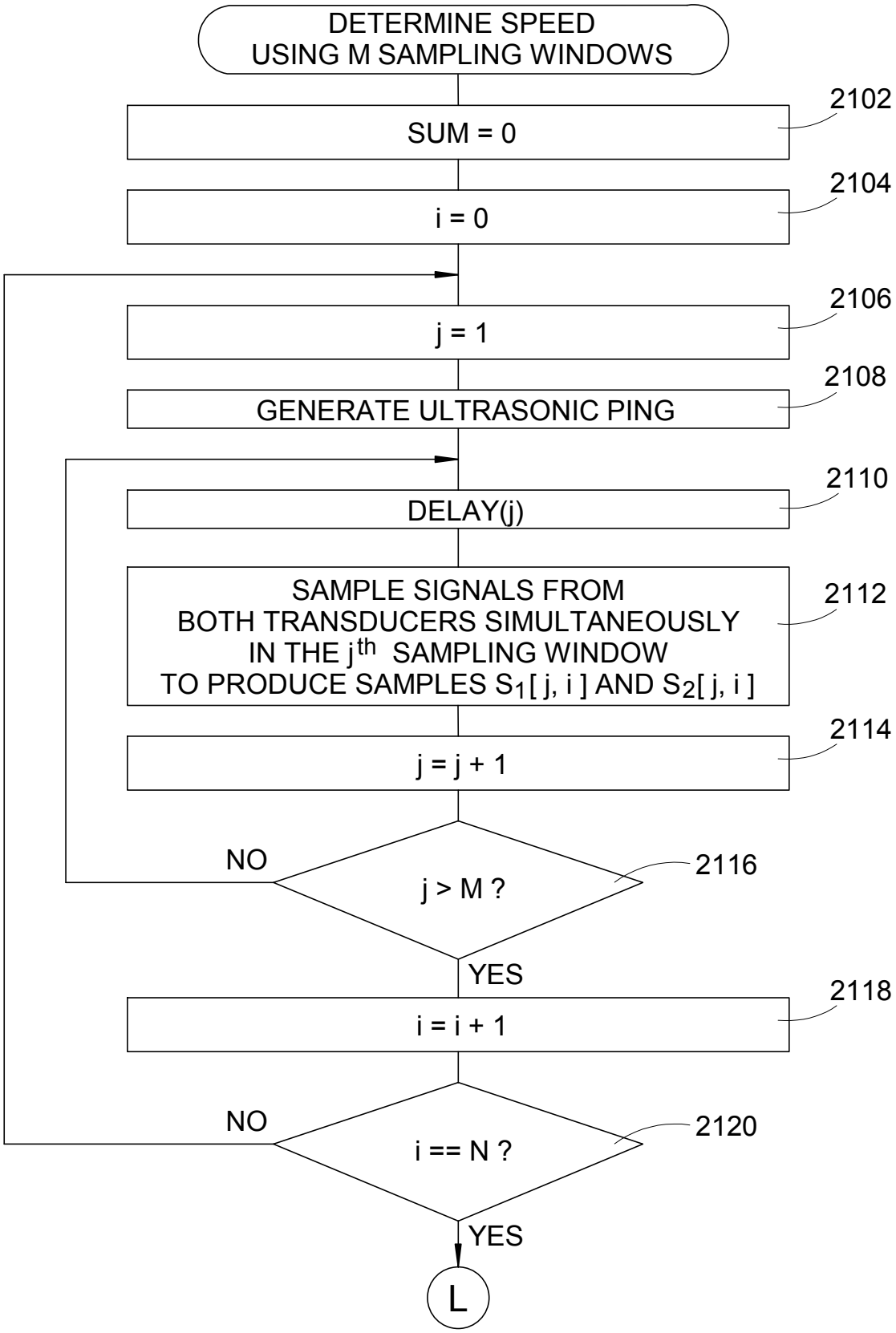
DETERMINE SPEED
USING M SAMPLING WINDOWS
2102
SUM = 0
2104
i = 0
2106
j = 1
2108
GENERATE ULTRASONIC PING
2110
DELAY(j)
2112
SAMPLE SIGNALS FROM
BOTH TRANSDUCERS SIMULTANEOUSLY
IN THE j^th SAMPLING WINDOW
TO PRODUCE SAMPLES S1[j, i] AND S2[j, i]
2114
j = j + 1
NO
2116
j > M ?
YES
2118
i = i + 1
NO
2120
i == N ?
YES
L

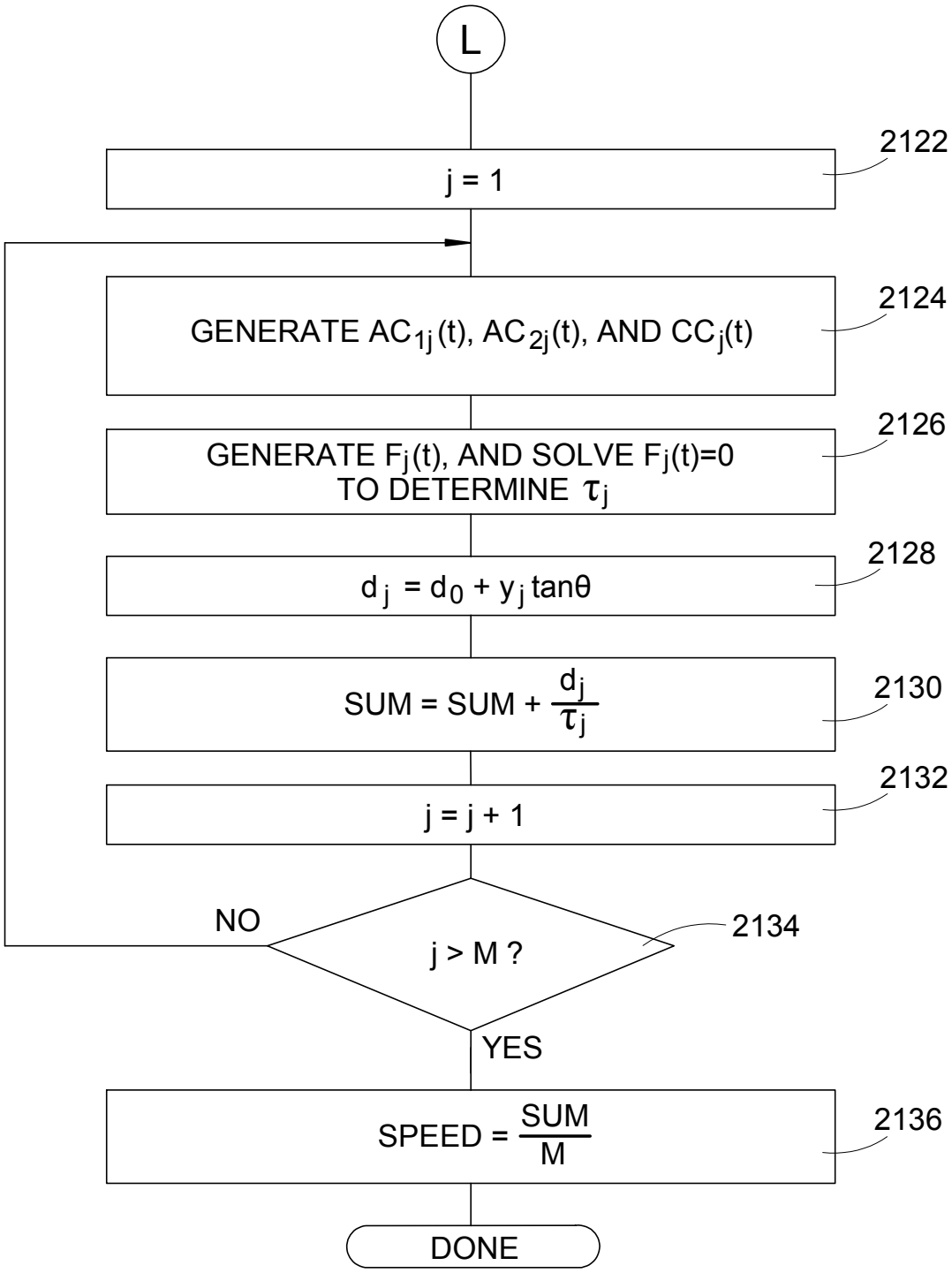
L
2122
j = 1
2124
GENERATE $AC_{1j}(t)$, $AC_{2j}(t)$, AND $CC_j(t)$
2126
GENERATE $F_j(t)$, AND SOLVE $F_j(t)=0$ TO DETERMINE τ_j
2128
$d_j = d_0 + y_j \tan\theta$
2130
SUM = SUM + $\frac{d_j}{\tau_j}$
2132
j = j + 1
2134
NO
j > M ?
YES
2136
SPEED = $\frac{SUM}{M}$
DONE

Fig. 21B

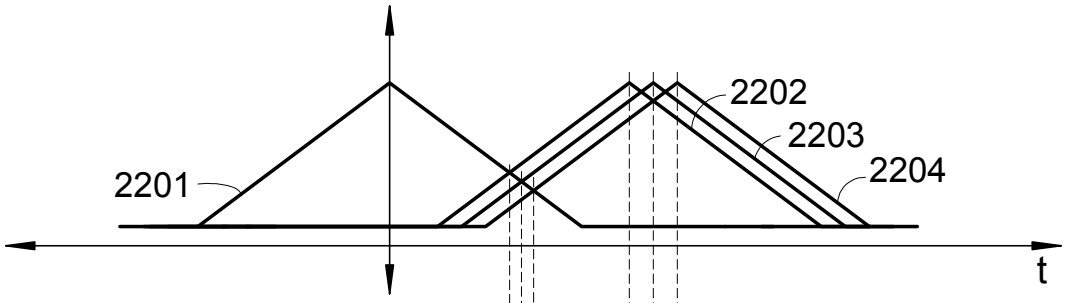

Fig. 22A

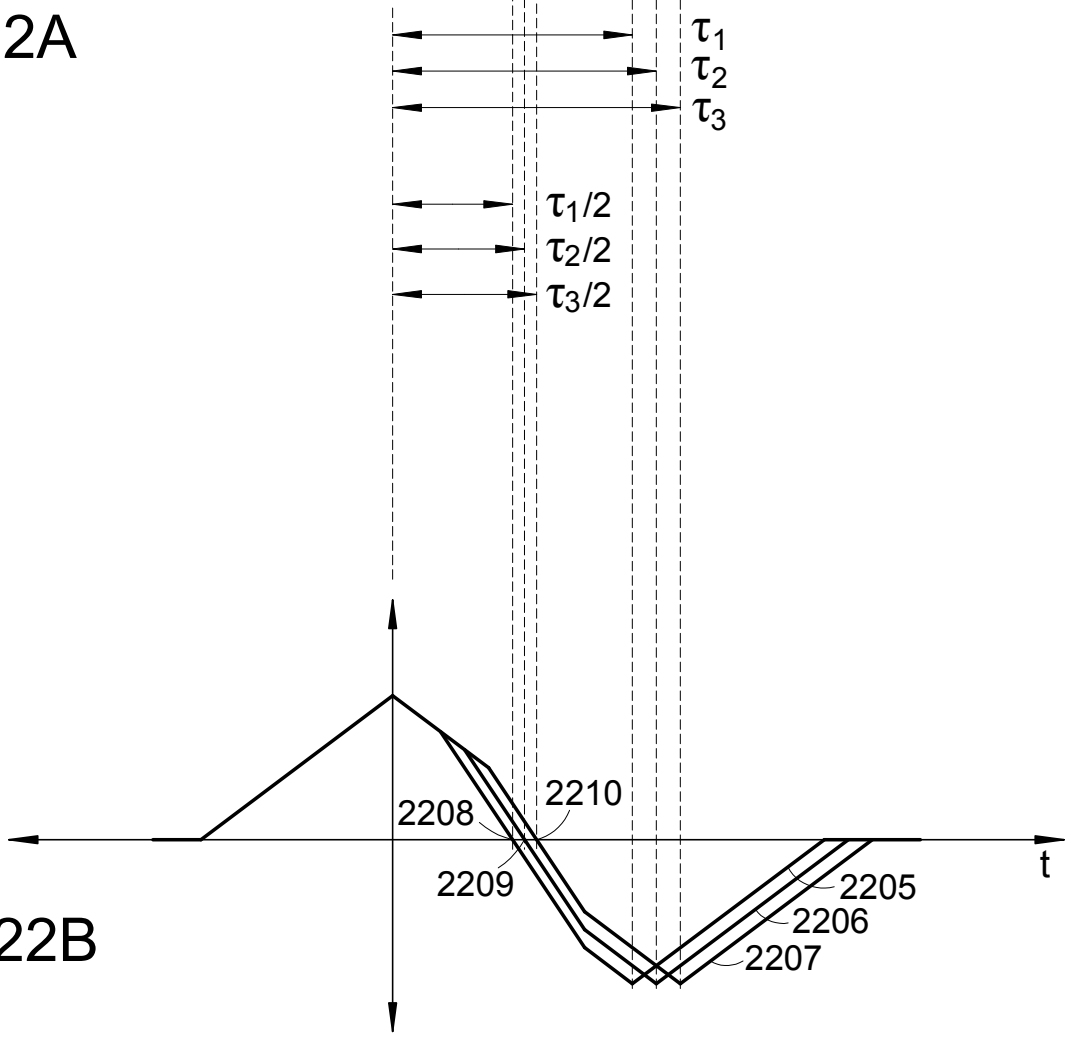

Fig. 22B

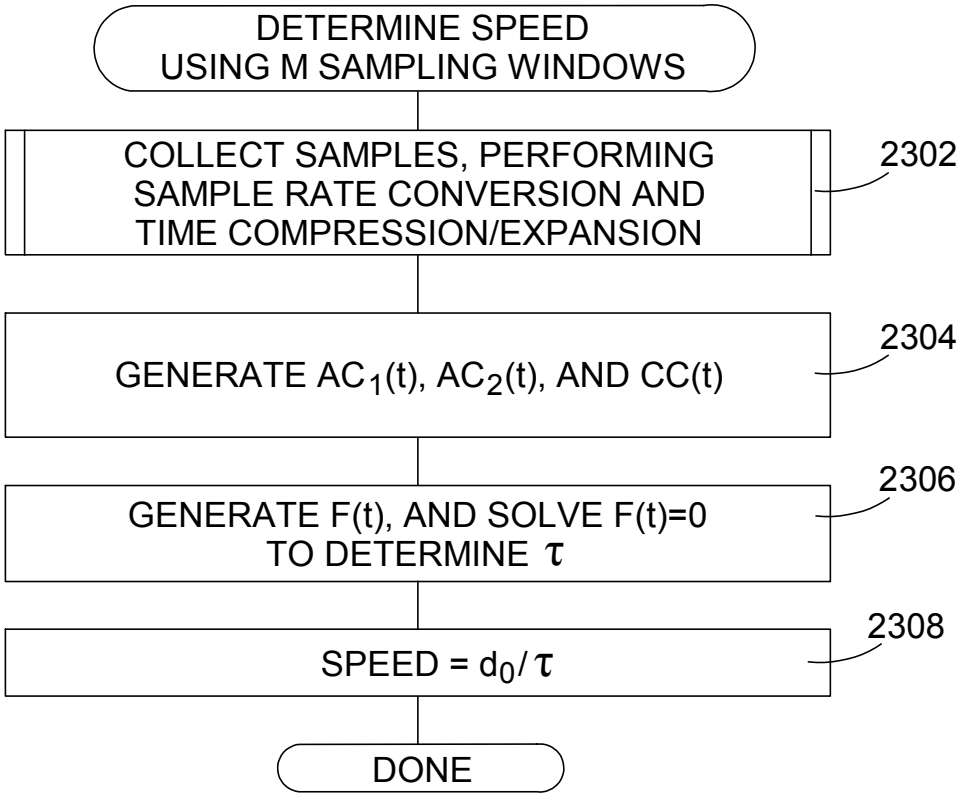
DETERMINE SPEED
USING M SAMPLING WINDOWS
COLLECT SAMPLES, PERFORMING
SAMPLE RATE CONVERSION AND
TIME COMPRESSION/EXPANSION
2302
GENERATE $AC_1(t)$, $AC_2(t)$, AND CC(t)
2304
GENERATE F(t), AND SOLVE F(t)=0
TO DETERMINE τ
2306
SPEED = d_0/τ
2308
DONE

Fig. 23

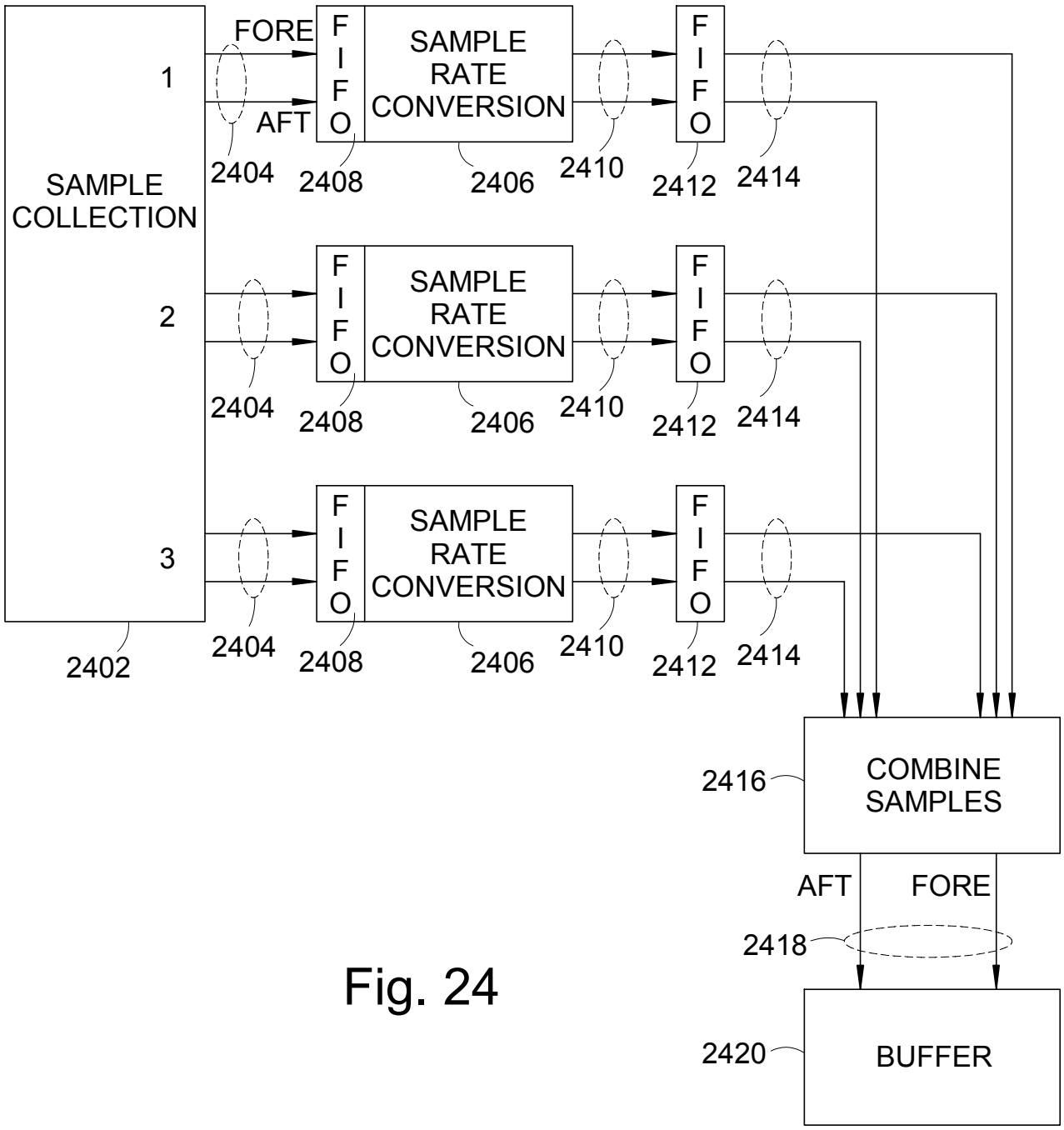
SAMPLE COLLECTION
1
2
3
2402
FORE
AFT
2404
FIFO
2408
SAMPLE RATE CONVERSION
2406
2410
FIFO
2412
2414
COMBINE SAMPLES
2416
AFT
FORE
2418
BUFFER
2420

Fig. 24

Fig. 25A

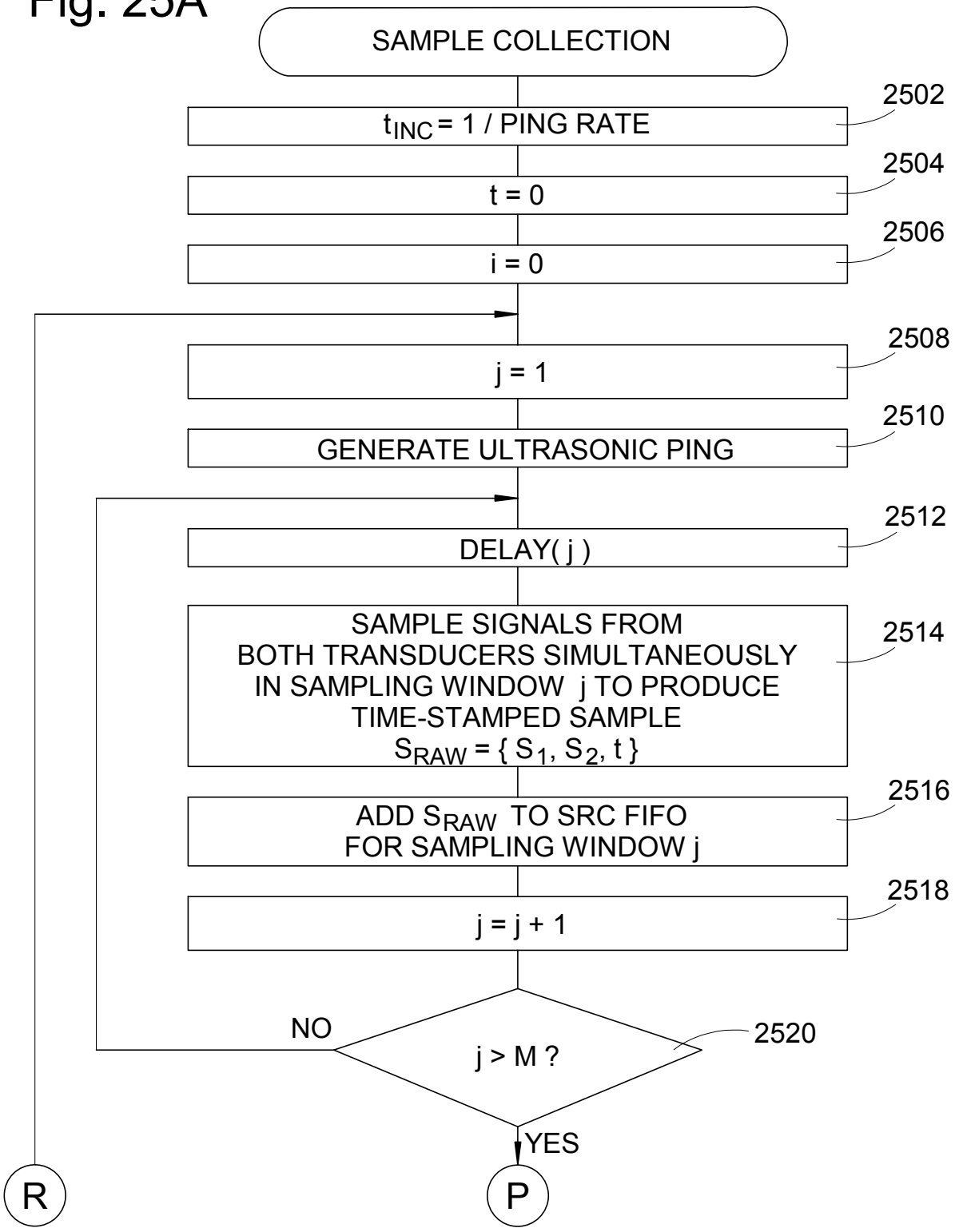
SAMPLE COLLECTION
2502
t_{INC} = 1 / PING RATE
2504
t = 0
2506
i = 0
2508
j = 1
2510
GENERATE ULTRASONIC PING
2512
DELAY(j)
2514
SAMPLE SIGNALS FROM
BOTH TRANSDUCERS SIMULTANEOUSLY
IN SAMPLING WINDOW j TO PRODUCE
TIME-STAMPED SAMPLE
S_{RAW} = { S_1, S_2, t }
2516
ADD S_{RAW} TO SRC FIFO
FOR SAMPLING WINDOW j
2518
j = j + 1
2520
j > M ?
NO
YES
R
P

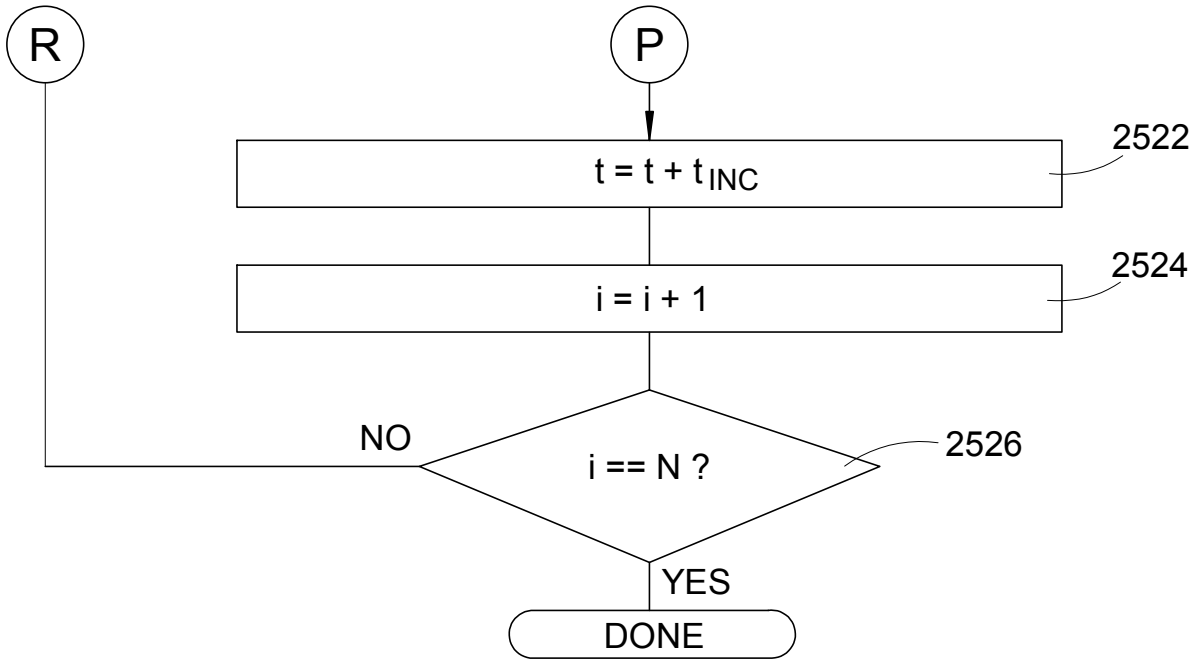

Fig. 25B

Fig. 26A

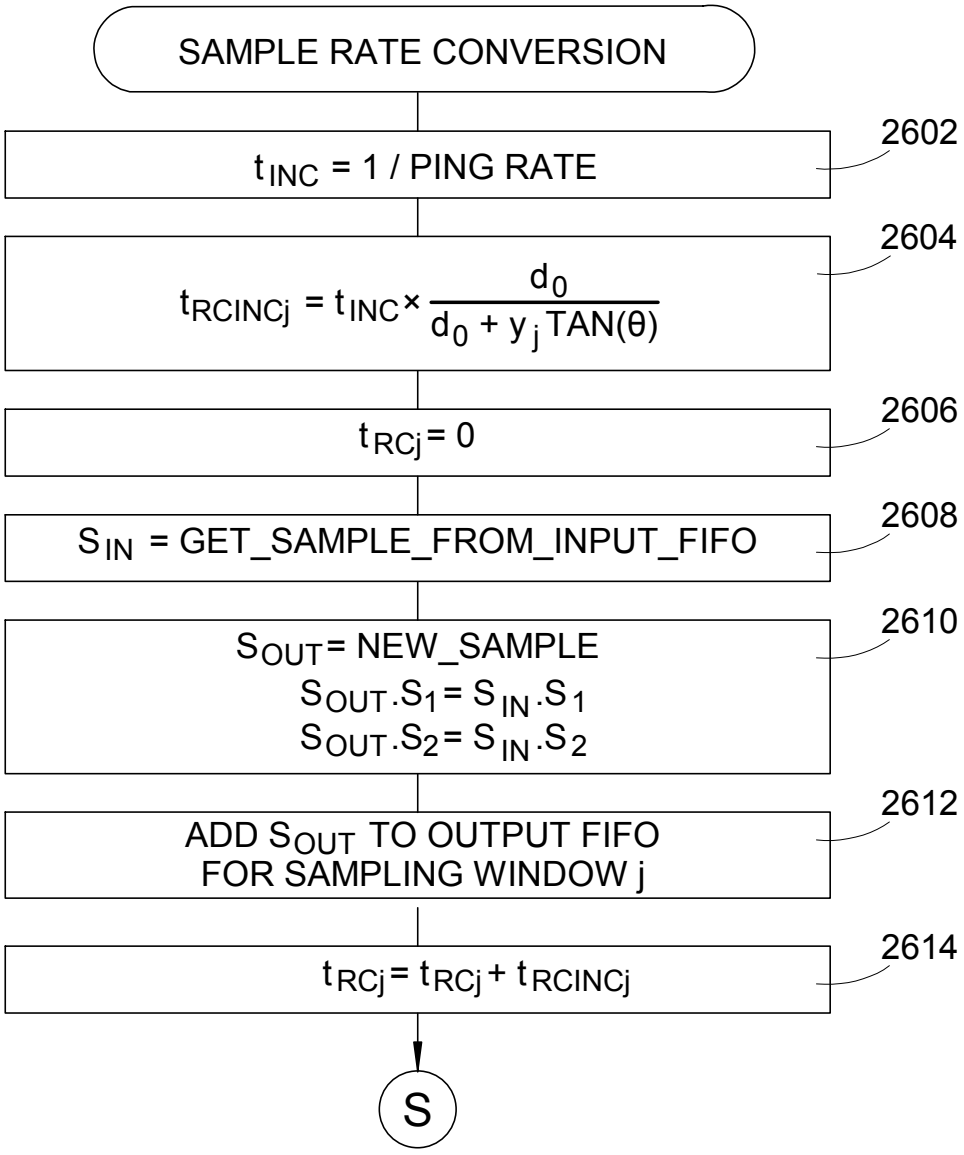
SAMPLE RATE CONVERSION
t_{INC} = 1 / PING RATE
2602
$t_{RCINCj} = t_{INC} \times \frac{d_0}{d_0 + y_j TAN(\theta)}$
2604
$t_{RCj} = 0$
2606
S_{IN} = GET_SAMPLE_FROM_INPUT_FIFO
2608
S_{OUT} = NEW_SAMPLE
$S_{OUT}.S_1 = S_{IN}.S_1$
$S_{OUT}.S_2 = S_{IN}.S_2$
2610
ADD S_{OUT} TO OUTPUT FIFO
FOR SAMPLING WINDOW j
2612
$t_{RCj} = t_{RCj} + t_{RCINCj}$
2614
S

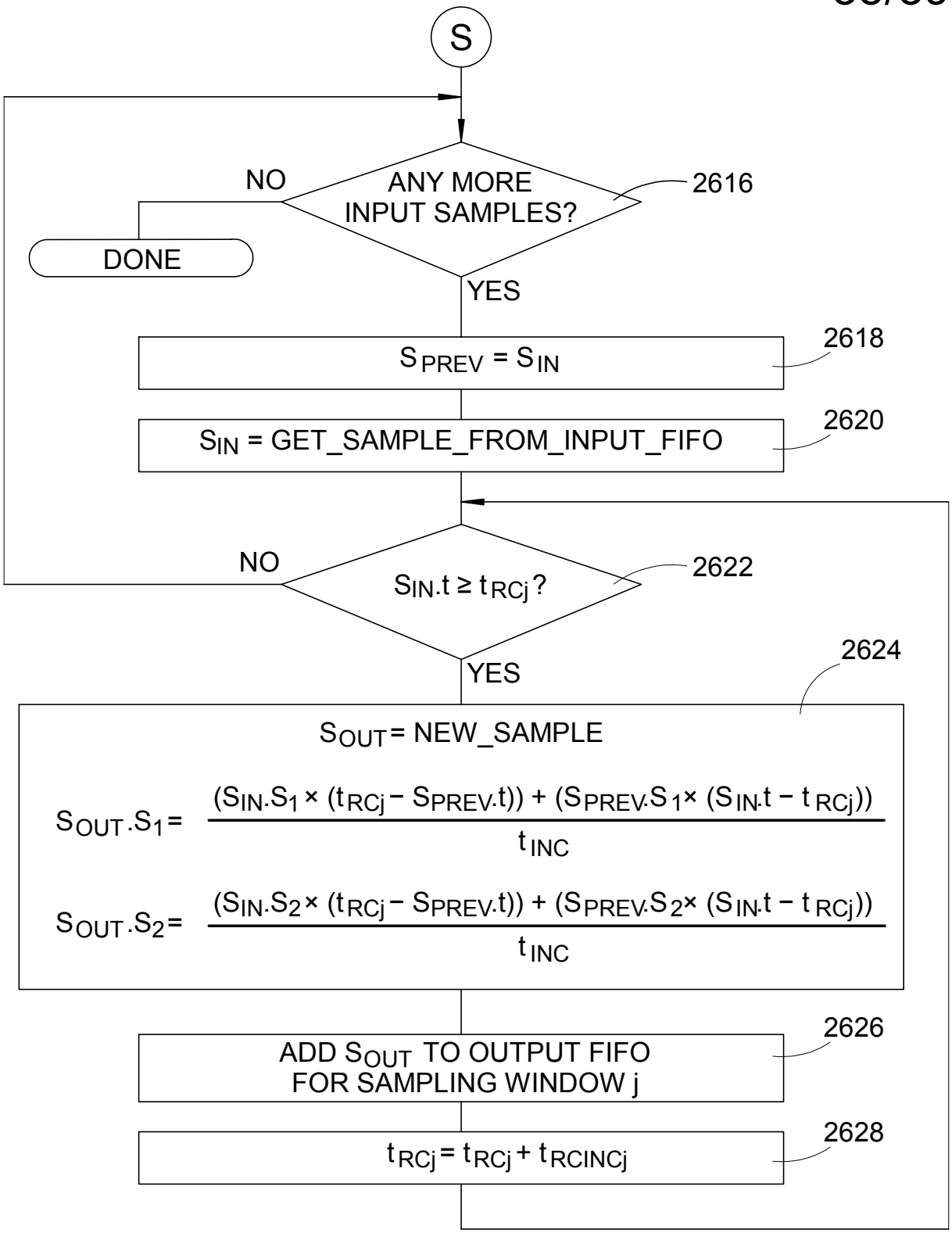
S
ANY MORE INPUT SAMPLES?
2616
NO
DONE
YES
$S_{PREV} = S_{IN}$
2618
S_{IN} = GET_SAMPLE_FROM_INPUT_FIFO
2620
$S_{IN}.t \geq t_{RCj}$?
2622
NO
YES
2624
S_{OUT} = NEW_SAMPLE
$S_{OUT}.S_1 = \frac{(S_{IN}.S_1 \times (t_{RCj} - S_{PREV}.t)) + (S_{PREV}.S_1 \times (S_{IN}.t - t_{RCj}))}{t_{INC}}$
$S_{OUT}.S_2 = \frac{(S_{IN}.S_2 \times (t_{RCj} - S_{PREV}.t)) + (S_{PREV}.S_2 \times (S_{IN}.t - t_{RCj}))}{t_{INC}}$
ADD S_{OUT} TO OUTPUT FIFO FOR SAMPLING WINDOW j
2626
$t_{RCj} = t_{RCj} + t_{RCINCj}$
2628

Fig. 26B

Fig. 27

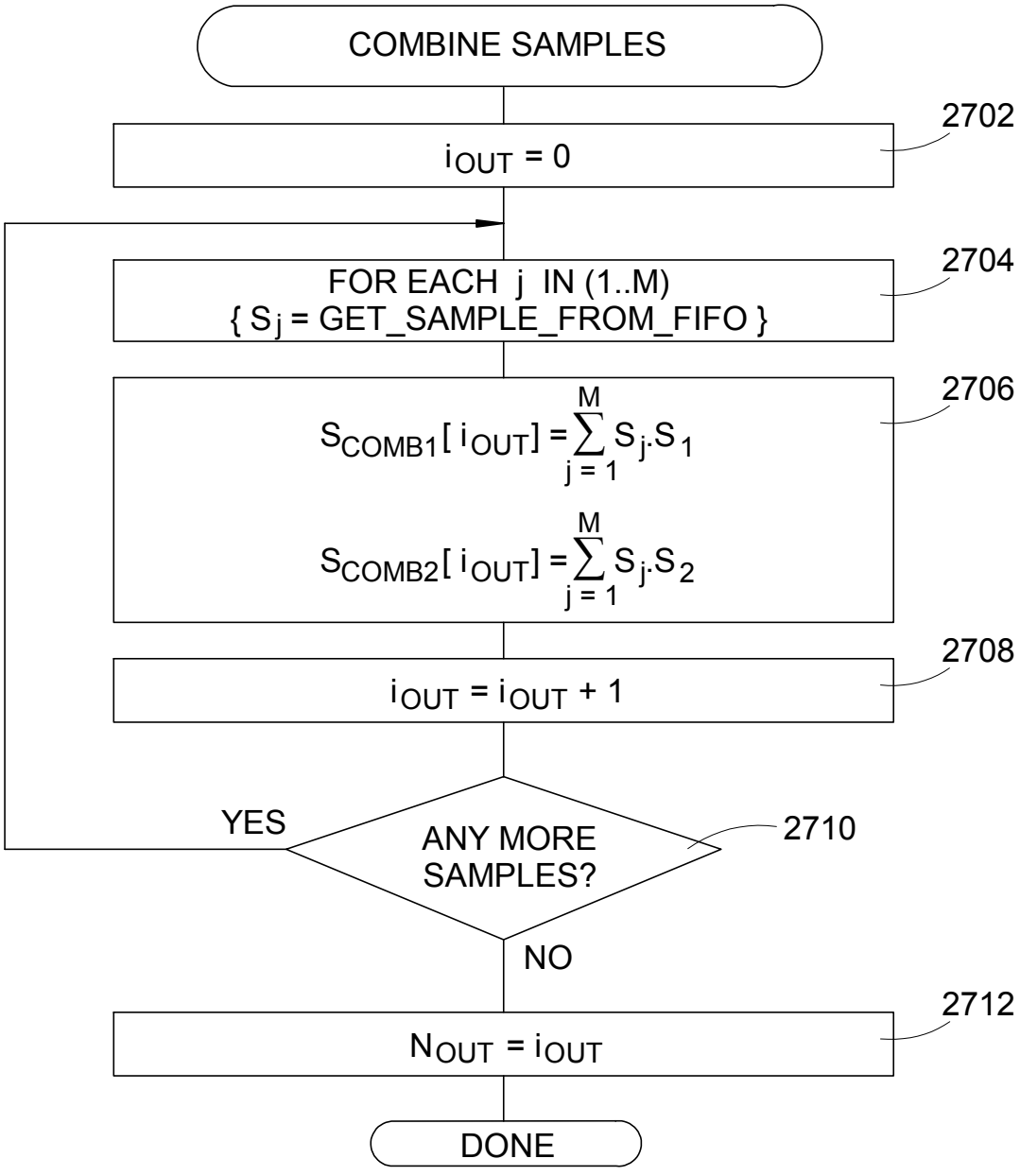
COMBINE SAMPLES
2702
$i_{OUT} = 0$
2704
FOR EACH j IN (1..M)
{ S_j = GET_SAMPLE_FROM_FIFO }
2706
$S_{COMB1}[i_{OUT}] = \sum_{j=1}^{M} S_j \cdot S_1$
$S_{COMB2}[i_{OUT}] = \sum_{j=1}^{M} S_j \cdot S_2$
2708
$i_{OUT} = i_{OUT} + 1$
YES
ANY MORE SAMPLES?
2710
NO
2712
$N_{OUT} = i_{OUT}$
DONE

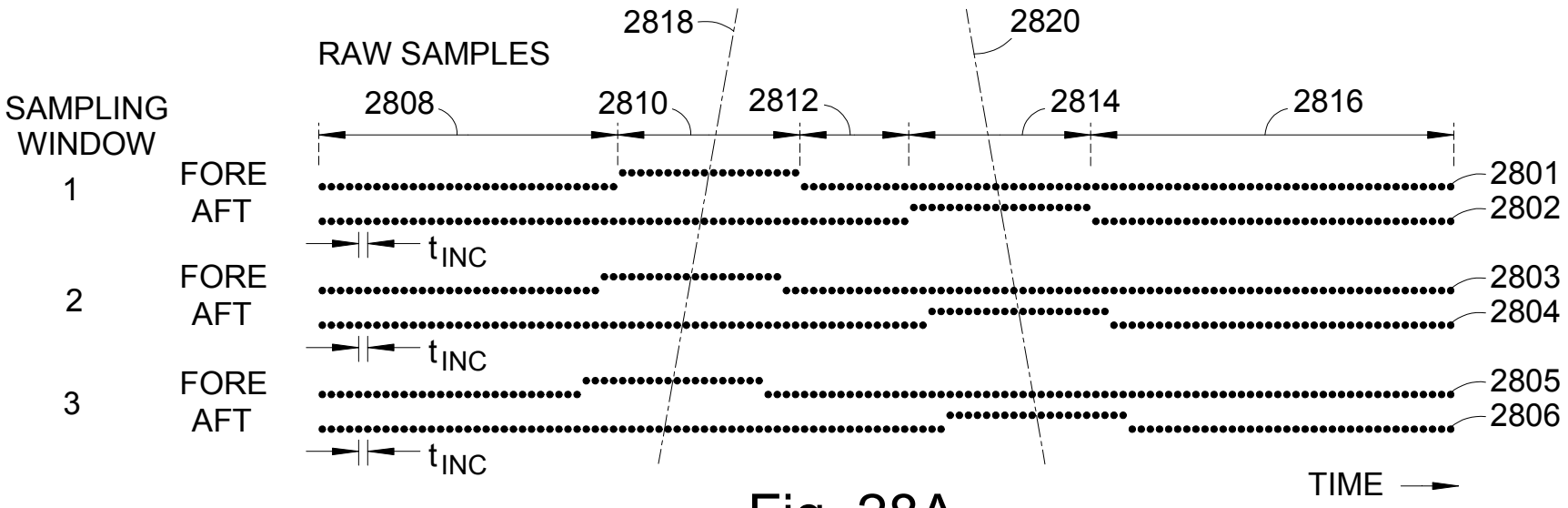

Fig. 28A

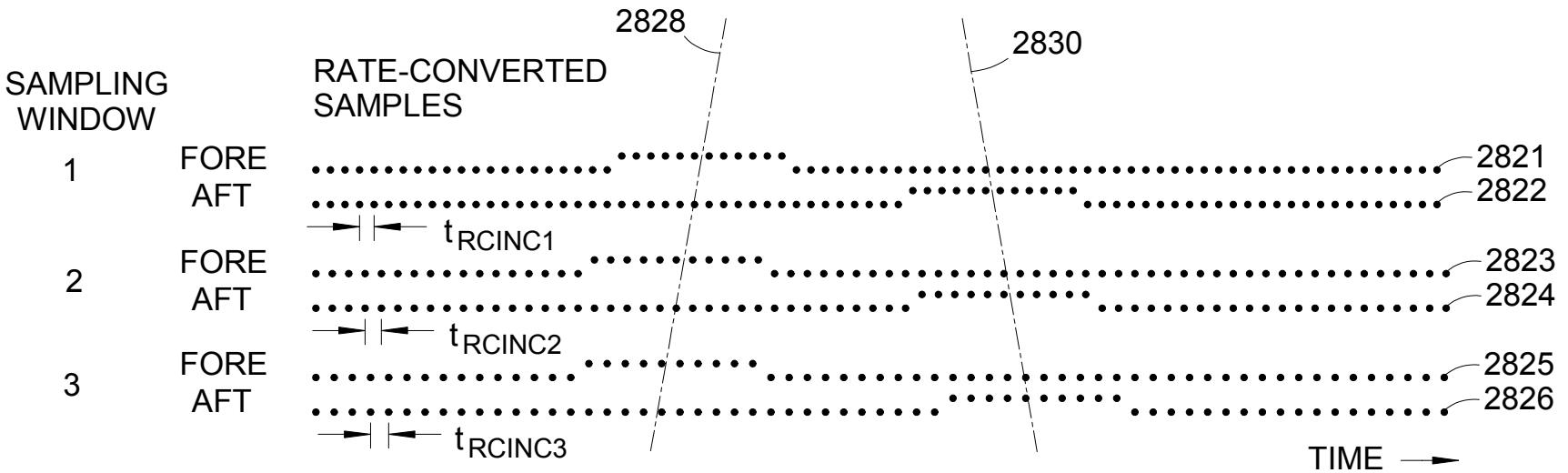

Fig. 28B

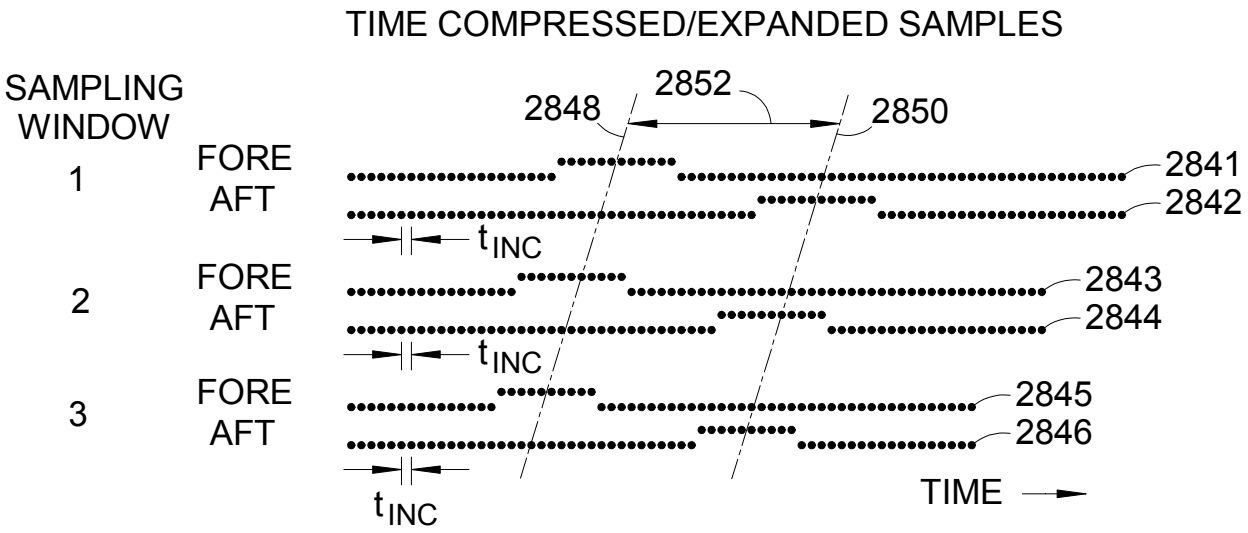

Fig. 28C

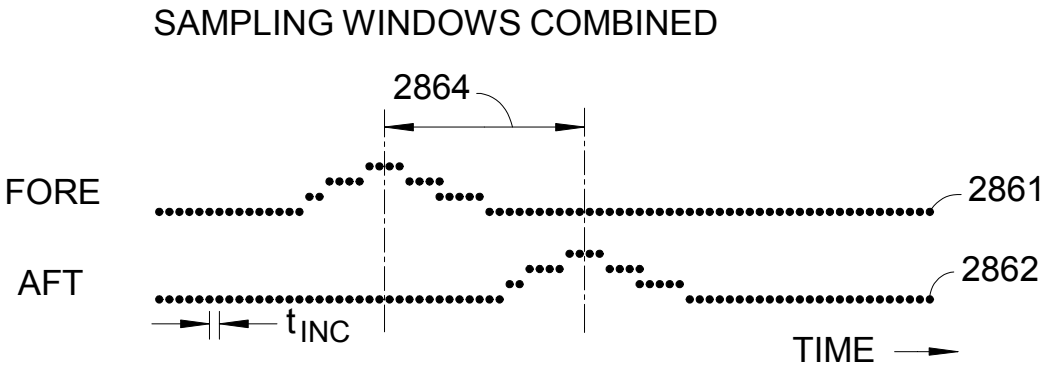

Fig. 28D

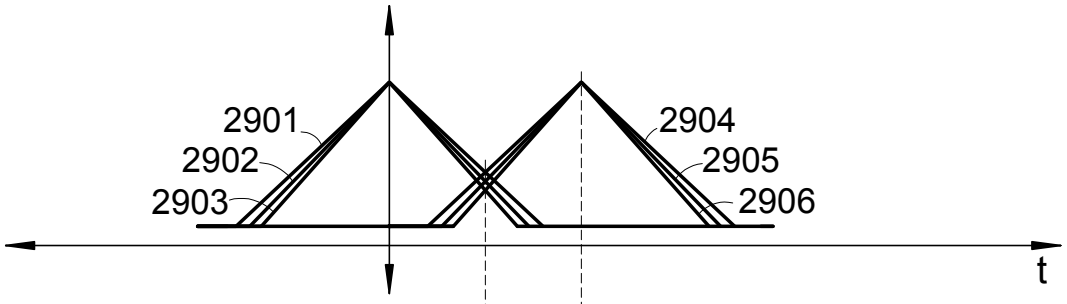

Fig. 29A

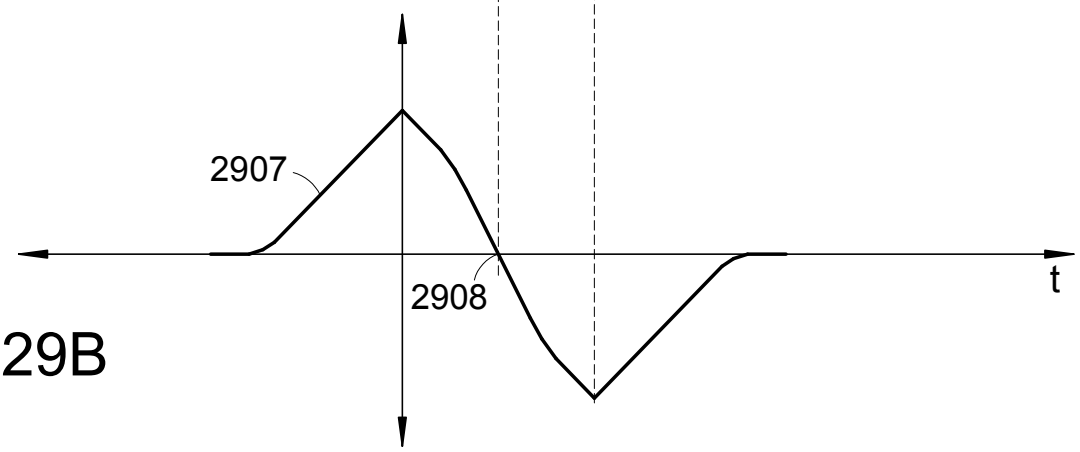

Fig. 29B